University of Southern Queensland
Faculty of Health Engineering and Science

A Dissertation submitted by

Daniel de Freitas Pessoa
0050097308

STATCOM DC Bus Voltage Control and Switching Strategy Analysis

Towards the degree of

Bachelor of Engineering (Electrical and Electronics)

Due October 29
Semester 2, 2015

ABSTRACT

Static Synchronous Compensators (STATCOMs) are employed within electrical networks to dynamically provide Reactive Power support to the when necessary. In 2012, Ergon Energy (the regional electricity supply utility in Queensland, Australia) commissioned its first STATCOM into the sub-transmission, at St. George Substation, and within its first year of operation experienced a number of trip operations on this device.

Due to the limited knowledge of the operational characteristics of this device Ergon Energy's Engineering team decided to investigate further and attempt to model the D-VAR® STATCOM.

This dissertation is the result of this work. While the initial intent was to fully develop a three phase model of the STATCOM, time and complexity constraints limited the outcome of the initial aim, but the following text presents a comprehensive depiction of the findings of the simulation results and establishes a solid base to any further work towards this initial aim.

By deriving a number of equations from first principles and applying these to develop a mathematical model which was implemented in MATLAB®, this project uncovers a number of interesting arguments which explain some of the operational characteristics of the D-VAR® STATCOM.

Considering the limitation of information from the manufacturer, this project deals with an open-loop controlled STATCOM in an attempt to investigate the DC bus levels of the STATCOM. A number of analysis was carried out, including:

- The Pulse Width Modulation (PWM) switching strategy to verify and explain its role in the DC bus operation,

- The effects of changes in the δ angle and voltage magnitude between the Grid (V_G) and the STATCOM (V_S),

- A network transient scenario was also investigated explaining one possible outcome of the DC bus reaction to under a network fault condition.

The theoretical approach considered throughout this work enabled a thorough validation of the model used for this project allowing interesting findings to be reached and conclusions to be drawn, including:

- The PWM switching strategy employed within this single phase STATCOM model does not intervene with the DC bus charging / discharging, as this is achieved by the changes in δ angle between the Grid and the STATCOM, when a number of initial conditions are met (e.g. the DC bus capacitors contain an initial charge which has been calculated to function as the starting charge for the simulation)

- Given an assumed severity of the network transient applied to the simulation, it was observed that upon return to steady-state the STATCOM's DC bus was able to recover from sudden voltage shift caused by the fault, although only a limited number of conditions were analysed and these kept a symmetrical change in the DC bus capacitors.

Leading from this project the development of a three phase model would be valuable in assisting to answer further questions on the overall operational characteristics of the D-VAR® STATCOM.

LIMITATIONS OF USE

The Council of the University of Southern Queensland, its Faculty of Health, Engineering & Sciences, and the staff of the University of Southern Queensland, do not accept any responsibility for the truth, accuracy or completeness of material contained within or associated with this dissertation.

Persons using all or any part of this material do so at their own risk, and not at the risk of the Council of the University of Southern Queensland, its Faculty of Health, Engineering & Sciences or the staff of the University of Southern Queensland.

This dissertation reports an educational exercise and has no purpose or validity beyond this exercise. The sole purpose of the course pair entitled "Research Project" is to contribute to the overall education within the student's chosen degree program. This document, the associated hardware, software, drawings, and other material set out in the associated appendices should not be used for any other purpose: if they are so used, it is entirely at the risk of the user.

CERTIFICATION OF DISSERTATION

I certify that the ideas, designs and experimental work, results, analyses and conclusions set out in this dissertation are entirely my own effort, except where otherwise indicated and acknowledged.

I further certify that the work is original and has not been previously submitted for assessment in any other course or institution, except where specifically stated.

Daniel de Freitas Pessoa

0050097308

_____

Signature

_____

Date

ACKNOWLEDGEMENTS

I would like to first and foremost thank my wife Catherine for all the support, understanding and patience throughout all these years in my pursuit of higher education.

Thank you to my daughter Holly and my son Ryan for the patience and understanding the reasons why I could not play and spend more time with you in the last 7 years of our lives. I can only hope that through my pursuit of a higher education, I have at least inspired you both to never give up your dreams and ALWAYS seek happiness, no matter what.

I am also extremely thankful for all the support, help and love from my mother and sister who taught me the best values and have always been role models of perseverance, insistence and drive in my life, this dissertation would not have been possible without you. Te amo (I love you).

I would like to thank Dr Andrew Hewitt for being a great friend and mentor, for the patience during this mentoring period and for providing me with the opportunity to learn so much in these last few years.

A huge thank you Dr Tony Ahfock, who has taught me so much in the area of Power Systems through a number of university subjects but also extra-curricular courses in Power System Protection.

This project would not have been possible without any of you.

Also thank you to American Super Conductor, especially to Matt Pugh for the provision of some insight on some operational features of the D-VAR® STATCOM (via correspondence with Dr Andrew Hewitt) without over-stepping your company's Intellectual Property's boundaries, I am very grateful for your assistance during this project.

Last but not least, thank you to Professor Siqueira from ATEG Brasil, who always believed in me and mentored me from a young age, showing me the first steps into this great industry that is electrical engineering.

TABLE OF CONTENTS

TABLE OF FIGURES

1 INTRODUCTION

Due to improvements in performance and cost of high power power-electronic devices Static Synchronous Compensators (STATCOMs) have become the preferred solution for providing electricity networks dynamic reactive power support. Also due to its improved response times and reduced harmonic generation STATCOM technology has become a most desired option over the much older Static VAr Compensator (SVC) technology.

While there has been much research on STATCOM operational characteristics, detailed operational information is often highly protected by manufacturers to protect hard earned intellectual property. Ergon Energy as an owner operator of a sub-transmission connected STATCOM device has first-hand experience of this.

1.1 PROJECT MOTIVATION

In 2012 Ergon Energy commissioned its first major STATCOM system. This system was manufactured by the American Super Conductor group who branded their system by the name D-VAR®. Since its installation Ergon Energy has experienced a number of faults due to fluctuations in the DC bus voltage. This experience has highlighted the fact that the way in which the DC bus in the D-VAR® STATCOM is built based on the power electronics switching strategy is not well understood by Ergon Energy. In addition, what is not well understood is how system transients affect the DC bus voltage.

This project will provide an analysis of the IGBT switching strategy techniques used by American Super Conductor in the D-VAR® STATCOM to provide a better understanding of the D-VAR® operation and to propose answers as to why fluctuations in the DC bus voltage might be occurring.

1.2 AIMS AND OBJECTIVES

The aim of this project is to develop a mathematical model which describes the open-loop DC bus operational capabilities of a single phase STATCOM and can assist in fault-finding the D-VAR® STATCOM at Ergon Energy's St. George Substation.

Based on some limited information provided by American Super Conductor (AMSC), the manufacturer of the D-VAR® STATCOM, the following specific aims are proposed for this project:

- The development of a mathematical model of a single phase STATCOM with open-loop control
- Implement and verify the mathematical model by using modelling software (MATLAB®) and compare it to theoretical results from derived equations within project
- Assess how the Pulse Width Modulation (PWM) switching strategy of the modelled STATCOM affects the DC bus voltage level
- Evaluate any effects of Network transients in the modelled open-loop controlled STATCOM

This is aimed to be achieved by analysing the Pulse Width Modulation (PWM) switching strategy utilised by AMSC to operate the converter electronic switches, insulated-gate bipolar transistor (IGBT), contained within the unit and assess its role (if any) in maintaining/controlling the DC bus voltage.

As the main objective, we have to explain possible reasons for the premature failures of the D-VAR® STATCOM's Dynamic Breaking Board (DBR) on an equivalent single scenario disregarding any control system response which form part of the three phase actual D-VAR® STATCOM.

While the initial main goal of this project was to develop a three phase model of the D-VAR® STATCOM to assist in answering the above questions, it became clear during the evolution of the project that the technical complexity of the overall project was under-estimated.

Also adding to this, the control system philosophy for this STATCOM is unknown, steering the modelling to be done by using an open-loop approach. This choice in itself is valid when considering the control system response speed of the STATCOM as reasonably slow when compared to a system transient.

1.3 BACKGROUND

In 2012 Ergon Energy commissioned its first STATCOM system into the sub-transmission network at St George Queensland. This STATCOM replaced an aged Static VAr Compensator (SVC) unit which had been deemed unsustainable due to reliability issues, and due to the fact that the SVC manufacturer was no longer available to provided technical support for the unit.

In addition to the classic advantages provided by STATCOM units over the older SVC technology the D-VAR® unit purchased by Ergon Energy also provided additional security through the use of two independent dynamic VAr units (called Power Module Enclosures or PMEs), a redundant Master Control Enclosure (or MCE) and three D-VAR® controlled 5MVAR capacitor banks.

1.4 AMERICAN SUPER CONDUCTOR AND ERGON ENERGY

In order for Ergon Energy to provide ongoing support (in collaboration with AMSC) for the St George D-VAR® STATCOM the Commissioning and Maintenance group worked closely with AMSC to gain a better

understanding of the protection, control and operational aspects of the D-VAR® STATCOM.

The training provided to Ergon Energy's personnel by AMSC was only to a functional block level and did not provide any real detail on how the system operated. Understandably AMSC also did not want to divulge specific detail of the D-VAR® design as this would surrender their hard earned intellectual property.

Based on the design information provided by AMSC and additional information requested, Ergon Energy developed protection and control system function diagrams to assist with understanding the operating characteristics of the D-VAR®. One of these functional diagrams is shown in Figure.1-2.

In the first year of operation of the D-VAR®, Ergon Energy experienced a number of trip events which either removed the D-VAR® from service or restricted its output capability. These events were investigated with support from AMSC and resulted in some control system and component changes.

These investigations also highlighted the fact the limited understanding that Ergon Energy had on how the unit operated also severely limited its ability to understand and critically assess the rectification information provided by AMSC.

One of the main concerns experienced was the high failure rate of the Dynamic Braking Resistor control board (or DBR board) which was used to help manage the DC bus voltage of the D-VAR®.

In essence the DBR board acts as an "overseeing controller" for the DC bus which is used to build the DC bus when the inverters are idle and to discharge energy from the bus when its voltage becomes too high.

One of the issues found after the failure of a number of these boards was that an upgrade of the board had been made in the factory prior to the delivery of the D-VAR® STATCOM which also required a software change.

Unfortunately, the software change had not been made and this caused the thermal rating of the new DBR boards to be exceeded resulting in premature failure.

Since the rectification of this error the number of DBR board failures has significantly decreased but there have still been a number of subsequent failures experienced.

In order to better understand the nature of why the DBR boards are failing we first need to understand how the board operates in context with the main control system.

As stated previously, the DBR board is not the primary control mechanism for the DC bus voltage but does act to a secondary control system overarching the main control system. In normal operation the DC bus voltage is controlled by the IGBT firing strategy which simultaneously generates an AC voltage on the output (for reactive power output) and maintains the DC bus voltage within its target range.

There are however two conditions where the IGBT firing strategy cannot perform its duty of maintaining the DC bus voltage, these are when the system is idle (that is the reactive power output is zero) and the other is when a system transient results in a high speed over or under voltage excursion of the DC bus voltage.

It is the latter of these two which it is hoped will provide some insight as to why the DBR boards might be failing. To explain what is happening within the D-VAR® under system transient conditions we first need to understand how the D-VAR® switching strategy achieves its two objectives.

1.5 ST. GEORGE SYSTEM CONFIGURATION

The D-VAR® was connected to the St George $33kV$ bus via two star-delta $33kV/480V$ transformers. The D-VAR® control system was designed to regulate the 66kV bus by injection/absorption of reactive power at the $33kV$

bus. The St George D-VAR® STATCOM configuration is shown in Figure.1-1

The two separate sections of the D-VAR® are interfaced into the $33kV$ via two Ring Main Units (RMU1 and RMU2) and these provide connection via RMU1 $33kV$ feeder and RMU2 $33kV$ feeder respectively into the $33kV$ bus system, this voltage level is then raised to $66kV$ to supply the local Sub-Transmission network through two step-up autotransformers and finally the $66kV$ local network, see Figure 1-1 for details.

From a contractual point of view, whilst American Super Conductor had previously commissioned a number of D-VAR® STATCOM throughout Australia the Ergon Energy D-VAR® STATCOM would be the first Australian system which would be operated by a government owned and operated supply utility. A key point of significance resulting from this was that unlike all previously installations AMSC could not be granted unlimited and uncontrolled access to the D-VAR® STATCOM which when commissioned formed part of the Ergon Energy operational network.

The AMSC experience at all previous installations was based on its ability to monitor, maintain and modify the D-VAR® STATCOM s as it deemed necessary to provide an operational system. Under this arrangement whilst AMSC was required to coordinate with the D-VAR® owner to gain access to the units it fundamentally managed and operated the D-VAR® STATCOM.

Due to security and operational constraints this type of arrangement was not possible for the Ergon Energy D-VAR® STATCOM. This change in the D-VAR® maintenance and management strategy meant that Ergon Energy would play a collaborative role with AMSC in the maintenance and management of the D-VAR® STATCOM.

The D-VAR® STATCOM is composed of a number of key sections / devices as depicted in Figure.1-2. AS one of the key primary plant devices within the STATCOM, the Power Module Enclosure (PME) interfaces the

STATCOM with the electrical Network via a three phase $33kV/480V$ $(Y-\Delta)$ transformer.

A number of inverter modules (Inverter 1 Upper / Lower, Inverter 2 Upper / Lower, Inverter 3 Upper / Lower, Inverter 4 Upper / Lower), operate simultaneously supplying the STATCOM output with the required amount of reactive power needed at any given time via separate current steering reactor modules $(2 \times 100\mu H)$ and each inverter is equipped with its own Dynamic Breaking Board (DBR) module.

The PME also contains a harmonic filter within, see Figure 1-2 for a diagrammatic depiction of the configuration.

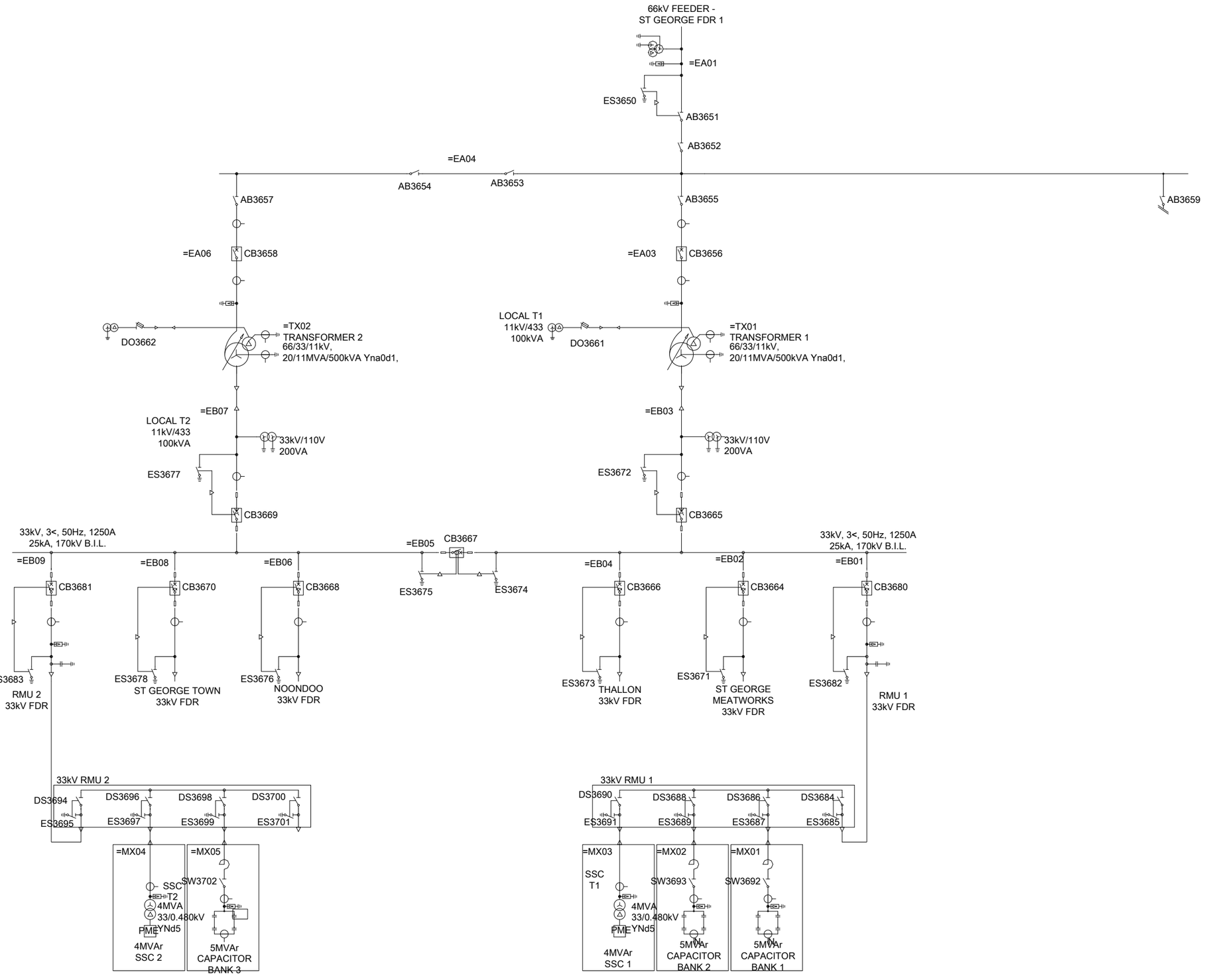

Figure 1-1 – St. George Substation final System configuration (Ergon Energy)

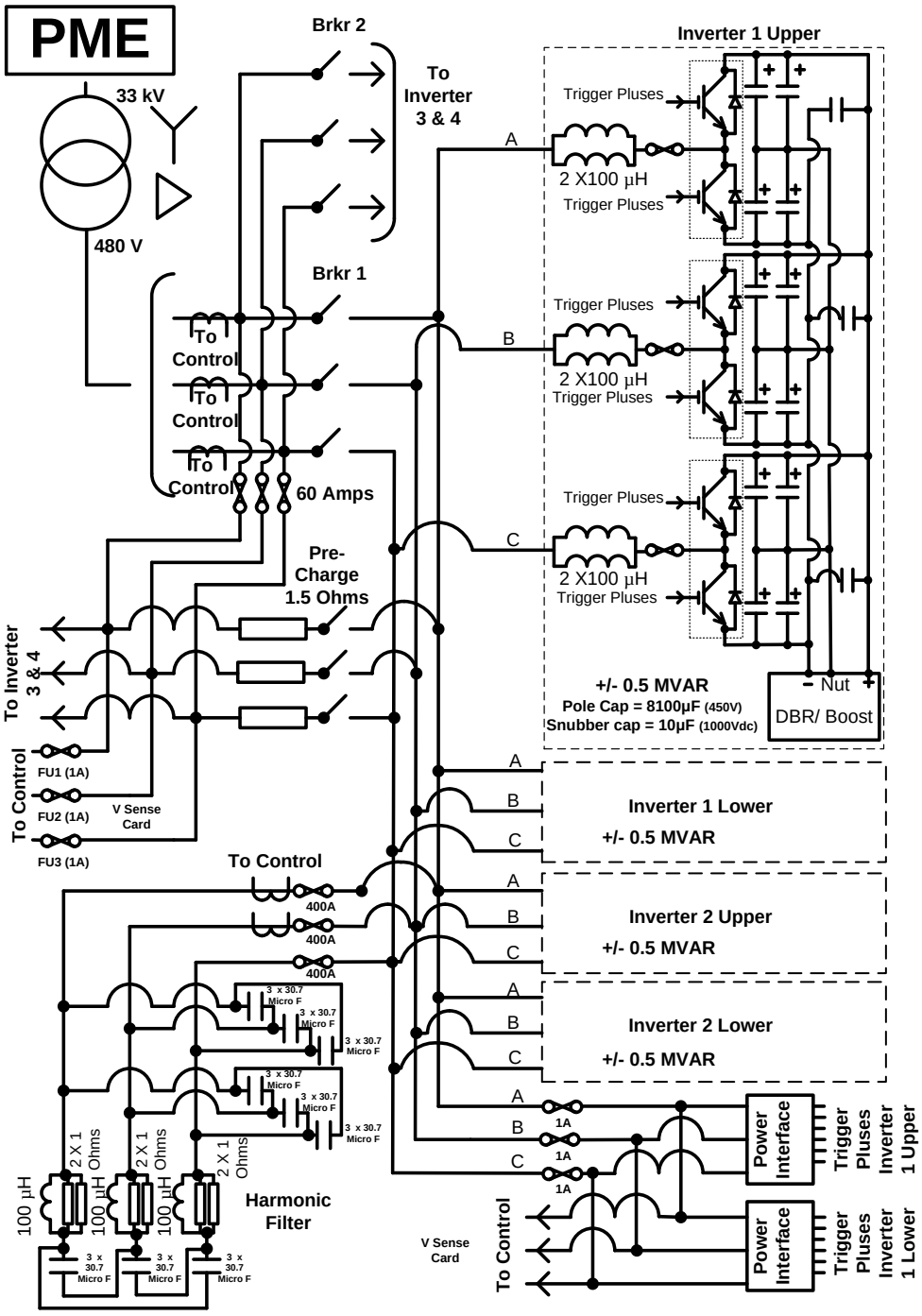

Figure 1-2 – D-VAR® - PME and general arrangement (Ergon Energy Pty)

1.6 PROJECT LIMITATIONS

This project has been developed to provide an insight in some of the operational capabilities of the D-VAR® STATCOM. While the highest degree of care has been taken to develop the whole project in such manner, with this very objective in mind, some hurdles were reached which limited the initial aims to be reached, the main reason described below:

The D-VAR® STATCOM is a three phase device:

- Without thorough knowledge of a single phase STATCOM model, it would have been impossible to develop a greater understanding of how a three phase version of this STATCOM may operate and for this reason this project has been "scaled down" to a single phase STATCOM

The theory developed throughout this dissertation applies to the very single phase model analysed within. While it is clear that some of the characteristics are similar between the single phase and the three phase devices, progressing with the single phase model only due to time constrains will ease any further / future analysis of a three phase STATCOM device.

The D-VAR® STATCOM control system:

- American Super Conductor (AMSC) utilises a number of controllers throughout the STATCOM and these are bound under AMSC's Intellectual Property policies.

While an attempt has been made to reach a higher understanding of this STATCOM, it has to be kept in mind that due to the lack of knowledge of the control system philosophy used it is not possible to accurately model a "perfect STATCOM" which will operate exactly as the D-VAR®.

We were informed by Matt Pugh from AMSC that the D-VAR® control system is segregated into 3 main areas, such as Master Controller, Power Module Enclosure Controller and Inverter Controller. That information

alone, unfortunately, does not provide enough information about the control system to enable this project to create a control system which will mimic the D-VAR® STATCOM to the level needed for the modelling.

With that in mind the approach taken was to consider the STATCOM control system as an open-loop control system and therefore assuming slow control systems responses during its operation.

The above arguments reinforce the reasons for the approach taken during this project, but does not diminish the level of work done and the accomplishments reached during the course of this work, especially considering the limited time allowed for the project to take place.

1.7 OVERVIEW OF DISSERTATION

This dissertation has been structured following the classic undergraduate thesis structure:

The first chapter, INTRODUCTION – Introduces the topic of STATCOM and the background information on the motivation, aims and objectives of the dissertation. The St. George Substation system configuration is introduced and an explanation is given is regards to any limitations reached during the project.

The second chapter, LITERATURE REVIEW – Describes the limited literature that was reviewed during the research process of this project. Introduces the reader to key concepts related to this dissertation, such as Reactive Power, its needs and the use of Reactive Power is managed by the electrical utilities and electrical network operators.

The third chapter, METHODOLOGY – Briefly describes the methodology used during the project and quickly introduces the reader to the model MATLAB® used during the dissertation process.

The fourth chapter, THEORETICAL ANALYSIS – Guides the reader through the steps taken to initiate a logical and reasonable line of thought,

explaining the reason for the analysis of each separate concept that so they can be merged together and used side by side in the final analysis of the STATCOM model.

The fifth chapter, MATHEMATICAL MODEL – Explains the MATLAB® model in a "block-by-block" manner, aimed to demonstrate a comprehensive understanding of the operational characteristics of the numerical solving MATLAB® blocks utilised within the model.

The sixth chapter, SIMULATION RESULTS / DISCUSSION – As obvious as its name, this chapter is aimed to present the results found during the validation process of the model. It is in this chapter that the simulation results were compared with a number of derived equations and some of the well-known theory to ensure the validity of the MATLAB® model itself. Only once the model was validated, discussions were developed to explain the STATCOM operational capabilities in an open-loop state.

The seventh chapter, CONCLUSION – This is where the conclusions drawn during the investigation process of the project are presented to the reader in a concise and yet comprehensive manner.

2 LITERATURE REVIEW

Static Synchronous Compensators have been widely used in power networks for decades around the world (Vedam & Sarma, 2009) and several authors have written about the topic at length.

STATCOMs operate interfaced in parallel to the network (Vedam & Sarma, 2009) and in the case of the D-VAR® the voltage support is provided by a capacitor bank with relatively small energy storage capability and it does not provide active power to the network during steady state operation (American Super Conductor (AMSC), 2013).

Used to supply the network with needed amounts of reactive power for voltage support and Power Factor correction (Ekanayake & Jenkins, 1996) and therefore increasing the power transmission capability of the network (Hingorani & Gyugyi, 2000), the amount of reactive power supplied by the STATCOM to the network can be easily explained by classical power transfer theory (Stevenson Jr., 1975), as can be seen in THEORETICAL ANALYSIS section of the dissertation.

A number of authors have described the main functionalities of STATCOMs, although much is unknown about proprietary techniques used by different manufacturers of the technology to build the DC bus voltage level higher than the peak value of the supply voltage.

Jenkins and Ekanayake explain that the capacitors in a STATCOM can be charged up to the peak value of the supply voltage by managing the switching strategy (Ekanayake & Jenkins, 1996), but their research does not extend to assessing the generation of a DC bus voltage to a greater nominal value than the input RMS voltage.

Marin describes differences, advantages and disadvantages of different techniques used to build the AC signal at the converter level in a multi-pulse level STATCOM (Marin, 2005) with an emphasis on the harmonic

cancellation characteristics of multi-pulse and multi-level converter configuration and also pulse width modulation.

American Super Conductor uses pulse width modulation to generate the output signal, with a switching frequency of approximately 4 kHz (American Super Conductor (AMSC), 2013). Beyond this they do not provide any detail of how the PWM technique also performs the building and maintenance of the DC bus.

This project is intended to fill the gaps found in relation to the lack of information on the specific IGBT switching strategy which enables the D-VAR® to build and maintain the DC bus voltage at $840V_{DC}$ from a $480V_{AC}$ system voltage.

2.1 REACTIVE POWER

The power network is used to deliver electrical energy to domestic, commercial and industrial customer throughout its reach. The electrical power network is required to meet certain criteria to operate effectively, efficiently and reliability; one of these criteria is voltage levels.

As described in section 4.51, sub-section (a), Power System Voltage Control, of NER v.68, "the Australian Energy Market Operator (AEMO) must determine the adequacy of the capacity of the *power system* to produce or absorb *reactive power* in the control of the *power system voltages"* (Australian Energy Market Commission, 2015).

AEMO must also agree, in consultation with the Network Service Providers, not only upon voltage limits / settings, but also reactive power production (or absorption) capacity among other appropriate limits to enable their use by AEMO in the maintenance of power system security (Australian Energy Market Commission, 2015).

Within the transmission network, at any given time, sufficient reactive power reserve must be available to maintain and restore the power system to a reasonable operating state after the most critical system abnormality

determined by previous analysis or periodic contingency analysis (Australian Energy Market Commission, 2015).

There are a number of Reactive Power supply methods available now a day and these are categorised by its capacity deliver approach.

2.2 DISCRETE REACTIVE POWER DEVICES

Discrete Reactive Power devices can be capacitive and / or inductive. They are used to provide a set amount of reactive power at strategic points of the electrical network. Some examples of discrete Reactive Power devices present in the electrical network are: Capacitor banks (usually shunt connected), shunt and line Reactors (Inductors).

2.2.1 CAPACITIVE DEVICES

Placed at strategic locations / substations within the electricity network, capacitor banks provide voltage support by the injection of Reactive Power into the network, improving the system power factor, supporting the system voltage and as result decreasing losses within the system. The decision to invest in this solution is the result from model analysis by the electricity supplier identifying the need for support at crucial periods of the day (Vedam & Sarma, 2009).

Capacitor banks are a cost effective solution when connected to points in the network where fast response times are not of major concern, such as domestic distribution areas.

2.2.2 INDUCTIVE DEVICES

Among the various types of Inductive devices used in the electrical network, shunt Reactors are a common solution to Reactive Power absorption within the electrical network.

Commonly located at substations where long High Voltage transmission lines arrive, shunt reactors absorb excess reactive power from the line when the line is lightly loaded, as result decreasing the line voltage to closer to the

nominal voltage value avoiding potential damage from equipment overvoltage.

2.3 DYNAMIC REACTIVE POWER DEVICES

Unlike discreet Reactive Power devices, dynamic Reactive Power devices are controlled by real times sampled systems. Their associated control systems manage how much Reactive Power is needed, to be absorbed or delivered, at any given time at the point of connection.

These control systems are commonly able to decide and operate within a few cycles of the fundamental frequency (at 50 Hz, 1 cycle is 20 ms), these fast reactions provide a seamless operation and considerable improvements in the power quality of the electrical system voltages.

2.3.1 STATIC VAr COMPENSATOR (SVC)

The Static VAr Compensator is an example of dynamically controlled Reactive Power system which uses capacitive and inductive banks to provide a variable amount of Reactive Power when needed.

Among the various technologies used within the SVCs, they commonly use Thyristor Controlled Reactors (TCR) and Thyristor Switched Capacitors (TSC) and these are strategically switched managing any requirement of Reactive Power need at the point of connection.

Due to its operational characteristics SVCs tend to generate a reasonable amount of low frequency harmonics (usually 5^{th} and 7^{th} harmonic), requiring the installation of harmonic filters for the above mentioned frequencies to be contained within its installed system minimising the amount of harmonic injected into the power system.

Until the “popularisation” of the STATCOMs, SVCs were widely installed around the World when dynamic Reactive Power control, with fast response time systems was needed.

2.3.2 STATIC SYNCHRONOUS COMPENSATOR (STATCOM)

Since it was first proposed by Gyugyi and Pelly in 1976, the use of "all silicon" solutions to the challenges of reactive power compensation in electricity networks has become very popular, eliminating the need for reactive storage components used in rectifier-inverter based system, such as the STATCOM (Krishna, 2014).

Considering its main control attributes, namely Negative Phase Sequence (NPS) correction and oscillation damping in electrical networks, the STATCOM has become a popular solution when some of these issues are to be solved in certain parts of the electrical network.

The main control attributes contained in the studied STATCOM are; Voltage control, VAr compensation, oscillation damping, voltage stability and NPS correction.

Furthermore, the STATCOM contains some inherent advantages, such as the non-generation of low frequency harmonics. This meaning that no harmonic filters are needed to be installed as part of a STATCOM system and therefore the foot print required for this solution is significantly smaller of that of the earlier Static VAr Compensator (SVC).

2.3.3 POWER INVERTERS

The STATCOM is one of the key Flexible Alternating Current Transmission Systems (FACTS) Controllers (Hingorani & Gyugyi, 2000) and has the converter (Inverter) as its main element. A STATCOM can be designed to operate using one of the two main types of inverter controls below:

- Voltage-Sourced Inverters (*VSI*) – Inverter which uses unidirectional DC voltage from a DC capacitor which is converted to AC through sequential device switching. By employing the correct converter topology, it is possible to fully control the voltage output, not only in magnitude, but also in any phase relationship to the AC system

voltage. This type of inverter when employed in a STATCOM uses a voltage level threshold as its target and attempts to keep its voltage output within the set range.

- Current-Sourced Inverters (*CSI*) – In the current-sourced inverter a DC current (supplied by an inductor) is converted into AC current (through sequential device switching) and is presented to the AC system and it can be varied in magnitude and phase angle in respect to the system voltage (its reference). This inverter dynamically controls its current output based on its set target range.

Inverter technology is well-known and has been used in a number of different applications since its development (Mohan, et al., 1989). Although both types of inverters were briefly described above the Current Source Inverters lay outside the scope of this project, since the inverter technology used by AMSC on the D-VAR® STATCOM is clearly of a VSI, as depicted in Figure 1-2 which shows that the DC bus is comprised of DC capacitors.

Voltage-source inverters (VSI) can be divided in 3 general categories, as described by (Mohan, et al., 1989), and these are:

- Pulse Width Modulated (PWM) – This type of inverter uses an essentially constant DC voltage input (in magnitude) and due to this the inverter itself must control the magnitude and frequency of the AC output voltages, which is achieved by pulse width modulation technique. While there are various schemes used to pulse width modulate the inverter switches operation in order to achieve the desired wave shape output, all of attempt to generate an output that is as close as possible to a “perfect sinewave”.

- Square wave inverters – In this type of inverter the control of the DC bus voltage is achieved externally to the inverter which allows the inverter to only need to control the output frequency of its output

signal. This type of inverter has an output shape which is similar to a square wave (hence the name)

- Single-phase Inverters with Voltage Cancellation – Inverters with single phase output, have the ability to control

While a number of inverter categories exist, the focus of this project is in PWM, which as described by AMSC, is the used technology to create its sinewave output modulated at 4 kHz.

2.3.4 PWM SWITCHING

Despite the many different switching techniques used in various "all silicon" DC/AC inverters / converters this project will give emphasis to PWM as this is the technique used on the D-VAR® STATCOM.

This type of inverter controls the generation of its output signal by comparing a control signal ($v_{control}$) to a triangular waveform switched at $f_s = 4$kHz (inverter switching or carrier frequency), which is kept constant alongside its amplitude $\hat{V}_{tri}$ (Rashid, 1988). The control signal ($v_{control}$) is effectively used to control the IGBT duty cycle and is switched at frequency (f_1), also called modulating frequency, which is the fundamental frequency of the inverter AC output.

2.3.5 D-VAR® SWITCHING METHOD

There are a number of ways in which a STATCOM can be configured to operate, each with their own advantages and disadvantages.

STATCOM manufacturers such as Siemens use sinewave stepped approximation as its method to generate its inverter output (Siemens, 2015). Based on the information provided by AMSC the D-VAR® STATCOM operates using a basic pulse width modulation technique.

While sinewave stepped approximation and PWM are well-known (Rashid, 1988), what has not been widely published is how a PWM switching strategy also controls the DC bus voltage. AMSC have provided a simple

explanation based on controlling the phase shift between the system and inverter voltages.

2.4 STATCOM OPERATION

To perform an analysis of the STATCOM, we re-define previously introduced terms, such as:

- $\hat{V}_{tri} \rightarrow$ carrier signal peak voltage
- $f_s \rightarrow$ carrier signal frequency
- $\hat{V}_{control} \rightarrow$ modulating signal peak voltage
- $f_1 \rightarrow$ modulating signal frequency

For a STATCOM system the modulating signal is defined in frequency by the grid or system voltage, that is, we generally use a phase lock loop to synchronise the STATCOM modulating signal to the system voltage. Thus the system fundamental frequency $f_1 = 50Hz$ is the STATCOM modulating signal frequency.

Based on the carrier and modulating signals we can define the amplitude modulation ratio as:

$$m_a = \frac{\hat{V}_{control}}{\hat{V}_{tri}}$$

Equation 2-1

and the frequency modulation ratio is:

$$m_f = \frac{f_s}{f_1}$$

Equation 2-2

It can be shown that the peak amplitude of the fundamental component of the PWM inverter output is given by:

$$\hat{V}_{out\_fund} = m_a \frac{V_d}{2} = \frac{\hat{V}_{control}}{\hat{V}_{tri}} \times \frac{V_d}{2}$$

Equation 2-3

provided that $\hat{V}_{control} \leq \hat{V}_{tri}$ (or $m_a \leq 1.0$). Here V_d is the DC bus voltage (that is from the positive to the negative rail).

Given the equation for the peak of fundamental component of the STATCOM voltage output we can approximate the values for P and Q delivered by the STATCOM as follows;

$$V_S = |V_S| \angle \delta = \left(m_a \frac{V_d}{2} \times \frac{1}{\sqrt{2}} \right) \angle \delta$$

Equation 2-4

V_G can be found using a load flow solution based on the source Thevenin impedance and a fixed power load.

Given V_S and V_G we can find P and Q using the previously derived equations (having the grid as the reference);

$$P = \frac{|V_G||V_S|}{\omega L_S} \sin(\delta) = \frac{|V_G| \left(m_a \frac{V_d}{2} \times \frac{1}{\sqrt{2}} \right)}{\omega L_S} \sin(\delta)$$

Equation 2-5

$$Q = \frac{|V_G|}{\omega L_S} \left[\left(m_a \frac{V_d}{2} \times \frac{1}{\sqrt{2}} \right) \cos(\delta) - |V_G| \right]$$

Equation 2-6

This approach could also be used when creating the STATCOM model to determine values for the modulation index (m_a) and the DC bus voltage for a given Reactive Power output. A simple and quick calculation like this can save significant time when trying to set up the model parameters to provide a steady state result to allow switching analysis to be performed.

3 METHODOLOGY

The studies performed in this thesis will be based on numerical modelling and the application of power electronic principles. A MATLAB® SimPowerSystems model has been developed and was used to validate the theoretical findings of this project.

The MATLAB model is used to develop a better understanding on how the IGBT switching strategy is employed to build and maintain the DC bus and once a full appreciation of the IGBT switching strategy was gained, an analysis of the effects of network transients on the DC bus voltage was performed.

To develop this theoretical approach a number of equations have been derived from first principles and these will assist in developing an understanding on possible mechanisms used by the manufacturer to achieve some key goals within the D-VAR® STATCOM functionalities.

3.1 STATCOM MODEL – MATLAB®

As a key part of this project a MATLAB® SimPowerSystems model of a single phase STATCOM was developed as to assist in the analysis process.

This model was developed relying only on a limited number of key details supplied by the manufacturer, AMSC, and keeping this in mind, the IGBT switching strategy analysis was performed only taking into consideration power electronics principles of operation with the DC bus control system in open-loop state, see Figure 3-1 for reference.

The main reason for this approach is the understandable reluctance from AMSC to provide specific information on operational details on the D-VAR® STATCOM due to intellectual property protection reasons.

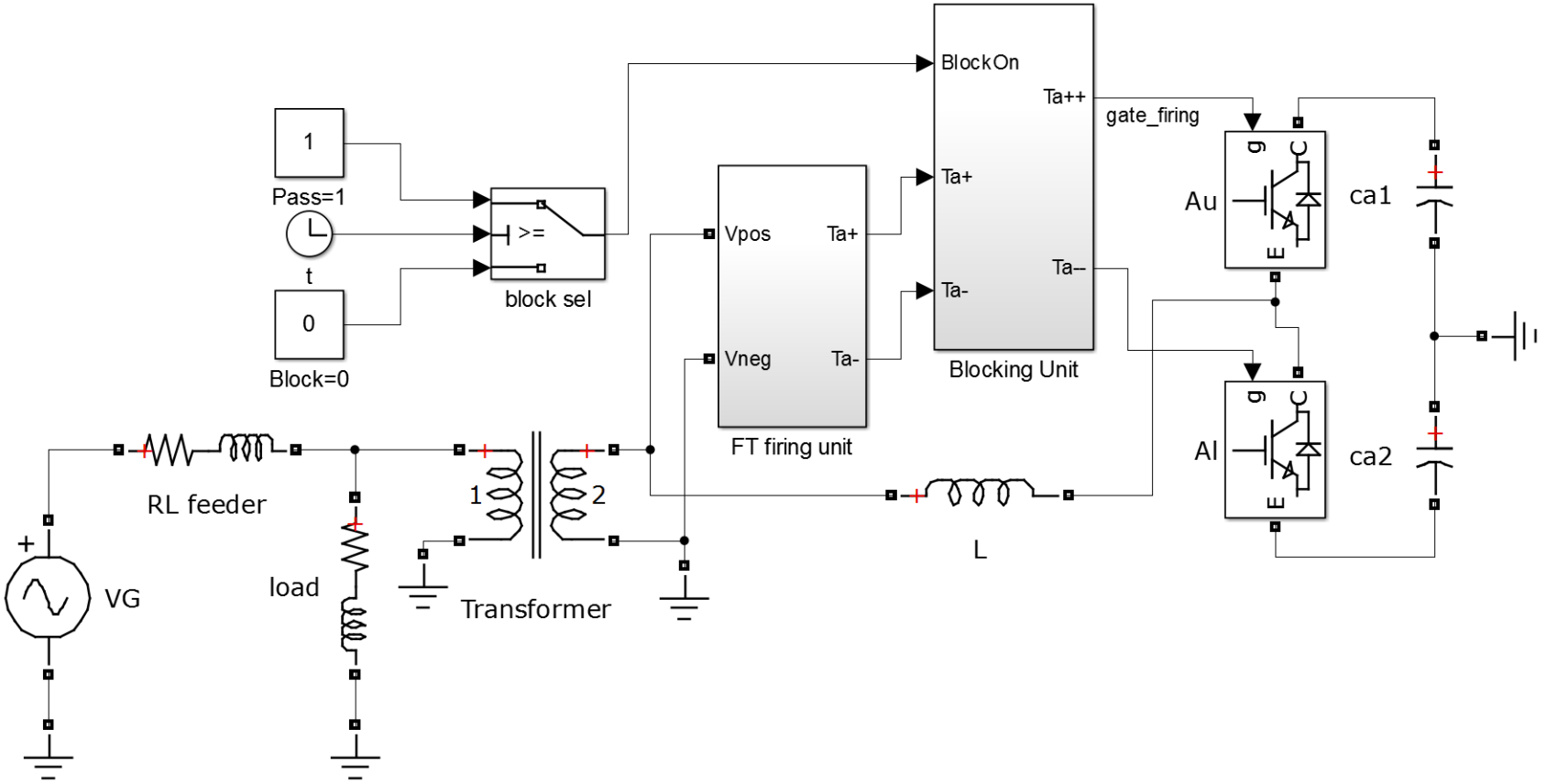

Figure 3-1 - SimPowerSystems ®MATLAB – Single Phase STATCOM Model

4 THEORETICAL ANALYSIS

To be able to reach a solution to the question at hand the development of theoretical understanding of the operational functionality of the STATCOM is essential and to achieve this, a number of approaches were taken.

From the Network's perspective the STATCOM acts as a Reactive Power source and to assist in the understanding of this concept power flow theory was considered and investigated.

Once full understanding was reached in regards to how a source (the STATCOM) delivers power into the Network, further investigation was carried out in the attempt to comprehend how the converter operates and manages its IGBT operation.

Finally allowing a complete analysis of how the switching strategy influences the DC bus voltage and how the STATCOM copes with a number of Network transients.

4.1 POWER FLOW

To explain how power flow takes place between the STATCOM and the network, we use the equivalent circuit depicted Figure 4-1.

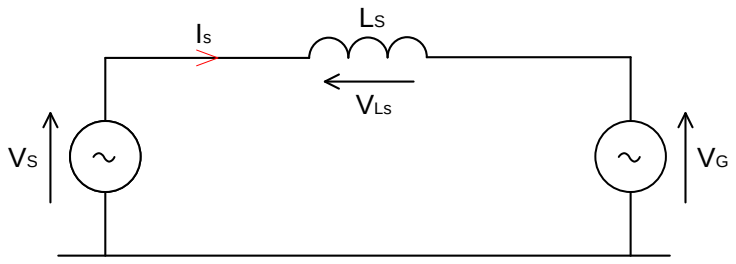

Figure 4-1 - STATCOM connected to the power network (equivalent circuit)

By analysing the above equivalent circuit, we conclude that the amount of Active and Reactive Power transferred between the STATCOM and the network follows two key formulae:

$$P = \frac{|V_G||V_S|}{\omega L_S} sin(\delta)$$

Equation 4-1

and

$$Q = \frac{|V_G|}{\omega L_S} \times (|V_S| cos(\delta) - |V_G|)$$

Equation 4-2

As it can be seen in Equation 4-1 and Equation 4-2 from an equivalent circuit approach, the STATCOM can be treated simply as a source (generator) connected to the grid when power transfer is investigated.

For completeness, the derivation of the above equations from first principles was carried out in APPENDIX B – GENERATOR EQUATION DERIVATION.

It can clearly be seen that both P and Q can be controlled by adjusting the values of V_S and δ using the STATCOM control system. In the STATCOM, the active power flow equation clearly shows that if the STATCOM voltage $V_S = |V_S| \angle \delta$ lags the grid voltage (that is $\delta < 0$) then $P < 0$, that is active power flows from the grid into the STATCOM.

If we consider the reactive power equation for $\delta = 0$ then we have

$$Q = \frac{|V_G|}{\omega L_S} [|V_S| - |V_G|]$$

Equation 4-3

which clearly shows that for $|V_S| > |V_G|$ we have $Q > 0$. From a network perspective this means that the STATCOM appears capacitive. Conversely,

for $|V_S| < |V_G|$ then $Q < 0$ and the STATCOM appears inductive to the network.

We must remember that $S = VI^*$ and thus;

- Capacitive current → Current leads voltage $\rightarrow Q < 0$
- Inductive current → Current lags voltage $\rightarrow Q > 0$

For the perspective of the STATCOM everything is reversed. Remember that when we derived the above equation for Q we did so it in terms of the STATCOM. *From the Grid perspective* we would have had:

$$S = P + jQ = -V_G I_S^*$$

Equation 4-4

which would give us;

$$P = -\frac{|V_G||V_S|}{\omega L_S}\sin(\delta)$$

Equation 4-5

That is – if the STATCOM voltage $V_S = |V_S|\angle\delta$ lags the grid voltage (that is $\delta < 0$) then $P > 0$, which means that active power flows from the grid into the STATCOM.

$$Q = -\frac{|V_G|}{\omega L_S}[|V_S|\cos(\delta) - |V_G|]$$

Equation 4-6

Which tells us that for $\delta = 0$ and $|V_S| > |V_G|$ we have $Q < 0$ which means that the STATCOM appears capacitive to the network. Note that previously

from the STATCOM perspective that this was $Q > 0$. This is because if the current lags the voltage from the STATCOMs' perspective then it leads from the grids' perspective.

Note – the reason we derive the above equations in terms of the active and reactive power delivered from the STATCOM with the grid voltage as the reference is that in practice we consider the grid voltage phase angle as fixed and the power to flow from the STATCOM into the grid in support of the grid voltage.

Whilst this may introduce some confusion (in that it may not be seen as conventional to treat the grid voltage as the reference source but then define the current as flowing from the STATCOM into that source) there are benefits in defining the system in this way. The main benefit is that for $\delta > 0$ we have $P > 0$ from the STATCOM perspective which aligns with the standard convention of a leading source will deliver active power to a load. The other real benefit of using the grid voltage as the reference it that when we want to calculate instantaneous power flow using the inductor current we can perform this calculation on either the STATCOM side or the grid side of the current steering reactor.

When we consider that in practice the voltage on the STATCOM side is a switched DC waveform then it becomes very apparent that is much simpler to use the grid side voltage. The main disadvantage is that for $|V_S| > |V_G|$ we have $Q > 0$ at the STATCOM which by standard convention represents inductive reactive power, however to the grid this would be seen as capacitive reactive power.

As we are primarily interested in the flow of active power we will in general persist with the above defined convention of current flow and voltage reference.

It should also be noted at this time that for a STATCOM which is performing only reactive power support for the network (that is two-

quadrant operation) then the control of P is commonly used to regulate the DC bus voltage.

Under steady state conditions this would in theory equate to the supply of I^2R losses in the STATCOM which would be quite small. Based on the derived power equations it could be argued that a change in $|V_G|$ and/or δ due to a system transient will affect P and Q flow between the STATCOM and the grid. The question then begs what is the consequence of this on the STATCOM reactive power output and the DC bus regulation in the short term for a system transient condition?

4.2 STATCOM THEORETICAL POWER FLOW ANALYSIS

For this theoretical analysis we will redefine the system as shown in the figure below.

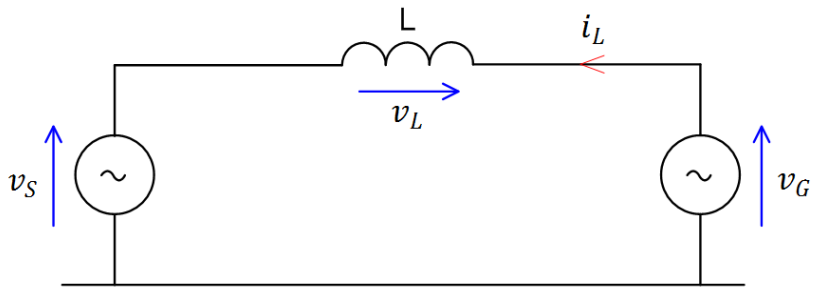

Figure 4-2 - STATCOM connected to the power network (equivalent circuit)

The reason for doing this is that it is much simpler mathematically and less confusing for the reader if we define the grid voltage as the reference source and the inductor current as flowing out of the chosen reference source. Previously we defined the current direction as positive when flowing out of the STATCOM as this better represented the system from a practical view point.

Unfortunately, the change in ‘convention’ for this part of the analysis may cause some minor confusion, however, it is much less confusing than trying

to maintain the previously established convention for the following derivations. In essence the only change by reversing the current direction for the following theoretical analysis is a sign change for the derived power flows.

Given that the grid and STATCOM voltages are defines as follows

$$v_{grid}(t) = \hat{V}_G \sin(\omega t)$$

Equation 4-7

$$v_{STATCOM}(t) = \hat{V}_S \sin(\omega t + \delta)$$

Equation 4-8

and using the grid as the reference (that is the grid voltage is taken as reference voltage and the current is assumed to flow out of the grid source towards the STATCOM) the inductor voltage can be expressed as;

$$v_L = \hat{V}_G \sin(\omega t) - \hat{V}_S \sin(\omega t + \delta)$$

Equation 4-9

$$\Longrightarrow v_L = \hat{V}_G \sin(\omega t) - \hat{V}_S[\sin(\omega t)\cos(\delta) + \cos(\omega t)\sin(\delta)]$$

$$\Longrightarrow v_L = \left(\hat{V}_G - \hat{V}_S \cos(\delta)\right)\sin(\omega t) - \hat{V}_S \sin(\delta)\cos(\omega t)$$

now

$$i_L = \frac{1}{L}\int v_L \, dt$$

Equation 4-10

$$\Longrightarrow i_L = \frac{1}{L}\int \left[\left(\hat{V}_G - \hat{V}_S\cos(\delta)\right)\sin(\omega t) - \hat{V}_S\sin(\delta)\cos(\omega t)\right] dt$$

Equation 4-11

$$\Longrightarrow i_L = \frac{1}{\omega L}\left[\left(\hat{V}_S\cos(\delta) - \hat{V}_G\right)\cos(\omega t) - \hat{V}_S\sin(\delta)\sin(\omega t)\right] + C$$

Equation 4-12

where C is the constant of integration. As we know that $\int_0^T i_L\, dt = \int_0^T \cos(\omega t)\, dt = \int_0^T \sin(\omega t)\, dt = 0$ thus C must be equal to zero. Now that we have an expression for the inductor current we can write an equation for the instantaneous apparent power flow on the grid side of the current steering reactor;

$$s(t) = v_{grid}(t) \times i_L^*(t)$$

Equation 4-13

Note that we use the conjugate of the current to get the correct polarity of the reactive power component. As the inductor current is not expressed in complex for we need to be able to determine what the conjugate is. Fortunately, because it has been written in terms of *sine* and *cosine* terms we can readily determine the real and imaginary components. That is, as the grid voltage has been taken as $v_{grid}(t) = \hat{V}_G\sin(\omega t)$ the *sine* term of i_L will be in phase with v_{grid} and the *cosine* term will be at 90° to v_{grid} and thus the *cosine* term represents the imaginary part of the current.

$$s(t) = \hat{V}_G\sin(\omega t) \times \frac{1}{\omega L}\left[\left(\hat{V}_G - \hat{V}_S\cos(\delta)\right)\cos(\omega t) - \hat{V}_S\sin(\delta)\sin(\omega t)\right]$$

Equation 4-14

$$s(t) = \frac{\hat{V}_G}{\omega L}\left[\left(\hat{V}_G - \hat{V}_S\cos(\delta)\right)\cos(\omega t)\sin(\omega t) - \hat{V}_S\sin(\delta)\sin^2(\omega t)\right]$$

Equation 4-15

$$s(t) = \frac{\hat{V}_G}{\omega L}\left[\frac{1}{2}\left(\hat{V}_G - \hat{V}_S\cos(\delta)\right)\sin(2\omega t) - \frac{1}{2}\hat{V}_S\sin(\delta)\left(1 - \cos(2\omega t)\right)\right]$$

Equation 4-16

$$s(t) = \frac{\hat{V}_G}{2\omega L}\left[\hat{V}_G\sin(2\omega t) - \hat{V}_S\cos(\delta)\sin(2\omega t) - \hat{V}_S\sin(\delta) + \hat{V}_S\sin(\delta)\cos(2\omega t)\right]$$

Equation 4-17

$$s(t) = \frac{\hat{V}_G}{2\omega L}\left[-\hat{V}_S\,sin(\delta) + \hat{V}_G\,sin(2\omega t) - \hat{V}_S\{cos(\delta)\,sin(2\omega t) - sin(\delta)\cos(2\omega t)\}\right]$$

Equation 4-18

$$s(t) = \frac{\hat{V}_G}{2\omega L}\left[-\hat{V}_S\sin(\delta) + \hat{V}_G\sin(2\omega t) - \hat{V}_S\sin(2\omega t - \delta)\right]$$

Equation 4-19

Alternately, we could derive expressions for the instantaneous power flow using the complex form of the inductor current. That is, we can rewrite the previously derived inductor current as a complex number using the grid voltage as the reference (that is using $sin(\omega t)$ as our reference) to give;

$$i_L = -\frac{\hat{V}_S}{\omega L} sin(\delta) + j\left\{\left(\frac{\hat{V}_S\, cos(\delta) - \hat{V}_G}{\omega L}\right)\right\}$$

Equation 4-20

From this expression we can see that the component of the current in phase with the grid voltage is given by:

$$i_{L\_active} = -\frac{\hat{V}_S}{\omega L} sin(\delta)\, sin(\omega t)$$

Equation 4-21

and the component of the current at 90° to the grid voltage is given by

$$i_{L\_reactive} = \left(\frac{\hat{V}_S\, cos(\delta) - \hat{V}_G}{\omega L}\right) cos(\omega t)$$

Equation 4-22

Thus the instantaneous active power flowing from the grid to the STATCOM will be given by

$$p(t) = v_{grid} \times i_{L\_active} = -\frac{\hat{V}_G \hat{V}_S}{\omega L} sin(\delta)\, sin^2(\omega t)$$

Equation 4-23

$$\Longrightarrow p(t) = -\frac{\hat{V}_G \hat{V}_S}{2\omega L} sin(\delta)\,(1 - cos(2\omega t))$$

Equation 4-24

$$\Longrightarrow p(t) = -\frac{\hat{V}_G \hat{V}_S}{2\omega L} sin(\delta) + \frac{\hat{V}_G \hat{V}_S}{2\omega L} sin(\delta)\, cos(2\omega t)$$

Equation 4-25

and the instantaneous reactive power will be given by

$$q(t) = v_{grid} \times -i_{L\_reactive} = -\frac{\hat{V}_G}{\omega L}\left(\hat{V}_S\, cos(\delta) - \hat{V}_G\right) cos(\omega t)\, sin(\omega t)$$

Equation 4-26

$$\Longrightarrow q(t) = -\frac{\hat{V}_G}{2\omega L}\left(\hat{V}_S\, cos(\delta) - \hat{V}_G\right) sin(2\omega t)$$

Equation 4-27

$$\Longrightarrow q(t) = -\frac{\hat{V}_G \hat{V}_S}{2\omega L} cos(\delta) + \frac{\hat{V}_G^2}{2\omega L} sin(2\omega t)$$

Equation 4-28

Note – we need to introduce the negative sign for the $q(t)$ calculation as we need to use i_L^* otherwise the sign of $q(t)$ will be incorrect. This is just a negative sign as $i_{L\_reactive}$ is the imaginary component of the inductor current.

The advantage of this derivation is that it provides expressions for both the instantaneous active and reactive power. These results are not surprising as we can see that in both cases the average power flowing from the grid into the STATCOM over one cycle will be given by:

$$P = -\frac{\hat{V}_G \hat{V}_S}{2\omega L} sin(\delta)$$

Equation 4-29

Previously we derived the same equation for P with the only difference being the negative sign. As stated at the beginning of this section the sign reversal comes from the fact that we have reversed the current direction.

Both equations are identical in that they tell us that for $\delta > 0$ (that is the STATCOM fundamental voltage output leads the grid voltage) active power flows from the STATCOM to the grid. That is, from the perspective of the grid the power flow is negative and from the perspective of the STATCOM the power flow is positive. The equations also show us that the converse of this is true for $\delta < 0$.

In order to assess the behaviour of the active power flow for varying phase shifts between the STATCOM fundamental output voltage and the grid voltage we need to go back to basics. We know that the general form for power flow is given by

$$S = VI^* = P + jQ$$

Equation 4-30

which tells us that

$$|S| = |V||I| = \sqrt{P^2 + Q^2}$$

Equation 4-31

$$\phi = tan^{-1}\left(\frac{Q}{P}\right)$$

Equation 4-32

and thus for a fixed Q and V (assumed constant grid voltage) if we increase P then I must increase in magnitude and the phase angle ϕ must decrease. Alternately, if we reduce P then I must become smaller and the phase angle must increase. Obviously the STATCOM will not be an exception to these rules but the question is how is this achieved through the control of active and reactive power within the STATCOM? Looking at the expressions for the average active and reactive power flow from the grid to the STATCOM (repeated here for convenience)

$$P = -\frac{\hat{V}_G \hat{V}_S}{2\omega L} sin(\delta)$$

Equation 4-33

and

$$Q = -\frac{\hat{V}_G}{2\omega L}\left(\hat{V}_S\, cos(\delta) - \hat{V}_G\right)$$

Equation 4-34

we can see that for a change in δ we both change the P and Q values. This is not really surprising when we look at our general power flow equations above but we need to be careful here as ϕ in the generic power flow equations is not the same as δ in the STATCOM power flow equations. We must remember that ϕ is the phase angle between the voltage and current whereas δ is the phase angle between the grid and STATCOM side voltages.

For a half bridge converter configuration using a PWM firing strategy the peak amplitude of the fundamental component of the converter output is given by (Mohan, et al., 1989):

$$\hat{V}_{out\_fund} = m_a \frac{V_d}{2} = \frac{\hat{V}_{control}}{\hat{V}_{tri}} \times \frac{V_d}{2}$$

Equation 4-35

and thus we can rewrite our expression for the average active and reactive power as

$$P = \frac{|V_G| \left(m_a \frac{V_d}{2} \times \frac{1}{\sqrt{2}} \right)}{\omega L_S} sin(\delta)$$

Equation 4-36

$$Q = \frac{|V_G|}{\omega L_S} \left[\left(m_a \frac{V_d}{2} \times \frac{1}{\sqrt{2}} \right) cos(\delta) - |V_G| \right]$$

Equation 4-37

The derivation and application of these equations will be further discusses in the subsequent section on STATCOM operation. What is important about these equations at this point in time is that they show that P and Q can be controlled by manipulation of the control variable = modulation ratio = m_a.

This means that the STATCOM can develop a fixed Q and adjust P. It can be shown (refer section on STATCOM operation) that the Q value will be constant provided that

$$m_{a\_n} = m_{a\_1} \times \frac{cos(\delta_1)}{cos(\delta_n)}$$

Equation 4-38

where m_{a_1} and δ_1 define the desired fixed value of Q and m_{a_n} is the modulation ratio required for a phase shift of δ_n to give the same Q value. As shown from the active power equation, a change in m_a will also affect the value of P. That is, active power flow is controlled not only by the phase angle δ but also m_a for a fixed Q output from the STATCOM.

To demonstrate this, plots of active and reactive power for a fixed m_a value over the range $-180° \leq \delta \leq +180°$ are shown in Figure 4-3.

As expected, the plot for active power has the form of a *sine* wave with $\delta$and Q has the form of a *cosine* wave with δ. As we are interested in the flow of active power to/from the STATCOM for changes in δ we can avoid the additional complexities caused by the changes in Q by adjusting the value of m_a as discussed above. This will allow us to investigate how the active power flow can be regulated under steady state conditions independent of Q. Plots of active power and $m_a$for a fixed Q are shown in Figure 4-4.

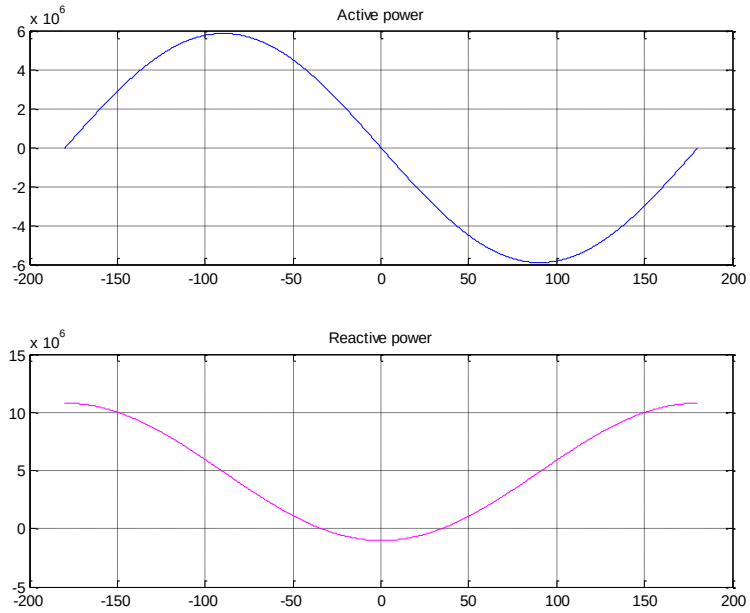

Figure 4-3 - Active and Reactive Power over δ angle

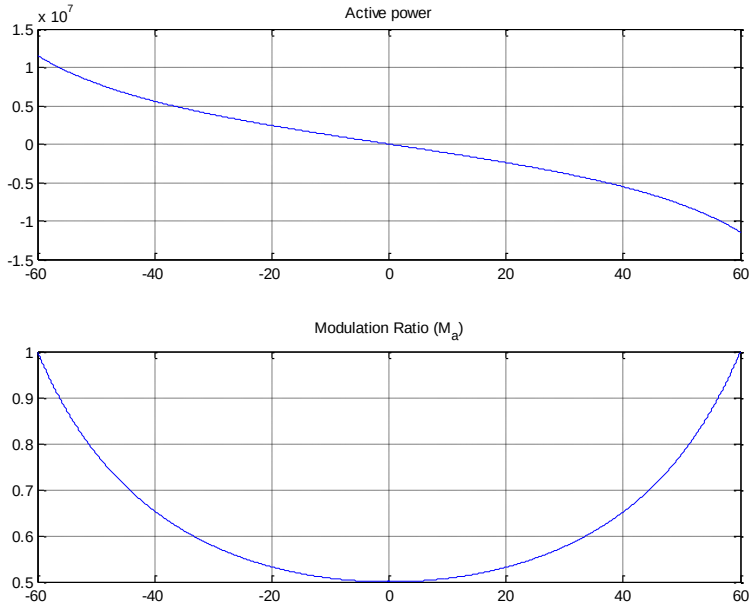

Figure 4-4 - Active Power and modulation ratio over δ angle

It should be noted that this time the plots are limited to the range $-60° \leq \delta \leq +60°$. The reason for this is that as can be seen from the plot of the

modulation ratio at the $\delta = \pm 60°$ the modulation ratio approaches 1.0 which is the limit for an "under-modulated" system (Mohan, et al., 1989). In practice we could use "over-modulation" or lower the Q value used or even increase the DC bus voltage but the behaviour of the modulation ratio would remain the same, that is, $m_a$will increase for a fixed Q output as we vary δ to control the active power flow.

As stated previously, we need to remember that δ does not represent the phase angle between the voltage and current (ϕ) which we commonly use when calculating active power but instead is the phase angle between the STATCOM fundamental and grid voltages.

If we consider the fundamental operation of a single phase STATCOM connected to a network, as represented by the figure below, we can see that the active power flow can be found by considering the phase angle between the inductor current i_L and the grid voltage v_G. In fact we have already seen that power equations can be readily derived for this system in terms of δ. What we have not investigated is the relationship between the well understood effects of ϕ (that is the phase angle between the voltage and current) on active power flow and δ.

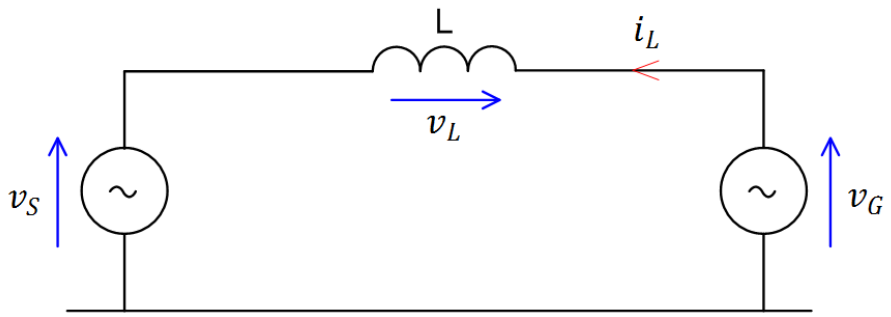

Figure 4-5 - Equivalent STATCOM / Grid connection

In order to investigate the relationship between these two angles we need to express the phase relationship between the inductor current and the grid voltage ϕ in terms of δ.

Alternately we could look at the phase relationship between the inductor current and the fundamental of the STATCOM voltage, however as we have used the grid voltage as our reference using this voltage makes the math a little easier. It will also be shown in the section on STATCOM operation that because in practice the STATCOM output voltage is a series of ±DC voltage pulses a sinusoidal grid voltage is much easier to work with when performing calculations. If we recall that the expression for the inductor current derived earlier (repeated here for convenience).

$$i_L = \frac{1}{\omega L}\left[\left(\hat{V}_S\, cos(\delta) - \hat{V}_G\right) cos(\omega t) - \hat{V}_S\, sin(\delta)\, sin(\omega t)\right]$$

Equation 4-39

was derived using the grid voltage as the reference (that is we let $v_{grid}(t) = \hat{V}_G \sin(\omega t)$) we can write the inductor current in phasor form as:

$$i_L = -\frac{\hat{V}_S}{\omega L} sin(\delta) + j\left\{\left(\frac{\hat{V}_S\, cos(\delta) - \hat{V}_G}{\omega L}\right)\right\}$$

Equation 4-40

From the phasor form of i_L we can readily see that the phase angle between the grid voltage and i_L is given by

$$\phi = \left[\pi - tan^{-1}\left(\frac{\hat{V}_S\, cos(\delta) - \hat{V}_G}{\hat{V}_S\, sin(\delta)}\right)\right] \;\; for \;\; sin(\delta) > 0$$

Equation 4-41

$$\phi = tan^{-1}\left(\frac{\hat{V}_S\, cos(\delta) - \hat{V}_G}{\hat{V}_S\, sin(\delta)}\right) \;\; for \;\; sin(\delta) < 0$$

Equation 4-42

Based on these equations we can see that the inductor current will be in phase with the grid voltage if:

$$\hat{V}_S\, cos(\delta) - \hat{V}_G = 0 \text{ for } sin(\delta) < 0$$

Equation 4-43

$$\Longrightarrow \cos(\delta) = \frac{\hat{V}_G}{\hat{V}_S}$$

Equation 4-44

$$\Longrightarrow \delta = \pm cos^{-1}\left(\frac{\hat{V}_G}{\hat{V}_S}\right)$$

Equation 4-45

Here the negative sign is required for the solution where $\delta < 0$ and the solution is only correct for $-\frac{\pi}{2} \leq \delta \leq 0$. The solution is positive for $\delta > 0$ in the range $0 \leq \delta \leq \frac{\pi}{2}$. It should also be noted that the inductor current will be 180° out of phase with the grid voltage for $\delta = \cos^{-1}\left(\frac{\hat{V}_G}{\hat{V}_S}\right)$.

What is interesting about this result is that the active power flow equation ($P = -\frac{\hat{V}_G \hat{V}_S}{2\omega L}\sin(\delta)$) clearly shows that the maximum power transfer occurs at $\delta = \pm\frac{\pi}{2}$. For $\delta \to \pm\frac{\pi}{2}$ this would require $\left(\frac{\hat{V}_G}{\hat{V}_S}\right) \to 0$ which means that $\hat{V}_G \to 0$ or $\hat{V}_S \to \infty$. As we assume that $\hat{V}_G$ is constant then we are left with $\hat{V}_S \to \infty$ as $\delta \to \pm\frac{\pi}{2}$. But we also know that $\hat{V}_S = m_a \frac{V_d}{2}$ and thus for a fixed DC bus voltage (V_d) this means that $m_a \to \infty$. We saw previously that m_a does increase as δ moves away from 0° but we stopped the simulation to at

$-60° \leq \delta \leq +60°$ to prevent m_a exceeding the value of 1.0. If we are only considering an "under-modulated" system then we know that the maximum value for m_a will be 1.0 so how can we say that $m_a \to \infty$? In fact we cannot, however, if we consider that for a fixed Q output given by

$$Q = -\frac{\hat{V}_G}{2\omega L}\left(\hat{V}_S\, cos(\delta) - \hat{V}_G\right)$$

Equation 4-46

we can see that

$$\left(\hat{V}_S\, cos(\delta) - \hat{V}_G\right) = -\frac{2Q\omega L}{\hat{V}_G}$$

Equation 4-47

and we know that the phase angle between the inductor current and the grid voltage for $\delta < 0$ was given by

$$\phi = tan^{-1}\left(\frac{\hat{V}_S\, cos(\delta) - \hat{V}_G}{\hat{V}_S\, sin(\delta)}\right)$$

Equation 4-48

thus we can express ϕ in terms of Q by

$$\phi = tan^{-1}\left(\frac{-2Q\omega L}{\hat{V}_G \hat{V}_S\, sin(\delta)}\right)$$

Equation 4-49

and if we make the substitution $\hat{V}_S = m_a \frac{V_d}{2}$ we get:

$$\phi = tan^{-1}\left(\frac{-4Q\omega L}{\hat{V}_G m_a V_d\, sin(\delta)}\right) = tan^{-1}\left(\frac{-k}{m_a\, sin(\delta)}\right)$$

Equation 4-50

where $= constant = \frac{4Q\omega L}{\hat{V}_G V_d}$. From this equation we can see that for $\delta \to \pm\frac{\pi}{2}$ and $m_a \to 1$ (which was required to maintain a constant Q output and maximum active power transfer) then $\phi \to \tan^{-1}(-k)$. This result is not really surprising as it tells us that in order to achieve unity power factor we must in fact relax the requirement of fixed Q and let $Q \to 0$. However, it does tell us how close we can get to unity power factor for a given Q output.

What we have not considered in our analysis of P with respect to δ too date is the effect of δ on the magnitude of i_L. Based on the complex form of the inductor current we can readily express the magnitude of i_L as

$$|i_L| = \frac{1}{\omega L}\sqrt{\hat{V}_S^2 sin^2(\delta) + \hat{V}_S^2 cos^2(\delta) - 2\hat{V}_G\hat{V}_S\, cos(\delta) + \hat{V}_G^2}$$

Equation 4-51

$$\Longrightarrow |i_L| = \frac{1}{\omega L}\sqrt{\hat{V}_S^2 - 2\hat{V}_G\hat{V}_S\, cos(\delta) + \hat{V}_G^2}$$

Equation 4-52

It can be seen from this expression that the inductor current magnitude will be a maximum for $\cos(\delta) = -1$ which means that the inductor current peak amplitude will occur at $\delta = \pm\pi$ with a maximum amplitude of

$$|i_L|_{maximum} = \frac{1}{\omega L}\sqrt{\hat{V}_S^2 + 2\hat{V}_G\hat{V}_S + \hat{V}_G^2}$$

Equation 4-53

$$\Longrightarrow |i_L|_{maximum} = \frac{1}{\omega L}\left(\hat{V}_G + \hat{V}_S\right)$$

Equation 4-54

Of course at $\delta = \pm\pi$ the active power will be zero as $\sin(\pm\pi) = 0$ and in practice the system will operate with $\delta < \pm\frac{\pi}{2}$. More importantly, we can see that for δ moving from zero towards $\pm\frac{\pi}{2}$ the magnitude of the inductor current, $|i_L|$, will be increasing (as $2\hat{V}_G\hat{V}_S\cos(\delta)$ will be decreasing in magnitude). A plot of the active power flow, ϕ, the inductor current magnitude and $\cos(\phi)$ for a fixed Q output is shown below over the range $-60° \leq \delta \leq +60°$ (that is $m_a \leq 1$).

We will see in the section on STATCOM operation that there is a calculable limit value for δ to keep $m_a \leq 1$ which will define the maximum active power flow.

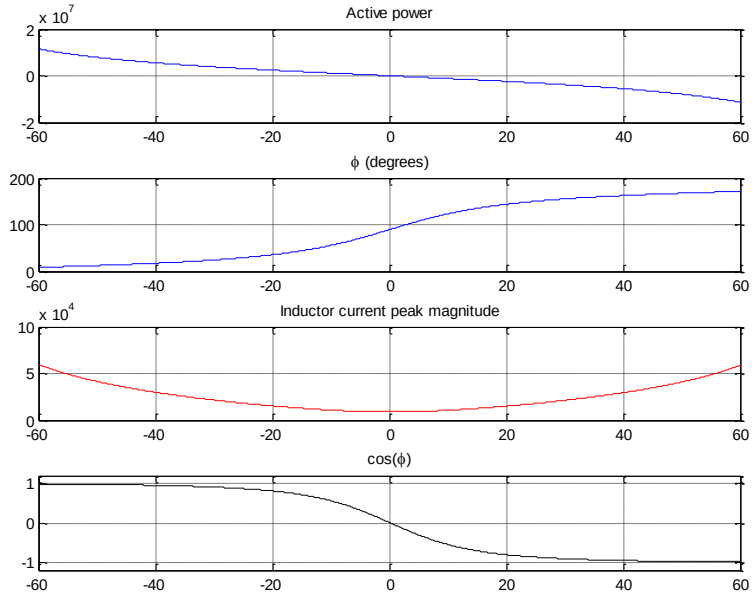

Figure 4-6 - $60° \leq \delta \leq -60°$ - Analysis

The reason for plotting $\cos(\phi)$ is that it directly relates to the active power magnitude through the well-known expression $P = VIcos(\phi)$.

These plots show that for $\delta = 0 \rightarrow -60°$ the phase shift between the inductor current and grid voltage falls from +90° toward 0° (or unity power factor). On the other hand for $\delta = 0 \rightarrow +60°$ the phase shift between the inductor current and grid voltage grows from +90° towards 180° (or unity power factor for reverse power flow). The fact that we have increasing current amplitude and tend towards $\pm$ unity power factor aligns fully with the active power equation derived earlier.

It should be noted that for a STATCOM acting as a reactive power support device we would only expect the phase angle δ to be adjusted by a small amount to compensate for losses to maintain the DC bus voltage. This means that in general the STATCOM will operate with a δ value close to zero. Looking at the active and reactive power equations

$$P = -\frac{\hat{V}_G \hat{V}_S}{2\omega L} sin(\delta)$$

Equation 4-55

and

$$Q = -\frac{\hat{V}_G}{2\omega L}\left(\hat{V}_S\, cos(\delta) - \hat{V}_G\right)$$

Equation 4-56

we can also see that for small changes in δ around zero we will have a greater rate of change in P that in Q due to the fact that *sine* has its peak slope at zero degrees whereas the slope of *cosine* is equal to zero at zero degrees.

In summarising this theoretical analysis it is important to realise that once we make the simplifying assumption that the STATCOM voltage (v_S) is sinusoidal then the apparent power flow question becomes quite simple and is defined by

$$S = VI^* = P + jQ$$

Equation 4-57

Thus if we fix Q and V (the grid voltage) and we want to adjust P we must adjust the phase angle (with respect to the fixed grid voltage) and magnitude of the inductor current. This can be readily seen from the simple sketch below.

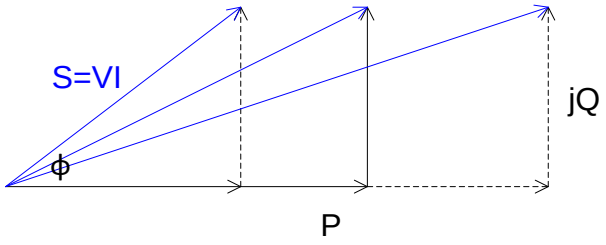

Figure 4-7 - Changes in ϕ and its effects in P

While this very simple analysis is completely correct what it does not explain is that within the STATCOM control system the simple "adjustment" to i_L to change P must be achieved through a change in phase angle between the grid voltage and the STATCOM fundamental voltage (δ) as well as the modulation ratio (m_a). In addition to this we need to understand the relationship between the δ and ϕ. Fortunately, this can be explained by equating our STATCOM active power equation with the well-known active power equation as follows;

$$P = -\frac{\hat{V}_G \hat{V}_S}{2\omega L} sin(\delta) = V_G I_L cos(\phi)$$

Equation 4-58

Here we can see that as $\sin(\delta) \to \pm 1$ we must have $\cos(\phi) \to 1$ or as $\delta \to \pm\frac{\pi}{2}$ we must have $\phi \to 0$. This is in essence what we found above but does not fully define how this is achieved within the STATCOM or any limits that might exist.

For completeness we should also acknowledge that the power flow analysis for the STATCOM is directly comparable to that of a generator. That is, we can consider the STATCOM as a generator capable of supplying and absorbing both active and reactive power from the grid. Based on this approach we can develop a capability diagram as shown below.

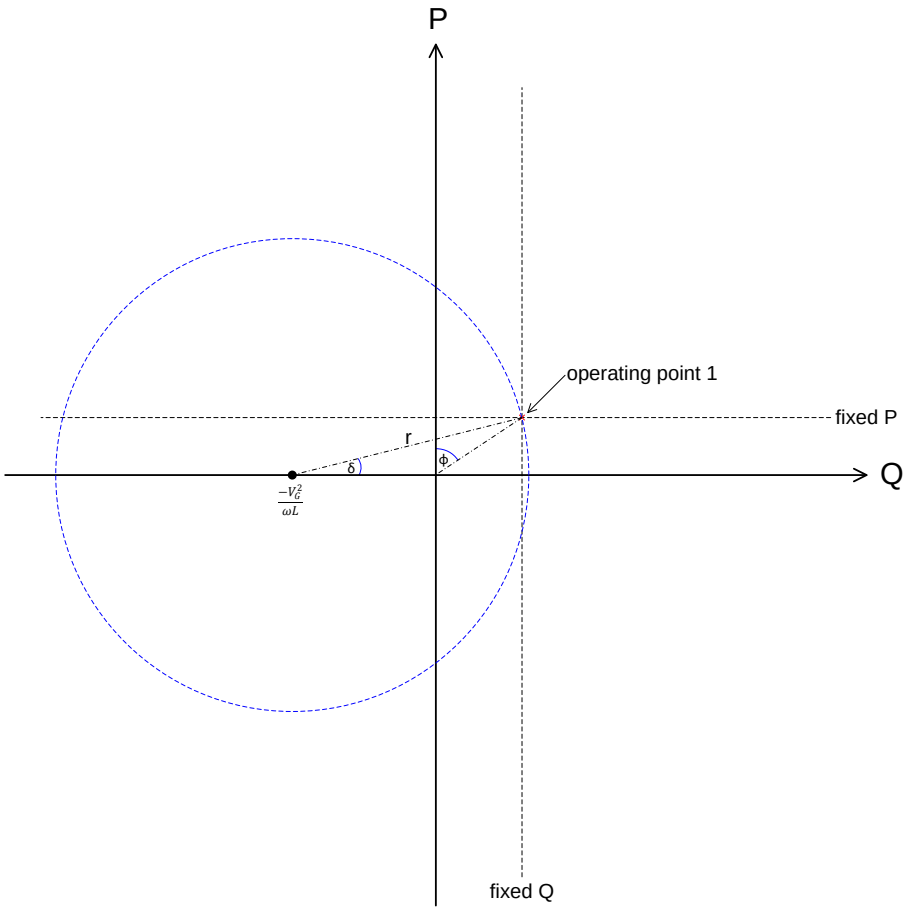

Figure 4-8 - STATCOM capability curve

To produce this capability diagram we define Q an P on the grid side which means that for $Q > 0$ this represents the injection of reactive power into the

grid (or a capacitive load) and similarly for $P > 0$ this represents an injection of active power into the grid (from the STATCOM). As shown the centre of the circle lies at $\left(-\frac{V_G^2}{\omega L}, 0\right)$ with a radius of $r = \frac{V_G V_S}{\omega L} = m_a \frac{V_G V_d}{2\omega L}$ which is defined by the operating point of the STATCOM. If we consider the behaviour of this diagram as we move along the fixed Q line to change our value of P we can see exactly the same results as we concluded from the above analysis. We could also show the operating limits on this diagram, for example $|\delta| < \pm\frac{\pi}{2}$ and $r \leq \frac{V_G V_d}{2\omega L}$ so that $m_a \leq 1$.

Note - The operating circle is defined from the STATCOM P and Q equations and the general form of a circle which for the chosen axes is:

$$(Q - h)^2 + (P - k)^2 = r^2$$

Equation 4-59

Which has a centre of (h, k) and radius r. From the STATCOM P and Q equations (note that these are the active and reactive power delivered from the STATCOM to the grid and thus are the negatives of those derived above)

$$P = \frac{\hat{V}_G \hat{V}_S}{2\omega L} sin(\delta)$$

Equation 4-60

$$\Longrightarrow P = \frac{V_G V_S}{\omega L} sin(\delta)$$

Equation 4-61

and

$$Q = \frac{\hat{V}_G}{2\omega L}\left(\hat{V}_S\, cos(\delta) - \hat{V}_G\right)$$

Equation 4-62

$$\Longrightarrow Q = \frac{\hat{V}_G \hat{V}_S}{2\omega L} cos(\delta) - \frac{\hat{V}_G^2}{2\omega L}$$

Equation 4-63

By inspection we can see that the circle will have a centre of $\left(-\frac{V_G^2}{\omega L}, 0\right)$ and thus if we substitute our expressions for Q and P into the general form of the circle equation we get;

$$(Q + \frac{V_G^2}{\omega L})^2 + (P - 0)^2 = r^2$$

Equation 4-64

$$\Longrightarrow r^2 = \left(\frac{V_G V_S}{\omega L} cos(\delta) - \frac{V_G^2}{\omega L} + \frac{V_G^2}{\omega L}\right)^2 + \left(\frac{V_G V_S}{\omega L} sin(\delta)\right)^2$$

Equation 4-65

$$\Longrightarrow r^2 = \left(\frac{V_G V_S}{\omega L} cos(\delta)\right)^2 + \left(\frac{V_G V_S}{\omega L} sin(\delta)\right)^2$$

Equation 4-66

$$\Longrightarrow r^2 = \left(\frac{V_G V_S}{\omega L}\right)^2 (cos^2(\delta) + sin^2(\delta))$$

Equation 4-67

$$\Longrightarrow r = \frac{V_G V_S}{\omega L}$$

Equation 4-68

The angle ϕ comes from

$$S = VI^* = P + jQ = |V||I|\angle\phi$$

Equation 4-69

that is

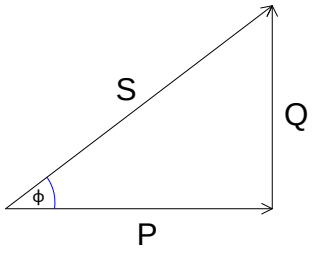

Figure 4-9 - The classical Power Triangle

Now that we have a sound understanding of the active power flow control for the STATCOM we can use this equation to predict the change in the DC bus capacitor voltage. If we call that the definition of active power is based on the rate of doing work = joules/second, then we can see that

$$change\ in\ energy = P \times \Delta t$$

Equation 4-70

That is, if we have a constant power P flowing into a capacitor for a time Δt then this will result in a change in the energy stored by the capacitor which

is equal to $P \times \Delta t$. Alternately this can be expressed mathematically as follows:

$$E = \int_{t1}^{t2} p\, dt$$

Equation 4-71

where E is the total energy transferred over the time interval from t_1 to t_2 and $p = p(t) = v(t)i(t)$ = instantaneous power transferred at any time over the time interval from t1 to t2. If we assume that $p = constant = P$ over the time interval then we get

$$\Delta E = \int_{t1}^{t2} P\, dt = P(t2 - t1) = P \times \Delta t$$

Equation 4-72

We also know that energy stored in a capacitor is given by

$$E_{cap} = \frac{1}{2} CV^2$$

Equation 4-73

and thus if we define V_1 as our initial voltage at time t and V_2 as our voltage at time $(t + \Delta t)$ then we can write

$$\frac{1}{2} CV_2^2 - \frac{1}{2} CV_1^2 = P \times \Delta t$$

Equation 4-74

$$\Longrightarrow (V_2^2 - V_1^2) = \frac{2P \times \Delta t}{C}$$

Equation 4-75

In our case it is the change in voltage ΔV we want to find and thus we rewrite V_2 as:

$$V_2 = (V_1 + \Delta V)$$

Equation 4-76

$$\Longrightarrow V_2^2 = V_1^2 + 2V_1\Delta V + (\Delta V)^2$$

Equation 4-77

Substituting into our previous equation gives us

$$2V_1\Delta V + (\Delta V)^2 = \frac{2P \times \Delta t}{C}$$

Equation 4-78

$$\Longrightarrow (\Delta V)^2 + 2V_1\Delta V - \frac{2P \times \Delta t}{C} = 0$$

Equation 4-79

$$\Longrightarrow \Delta V = \frac{-2V_1 \pm \sqrt{4V_1^2 + 4\frac{2P \times \Delta t}{C}}}{2}$$

Equation 4-80

$$\Longrightarrow \Delta V = -V_1 \pm \sqrt{V_1^2 + \frac{2P \times \Delta t}{C}}$$

Equation 4-81

From this equation we can see that the solution will only be practical for

$$\Delta V = -V_1 + \sqrt{V_1^2 + \frac{2P \times \Delta t}{C}}$$

Equation 4-82

where the change in voltage will be positive for P flowing into the converter and negative for P flowing out of the converter. The reason that the other solution cannot be valid is that it would give a change in voltage magnitude of greater than the initial bus voltage which is not practical around the operating point.

Note that P is in fact the average power over one cycle, that is

$$P = \frac{1}{T}\int_0^T v(t)i(t)dt$$

Equation 4-83

We can consider P as the "instantaneous average" in that it represents the instantaneous active power averaged over one cycle. This means that in effect the term instantaneous is not in time but over a cycle. The consequence of this is that technical when we say above that "P is constant over the time interval Δt" this time interval must be an integer multiple of the period T.

It is also clear from Equation 4-1 and Equation 4-2 that both P and Q can be controlled by adjusting the values of V_S and δ, but whilst Equation 4-1 and Equation 4-2 clearly provide a way of calculating the resultant active and reactive power flow in/out of the D-VAR® they do not show how the 480V system side voltage is used to maintain a 840V DC bus voltage.

In order to understand how this is achieved a single phase SimPowerSystems® MATLAB model of the STATCOM will be used.

This model will help to understand how the IGBT switching strategy simultaneously builds the DC bus voltage as well as generates the inverter AC output. Once verified this model can also be used to assess the effects of a system transient in the DC bus.

4.3 SINGLE PHASE STATCOM SWITCHING

To explain the basic principles of operation of the STATCOM we now consider the following simplified single phase circuit.

In Figure 4-10 the inductor current i_L is shown as positive when flowing from the STATCOM to the network and the capacitor currents i_{C1} and i_{C2} are shown as positive when they flow such that they cause their respective capacitances to charge.

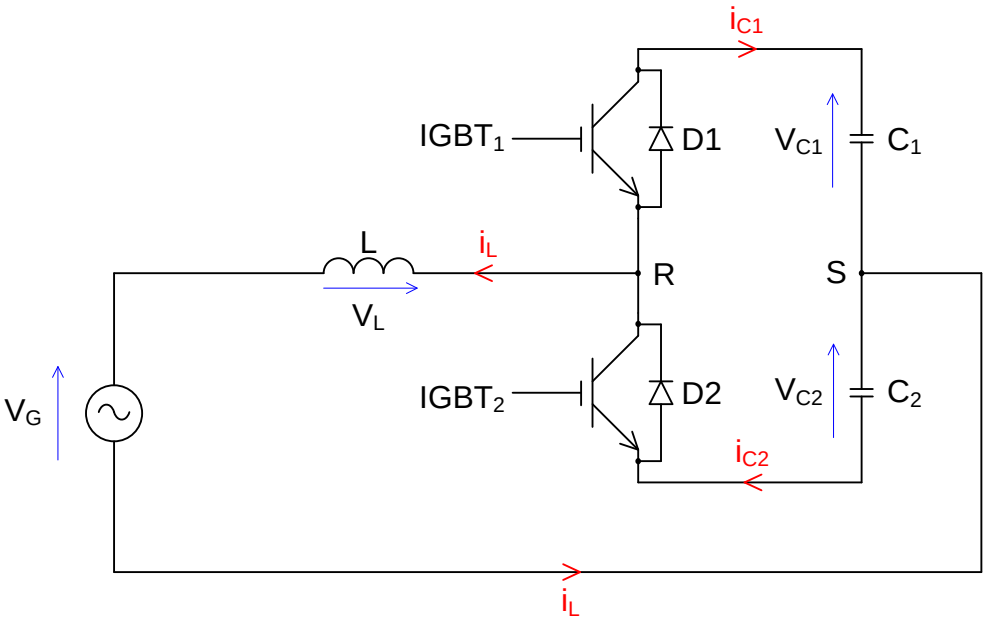

Figure 4-10 - Simplified single phase STATCOM

In this instance the convention for the inductor current has been chosen to provide a different perspective when considering the derived power flow equations between the network and the STATCOM.

For $i_L < 0$ (that is the current is flowing into the STATCOM)

- When IGBT1 is 'on' the current i_L cannot flow in IGBT1 as it is a reverse biased. Based on the gate firing strategy when IGBT1 is 'on' then IGBT2 must be in the 'off' state. This means that for $i_L < 0$ the inductor current must flow in D1 which causes C1 to charge.

It should also be noted that when IGBT1 is in the 'on' state this means that point R is connected to the positive DC rail and thus diode D2 will become reverse biased which makes $i_{C2} = 0$.

- When IGBT1 is switched 'off' then IGBT2 will be switched 'on'. This will cause D1 to become reverse biased (as point R will now be connected to the negative DC rail) and thus the current i_L will flow in IGBT2 to discharge C2. (Diode D2 is reverse biased as the current is attempting to flow from R to S.)

For $i_L > 0$ (that is the current is flowing out of the STATCOM) –

- When IGBT1 is switched ‘on’ then IGBT2 will be switched ‘off’ and diode D2 will be reverse biased (point R is now connected to the positive DC rail). This means that the current i_L will flow in IGBT1 to discharge C1.

- When IGBT1 is switched ‘off’ then IGBT2 will be switched ‘on’ which causes diode D1 to become reverse biased and diode D2 to become forward biased (note that i_{C2} cannot flow in IGBT2 as this is reverse polarity). This means that current i_L flows in diode D2 to charge C2.

Based on the principle of operation described it can be clearly seen that the DC capacitors (C1 and C2) are changed by current flowing in their respective diodes and discharged by the conduction of their corresponding IGBTs.

Based on the above mentioned operation modes, the model was run and the appropriate solution compared to provide clarification and validation of the theory of operation.

Figure 4-11 shows the current directions in and out of the STATCOM at any given instant within a complete power system cycle (20 ms).

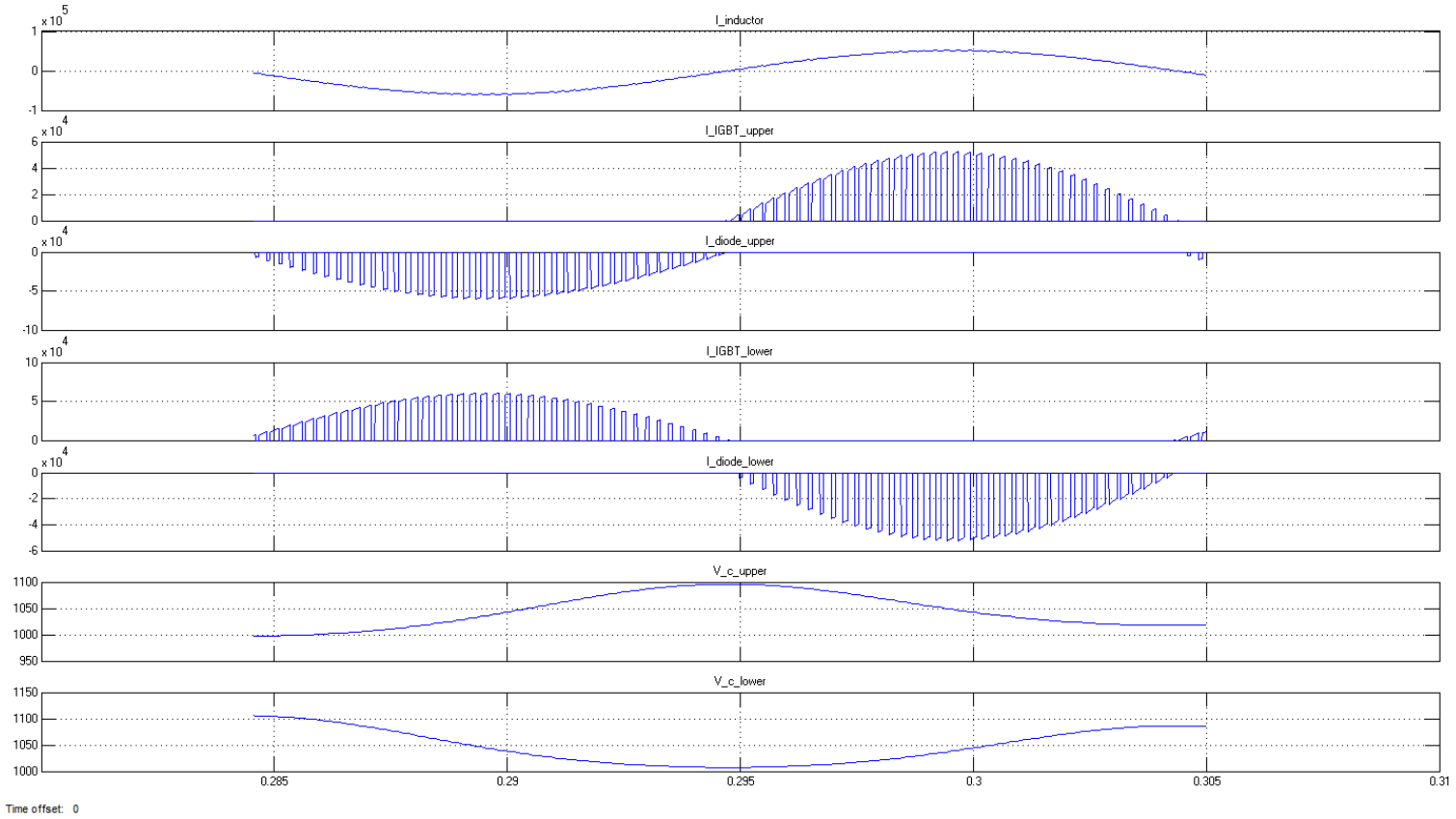

Figure 4-11 - STATCOM current firing over one cycle (over 1 cycle / 20 ms)

So, considering a STATCOM operating to provide reactive power support only (that is 2-quadrant operation) and if we can neglect all losses then we know that over a power system cycle the net power transfer is zero.

Based on the above operating principles for the STATCOM, in order to increase the DC bus voltage (or capacitor charge) for a fixed reactive power output at least one or more of the following would need to occur;

- The conduction time of the diodes must be increased – for a fixed switching strategy the diode conduction time is fixed by the IGBT switching times. That is, for a fixed modulation ratio, carrier and modulating signals the switching times will not change. It is important to remember here that for a STATCOM operating only in 2 quadrants (that is for reactive power support only) at steady state the modulating signal will be phase locked with the system volts with only small phase deviations to compensate for the system losses (in general the losses will be managed by the control system through the management of the DC bus voltage).

- Even if we consider the case where it is the grid voltage phase angle was shifted then we would also need to adjust the modulation index to maintain a fixed Q output.

- The current magnitude during the diode conduction time was increased – based on the theoretical analysis performed this is likely as we see an increase in the inductor current due to a phase shift.

- Reduce the capacitor discharge time – is this possible if we assume a constant reactive power output from the STATCOM?

- Reduce the current magnitude during capacitor discharge - is this possible if we assume a constant reactive power output from the STATCOM?

4.4 STATCOM CURRENT

The inductor current for a half bridge synchronous PWM converter can be approximated as follows;

To calculate the inductor current, we first need to consider the inductor voltage over an individual switching period. If we assume that the DC bus voltage is constant, then the voltage across the inductor at any instant in time is given by;

$$v_L(t) = \pm\frac{V_d}{2} - v_G(t)$$

Equation 4-84

This is shown in the Figure 4-12 where the STATCOM voltage = $V_s = +\frac{V_d}{2}$ when Sw+ is closed (Sw- open) and $V_s = -\frac{V_d}{2}$ when Sw- is closed (Sw+ open). It should be noted that based on a PWM switching strategy there will always be one and only one of the switches closed at any instant in time.

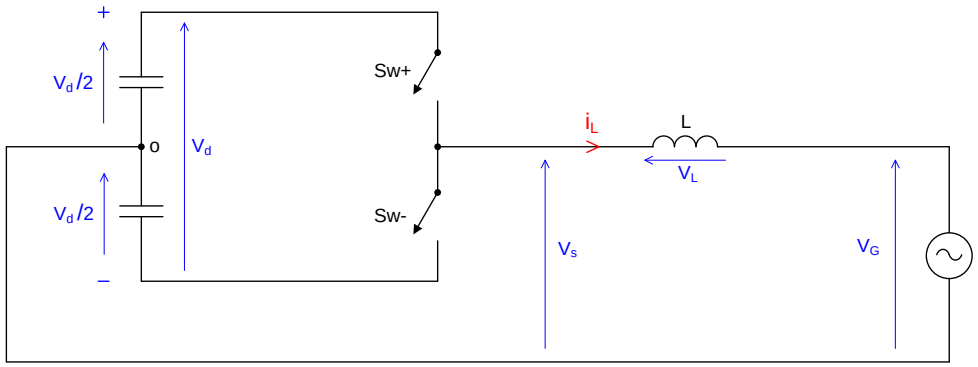

Figure 4-12 - Simplified STATCOM device connected to grid

Representations of the control and voltage waveforms for a single phase half bridge PWM converter are shown below. Here we can see the sinusoidal modulation signal (V_{mod}) and the triangular carrier signal (V_{car}). The gate switching strategy for this scheme is given by;

If $V_{mod} \geq V_{car}$ then:

$$V_S = +\frac{V_d}{2}\ (close\ Sw+)$$

Equation 4-85

If $V_{mod} < V_{car}$ then :

$$V_S = -\frac{V_d}{2}\ (close\ Sw-)$$

Equation 4-86

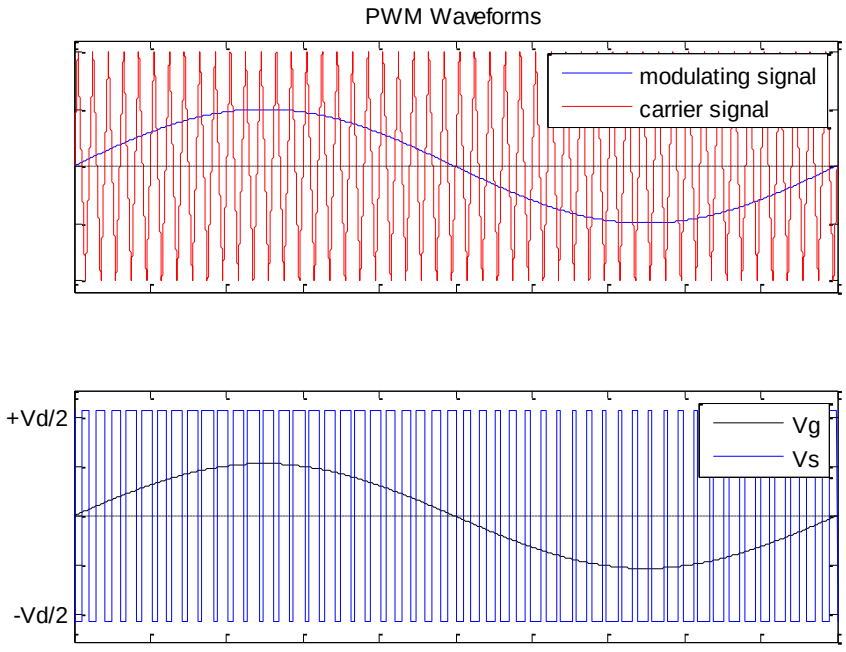

Figure 4-13 - PWM waveform

Given that we now have a simple equation for $v_L(t)$ we can find the inductor current using;

$$i_L = \frac{1}{L}\int v_L(t)\,dt = \frac{1}{L}\int \left\{\pm\frac{V_d}{2} - v_G(t)\right\} dt$$

Equation 4-87

The challenge we face in performing this integration is that while $v_G(t)$ is a simple sinusoid the fact that we are alternately switching between $\pm\frac{V_d}{2}$ means that we have a switched DC component with a time varying sinusoid.

We can however make the simplifying assumption that $v_G(t)$ = average voltage over the switch period (that is over the time interval in which a switch is closed). This approximation is reasonable provided that the frequency of the carrier signal is much greater than that of the modulating signal (in the limit $f_{carrier} \longrightarrow \infty$ this would no longer be an approximation).

In practice the inductor current may contain a steady state and a transient component due to the initial starting conditions. However, if we assume that we are operating under steady state conditions where all transients have decayed to zero then we can say that the inductor current will be fundamentally sinusoidal with no DC offset. This statement is justified based on the following facts:

- The system will in reality contain a resistive component which will cause any initial starting transients to decay to zero in time
- The grid side voltage is fundamentally sinusoidal
- The converter DC bus voltage can be considered constant for the system operating under steady state conditions
- The PWM inverter output voltage under steady state conditions can be considered to be a sinusoid at the system frequency plus higher frequency harmonics due to the power electronic switching

- The control system will act to remove any DC offset in the current or voltage output of the converter. Given that we are operating under steady state conditions then the control system will be able to achieve this target.

If we denote this constant average grid voltage over a switch period as $\tilde{V}_G$ then the inductor current over that period is given by;

$$i_L = \frac{1}{L}\int \left(\pm\frac{V_d}{2} - \tilde{V}_G\right) dt = \frac{1}{L}\left(\pm\frac{V_d}{2} - \tilde{V}_G\right)t + C$$

Equation 4-88

This equation shows that the inductor current will be composed of a series of piecewise linear ramps with positive slope when Sw+ is closed and negative slope when Sw- is closed. The integration constant (C) in this equation must be found using an initial condition for i_L. As the inductor current at steady state will be symmetric about the time axis then there should be no DC offset in the waveform over one period of grid voltage and this can be used to determine the value of C.

The derivation of the inductor current with a phase shift is as follows;

$$v_L(t) = \hat{V}_S \sin(\omega t \pm \phi) - \hat{V}_G \sin(\omega t)$$

Equation 4-89

$$\Longrightarrow v_L(t) = \hat{V}_S \sin(\omega t)\cos(\phi) \pm \hat{V}_S \cos(\omega t)\sin(\phi) - \hat{V}_G \sin(\omega t)$$

Equation 4-90

$$\Longrightarrow v_L(t) = \left(\hat{V}_S \cos(\phi) - \hat{V}_G\right)\sin(\omega t) \pm \hat{V}_S \sin(\phi)\cos(\omega t)$$

Equation 4-91

It is well know that $\int_0^T \sin(\omega t)\,dt = \int_0^T \cos(\omega t)\,dt = 0$ and thus $\int_0^T v_L dt = 0$. As the inductor current and voltage are directly related through

$$v_L = L\frac{di_L}{dt}$$

Equation 4-92

the inductor current can be written using

$$i_L = \frac{1}{L}\int v_L\,dt$$

Equation 4-93

$$\Longrightarrow i_L = \frac{1}{\omega L}\left[\left(\hat{V}_G - \hat{V}_S\cos(\phi)\right)\cos(\omega t) \pm \hat{V}_S\sin(\phi)\sin(\omega t)\right] + C$$

Equation 4-94

$$\Longrightarrow \frac{1}{T}\int_0^T i_L\,dt = C$$

Equation 4-95

where C is the constant of integration which would represent the DC offset in the inductor current. Generally the value for C would be found using an initial condition for $i_L$but we know that the inductor current will in general not have any DC offset or $\int_0^T i_L dt = 0$.

As shown previously, the inductor current can in fact be approximated as a series piecewise linear ramps. This approximation came from the simplification that the grid voltage can be assumed constant over the switch

period. This means that the inductor current cannot in fact be truly represented as a singular sinusoidal signal.

Whilst this is true we can still use the above arguments for the inductor current and voltage. The reason that these arguments hold true is that we could consider out waveforms as a Fourier series as we know that they are periodic functions (that is $f(t) \equiv f(t+T)$ where T is the period of the waveform). Thus we can represent our waveforms using the classic Fourier series form;

$$f(t) = a_0 + \sum_{k=1}^{\infty} [a_k \cos(k\omega_0 t) + b_k \sin(k\omega_0 t)]$$

Equation 4-96

As this form is in fact just the sum of *sine* and *cosine* terms it can be readily seen that $\frac{1}{T}\int_0^T f(t)dt = a_0$ which is the same result as we found previously for a purely sinusoidal waveform.

Note – even if relaxed the assumption of constant grid voltage over the switch period we would still get a series of piecewise almost linear ramps. To be absolutely correct the piecewise ramps would be curved with the curvature given by the sinusoidal component of the grid voltage. In any case the above discussion would still hold true. Simulation were performed using both methods with no appreciable difference found – it should be noted that the simulation itself is discrete in that calculations are performed at discrete time steps which also introduce error as averaging is required over these periods.

From a purely mathematical perspective, we can associate this error with integration by using trapezoidal method / rule, which is a form of integration by parts, error and the results of the simulation show that this error will be somewhat insignificant for this approximation.

For the purposes of this discussion and analysis we will assume a synchronous switching strategy based on symmetrical modulating and carrier signals where the frequency modulation ratio ($m_f = \frac{f_s}{f_1}$) is an integer value. There has been much research performed on the effects of non-synchronous switching (Gharedaghi, et al., 2011), however, these will not be covered nor discussed further here.

Any DC offset generated in the converter output should be minimised by the control system to avoid distortion in the system voltage. It can be shown that for a single phase half bridge converter that non-symmetry in the inductor current (that is due to DC offset) the two DC capacitors which form the DC bus will become unevenly charged which results in a DC offset in the converter output voltage.

Ideally DC offset should be eliminated, as described by (Ahfock & Bowtel, 2006), as injection of excessive DC signal into AC networks leads to corrosion in underground equipment, transformer saturation and magnetisation current distortion, metering errors and malfunction of protective devices. For these reasons, Australian Standards such as AS4777.2-2015 (section 5.9) sets limits for the amount of injected DC current into the AC network by inverter systems.

Note that it is a requirement form for correct converter operation that $\left|\frac{V_d}{2}\right| > \left|\tilde{V}_G\right|$ at any instant in time. It is also assumed that the DC bus voltage remains constant which may not be instantaneously true at all times in practice.

Having calculated the inductor current, we can calculate the instantaneous power flow to/from the converter. This calculation can be performed on either side of the current steering reactor using the well-known equation for instantaneous power;

$$p(t) = v_{grid}(t) \times i_{inductor}(t)$$

Equation 4-97

$$p(t) = v_{STATCOM}(t) \times i_{inductor}(t)$$

Equation 4-98

It should be noted that while these two equations will not give the same instantaneous values they will have the same value when averaged over one period of the grid voltage.

Note that this is a theoretical estimate only as in practice the DC bus voltage will not be fixed over the period of a cycle. The MATLAB and SimPowerSystems models allow us to see the ripple in the DC bus voltage.

What the theoretical prediction allows us to do is to provide a qualitative explanation of the active power flow when a phase shift between the grid voltage and the fundamental of the converter output voltage is introduced.

5 MATHEMATICAL MODEL

5.1 STATCOM MODEL

A single phase SimPowerSystems model was built to validate the results reached by the initial theoretical assessment and on the operational characteristics of the STATCOM. The D-VAR® STATCOM is comprised of a half bridge inverter and this forms the base to the single phase model developed.

Gaining an understanding on a single phase STATCOM equivalent will ease any future assessment of operational characteristics of a complete 3 phase STATCOM system as this is the focus of some future investigation.

The complete STATCOM model developed can be seen Figure 5-1.

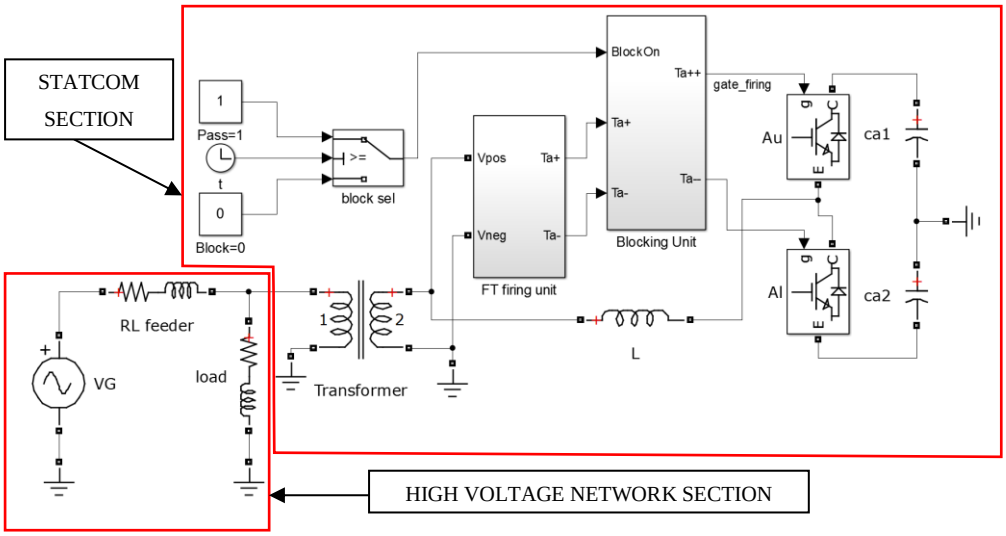

Figure 5-1 - Single phase STATCOM model

Both portions of the above MATLAB model are explained in detail below as to provide a comprehensive understanding on the reasoning to the final model configuration.

5.1.1 HIGH VOLTAGE NETWORK SECTION

The High Voltage Network portion of the model is represented by three separate elements which are equivalent representation of the network.

This model uses an infinite voltage source, a RL (resistive and inductive) feeder and a load.

- V_G is an infinite Voltage Source and represents the Thevenin equivalent voltage source of the whole network that interfaces with the STATCOM

- *RL feeder* represents the Thevenin equivalent source impedance

- *load* is the actual load which the STATCOM is to supply Reactive Power to during the simulation

The three above described devices in this model form the network portion of the MATLAB model and provide known values of Voltage, and impedances which assist in the analysis of the operation of the STATCOM during simulation.

5.1.2 STATCOM SECTION

The STATCOM portion of the model consists of a number of devices that essentially represent basic aspects of a STATCOM. It is stressed that this is only a representation of the power electronic devices within a STATCOM, as any analysis and implementation of a control system affiliated with the STATCOM is beyond the scope of the project.

The model STATCOM constructed for this project contains the following devices / blocks:

- *Blocking Signal switch*; this switch is the trigger to the blocking signal of the STATCOM

- *Blocking unit*; is the unit responsible for blocking the operation of the STATCOM for a set time, aiding the analysis of the results after the simulation period lapses

- *FT firing unit*; this unit is responsible the firing pulses for the IGBT switching within the STATCOM model

- *Transformer*; this device is responsible for the interface of the STATCOM system Voltage $(480V_{ac})$ with Network Voltage level of the substation under study, which in this case is $\frac{33kV}{\sqrt{3}}$ or $19.05kV$ (phase to ground)

- *L* is the steering current reactor within the STATCOM and its functionality can be described as to smooth the output waveform of the STATCOM

- *Insulated-Gate Bipolar Transistors (IGBTs)*; functions as the actual electronic switch of the inverter

- *Capacitors*; these devices are the main component of the DC bus in the STATCOM

More detailed explanation of key devices within this model is provided below:

5.1.2.1MATLAB MODEL BLOCKING UNIT

The blocking unit used in this model is responsible for relaying the firing unit's signal from the firing unit to the IGBT switches in the STATCOM.

This unit is also responsible for blocking the firing signal from initialising the operation of the STATCOM before the allocated blocking time has elapsed.

The main reason for the blocking unit to be of such important within this model is that it provides us the ability to "wait" until the firing unit is ready to operate and this depends on the Discrete Fourier Transform (DFT) block contained within the firing unit itself.

This initial delay within the firing unit is of 20 ms, but for convenience the blocking signal has an added 20 ms (making it a 40 ms block in total), as to provide easy on a pre and post STATCOM operation analysis.

A view of the internal function blocks within the blocking unit is depicted Figure 5-2.

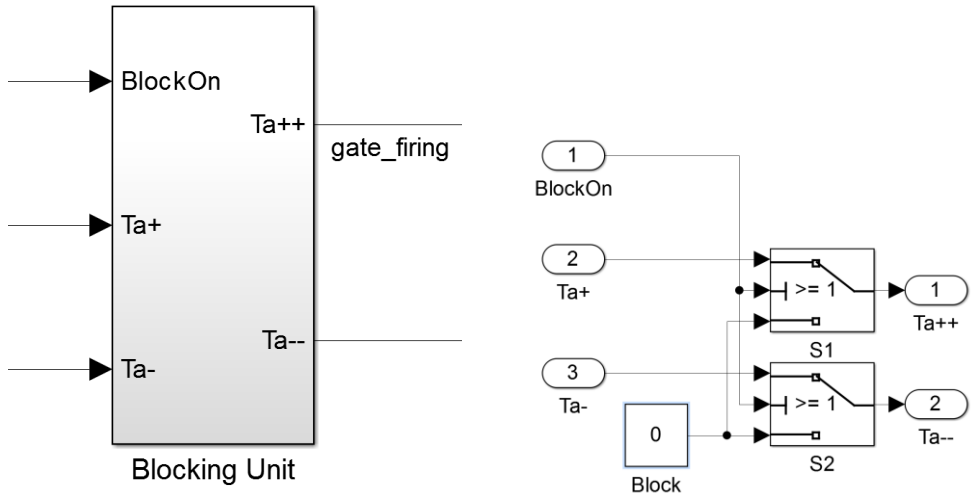

Figure 5-2 - MATLAB model Blocking unit and its internal configuration

We can also see Figure 5-3 the blocking unit output wave form for the first 60 ms of the simulation, which include a 40 ms firing block and 20 ms depicting a $50Hz$ cycle period of firing.

Figure 5-3 - Blocking unit output waveform for the initial 60 ms of simulation

5.1.2.2MATLAB MODEL FIRING UNIT

In this MATLAB model the firing unit (FT firing unit) is responsible for generating the switching / firing pulses for the correct IGBT, ensuring correct converter operation.

At its first stages it samples the input voltage from the secondary side of the transformer $480V_{ac}$, and uses its phase information to generate the modulating signal for the PWM output. The modulation ratio (maGainA) is then applied to this signal which is used to switch each IGBTs on and off as required by comparing it to the carrier signal (Vtriangle block), as seen in Figure 5-4.

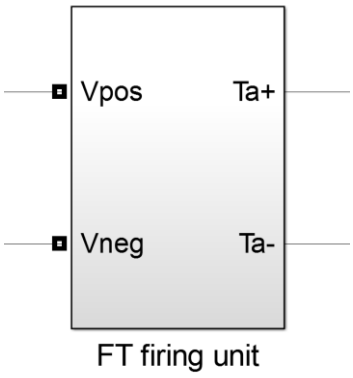

Figure 5-4 - STATCOM model firing unit

The below figure shows the internal function blocks within the firing block.

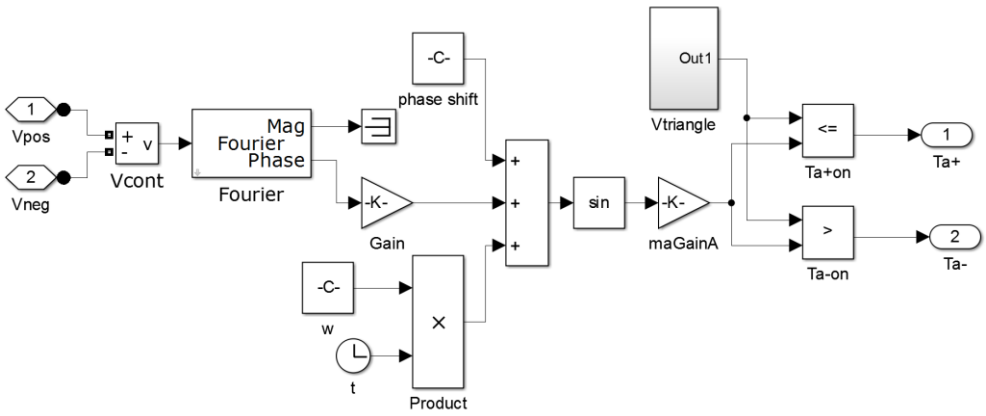

Figure 5-5 - STATCOM model firing block internal functionality

The output waveform generated by the firing unit can be seen in Figure 5-6.

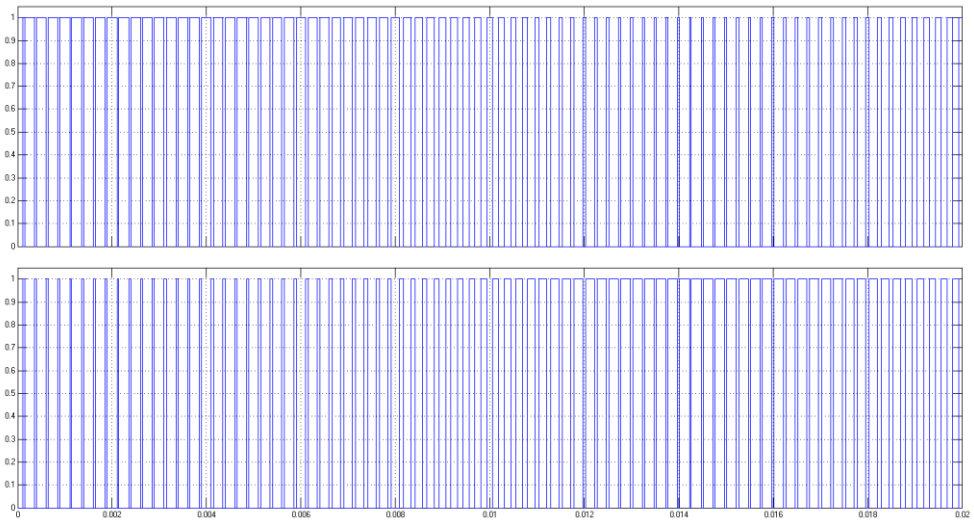

Figure 5-6 - Firing unit output waveform over one fundamental frequency cycle (20 ms)

Whilst the STATCOM model was developed using limited information provided by AMSC, a triangular waveform generator block was also constructed to provide full flexibility in the simulation process and the internal devices used within this block (Vtriangle) is depicted Figure 5-7.

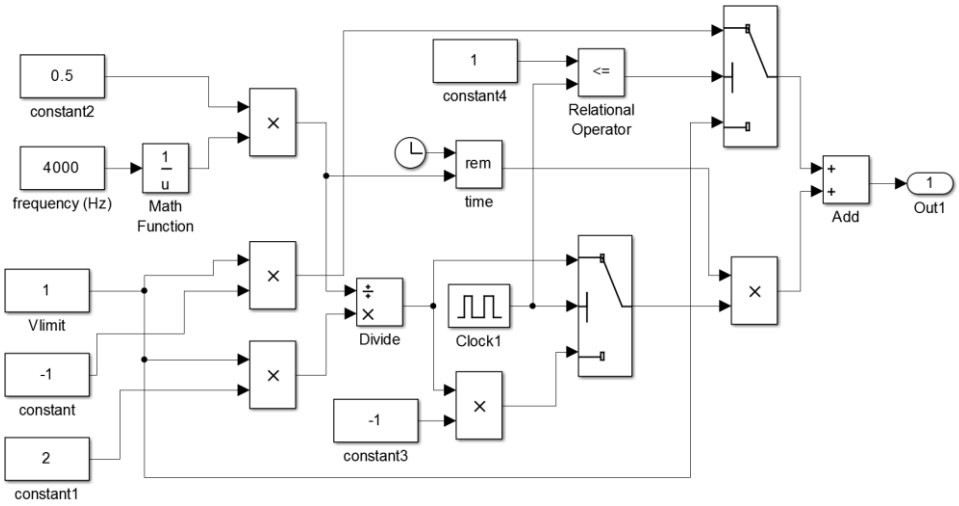

Figure 5-7 - Vtriangle block (within firing block)

The above mentioned block generates the $4kHz$ triangular carrier signal used for pulse width modulate the output of the converter and its waveform output can be seen in Figure 5-8.

Figure 5-8 - Vtriangle block output waveform (over 20 ms)

For convenience a zoomed in view of the Figure 5-8 waveform is depicted in Figure 5-9 over a 2ms period (zoomed).

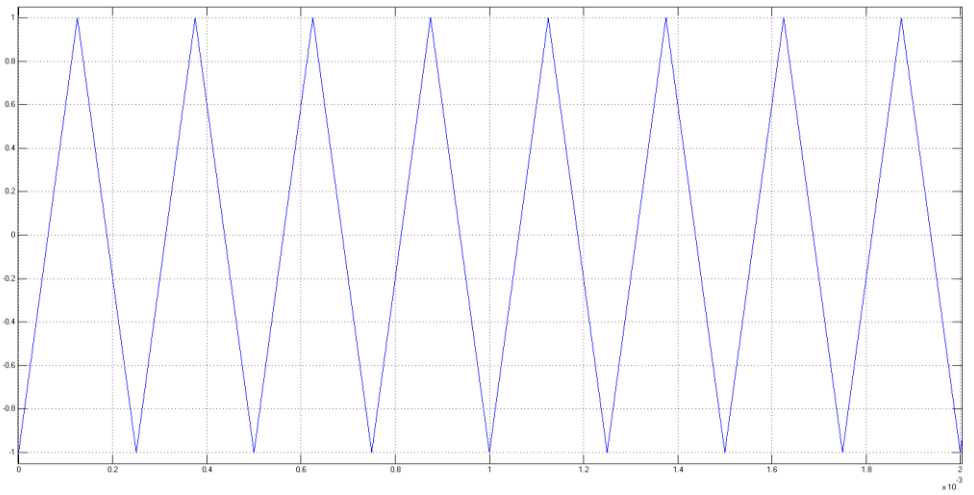

Figure 5-9 - Vtriangle block output waveform (over 2 ms)

5.2 STATCOM INDUCTOR CURRENT AND POWER FLOW SIMULATION

The code uses a discrete time step approximation for all waveforms. We start by generating the modulating and carrier waveforms. For the modulating waveform the calculation is simple as all we need is a vector of values which represent a sinusoidal waveform at the defined time steps. For

the carrier signal we need to generate a triangular waveform with the desired carrier frequency $\left(\mathrm{f}_{\mathrm{carrier}} \gg \mathrm{f}_{\mathrm{modulating}}\right)$.

The carrier signal has been generated using the following approach:

- Start at time $t = 0$ (note that we have also chosen the grid voltage as $\hat{V}_{grid} sin(\omega t)$) and ramp to the peak value.

- Once the peak value has been reached ramp with an equal magnitude but opposite sign slope to the opposite side peak magnitude. This strategy is repeated until we reach the end of the simulation period. The slope of the piecewise linear waveform can be calculated using;

$$T_{carrier(ms)} = \frac{1}{f_{carrier}}$$

Equation 5-1

$$\frac{\Delta V}{\Delta t} = \frac{2 \times V_{peak}}{\frac{T_{carrier}}{2}} = \frac{4 \times V_{peak}}{T_{carrier}}$$

Equation 5-2

If we now use the incremental calculation

$$v_{carrier}(n+1) = v_{carrier}(n) + \frac{\Delta V}{\Delta t}\Delta t$$

Equation 5-3

and account for the change in sign of $\frac{\Delta V}{\Delta t}$ when the peak voltage is reached then the carrier wave can be approximated at each of the discrete time steps used in the simulation.

Unfortunately, this approach can result in 'overshoot error' at the peak value of the waveform and these errors are propagated through the remainder of the solution causing a compounding error. This error and its cause can be seen in the diagram below;

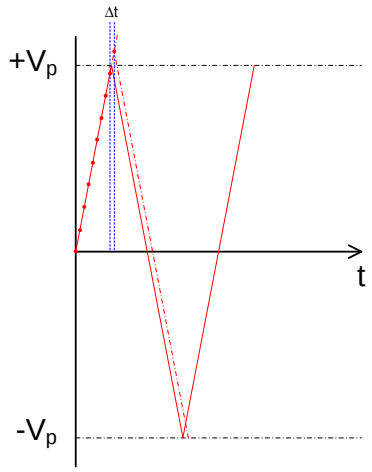

Figure 5-10 - Overshoot error

The error is fundamentally caused by the fact that we do not change direction (reverse the slope polarity) until we reach or exceed the peak voltage. To correct for this, we can simply set the voltage equal to the peak value at the same time as we reverse the slope polarity.

This effectively resets the peak value every time it is reached to the exact value to eliminate propagation of the error.

Now that we have values for the carrier and modulating signal at each of the time steps we can readily generate the STATCOM output voltage using the following standard PWM logic for the two cases:

$$V_{mod} \geq V_{car}\ then\ V_S = +\frac{V_d}{2}\ (close\ Sw+)$$

Equation 5-4

$$V_{mod} < V_{car}\ then\ V_S = -\frac{V_d}{2}\ (close\ Sw-)$$

Equation 5-5

The results for the switched output generated by the code are shown below.

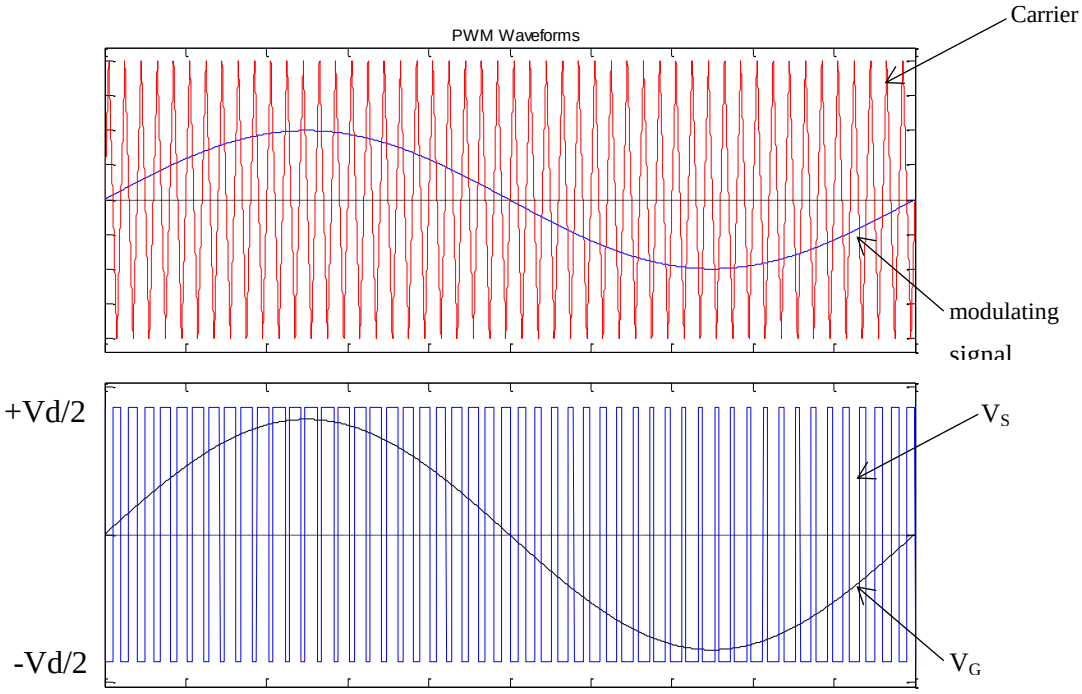

Figure 5-11 - STATCOM switched output

Note that there exists an error in the output waveform due to the fact that at any time instant the output voltage cannot be simultaneously two magnitudes. This means that the transitions between $+\frac{V_d}{2}$ and $-\frac{V_d}{2}$ will occur at times t and $(t + \Delta t)$. This error will be small provided that Δt is made sufficiently small.

Now that we have calculated values for the STATCOM switched output voltage we can calculate the current steering reactor current using the equation;

$$i_L = \frac{1}{L}\left(\pm\frac{V_d}{2} - \tilde{V}_G\right)t + C$$

Equation 5-6

In the code this is done by first calculating the average of the sinusoidal grid voltage over a switch period (note that a 'switch period' is defined as the time at which the STATCOM output is at $+\frac{V_d}{2}$ or $-\frac{V_d}{2}$ and will change over the modulation cycle).

The average voltage can be found by using the average of the grid voltages calculated at the time the output voltage transitions from $-\frac{V_d}{2}$ to $+\frac{V_d}{2}$ and at the transition from $+\frac{V_d}{2}$ to $-\frac{V_d}{2}$ for a positive going output pulse and vice versa for a reverse going pulse. The average grid voltages calculated by the code are shown in the figure below.

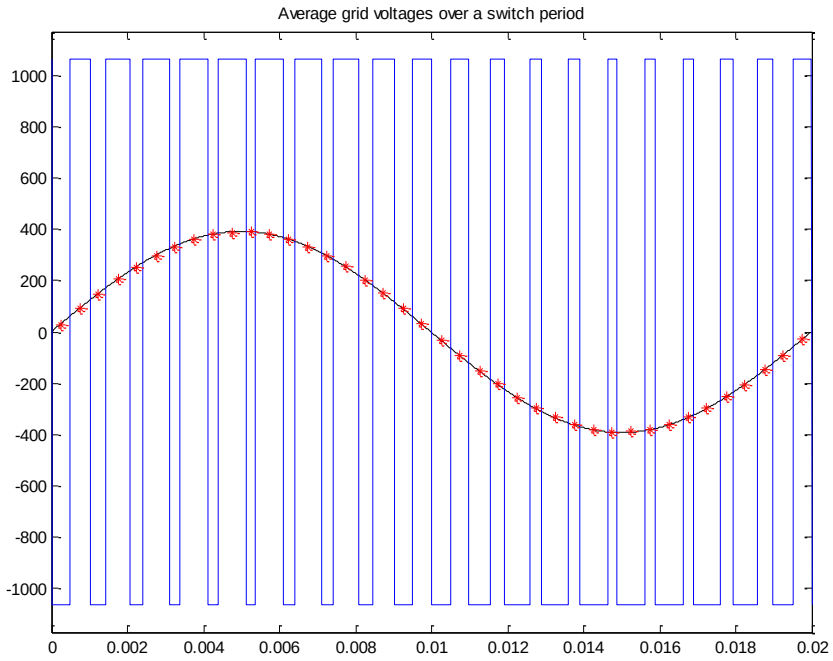

Figure 5-12 - Average grid voltages over a switching period

Note that in this figure the carrier frequency was reduced to allow for reader to clearly see the calculated results.

To calculate the inductor current, the code is set to give an initial (t=0) value of zero and then the current is ramped in accordance with its defining equation. As can be seen from this equation the current ramp slope is given by;

$$\frac{\left(\pm\frac{V_d}{2}-\tilde{V}_G\right)}{L}$$

Equation 5-7

and thus the inductor current at each time step can be calculated using;

$$i_{inductor}(n+1)=i_{inductor}(n)+\frac{\left(\pm\frac{V_d}{2}-\tilde{V}_G\right)}{L}\Delta t$$

Equation 5-8

Whilst this approach does provide a good approximation to the inductor current wave shape it will not have the correct DC offset as we arbitrarily chose the starting current to be zero. As discussed previously the inductor current should be symmetric about the time axis so that $\int_0^T i_L dt = 0$.

We can use this to calculate the required DC offset for the found inductor current. The calculation for the DC offset is as follows, so Let:

$$i_L = \hat{I}\sin(\omega t)+C$$

Equation 5-9

where C is the DC offset in the current. If we now take the integral of the current over one period, we get

$$\hat{I}\int_0^T \sin(\omega t)\,dt + \int_0^T C\,dt = 0 + CT$$

Equation 5-10

That is, if we integrate the calculated waveform for the inductor current over one period and divide this value by the period we will have the DC offset for the waveform. We can then use this value to offset the calculated inductor current so that it is now symmetrical over the grid voltage period. Of course the integration must be performed numerically based on the chosen time step and this will introduce some error in the results.

Due to the fact that the time discretisation has been chosen as uniform over the simulation period the code uses the well-known trapezoidal method to perform the numerical integration calculation. It should also be noted that the error in using this method is minimised by the fact that the inductor current is piecewise linear and thus the approximation of the function value over the time step used by the trapezoidal rule is exactly correct.

The calculated inductor current is shown in the figure below.

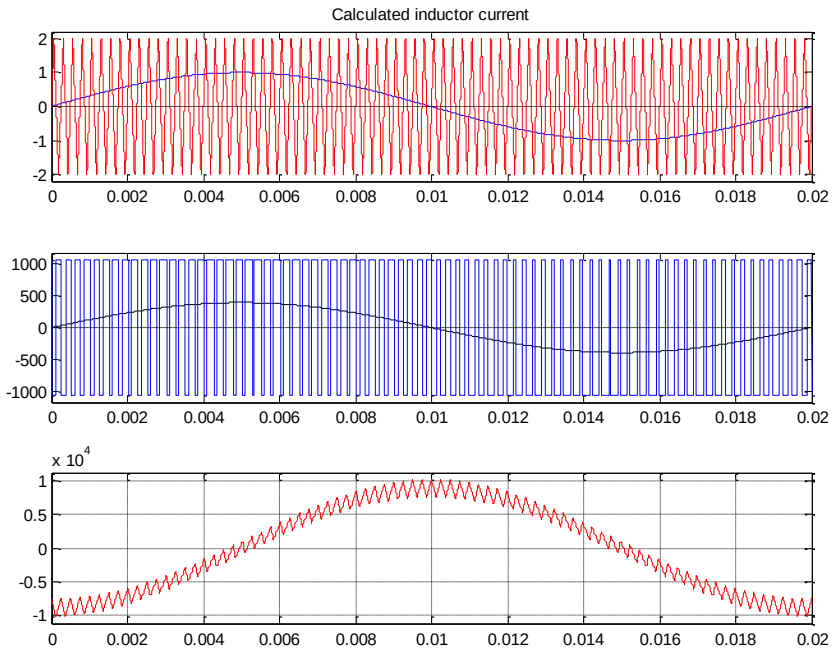

Figure 5-13 - Calculated inductor current

Having calculated the inductor current, we can now calculate the instantaneous power entering/leaving the STATCOM. As stated previously this can be done one either side of the current steering reactor. In the code the calculation of instantaneous power is performed by multiplying the calculate inductor current with the grid or STATCOM switched voltage at every sample time.

The calculate instantaneous power can then be integrated over one cycle period (of the grid voltage) and divided by the period to give average power flowing to/from the STATCOM over one cycle of the grid voltage.

The code uses the trapezoidal method to perform the numerical integration calculation of the calculated power.

The calculated instantaneous power flow is shown in the figure below.

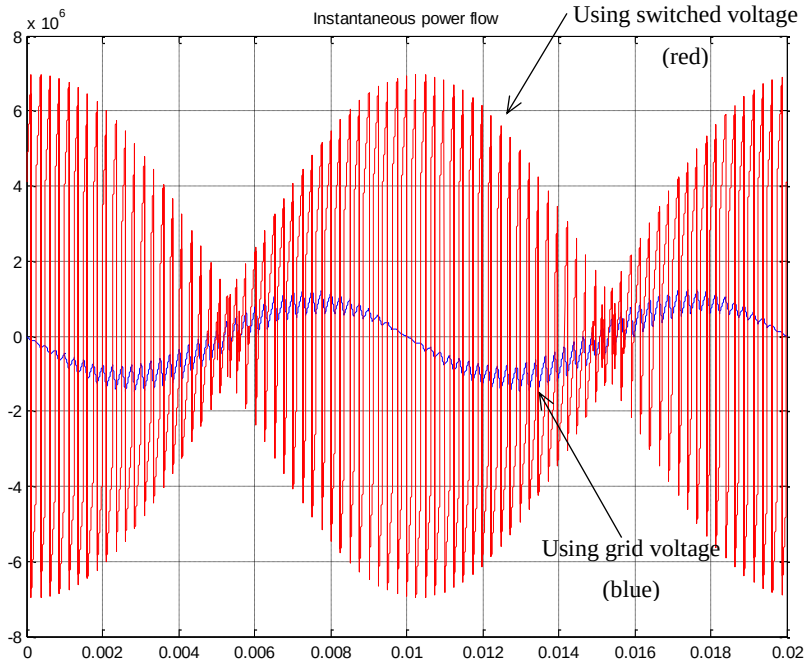

Figure 5-14 - Instantaneous Power Flow

6 SIMULATION RESULTS / DISCUSSION

6.1 MODEL VALIDATION

Having arrived to the above equations, we can start to validate some of the results in terms of Active and Reactive Power flow into the load in our model.

As it can be seen in Figure 6-2, the delivery of Reactive Power by the source is compensated by the STATCOM operation and this occurs as follows:

- 0 ms to 20 ms of simulation; - the graph shows no Active or Reactive Power output and also 0 Power Factor angle, this is due to the Discrete Fourier Transform (DFT) block which is used to capture the measurement. As it is well-known DFT needs a minimum of 1 cycle, that is 20 ms for a 50 Hz system, to perform its operation and provide a result / output.

- 20 ms to 40 ms of simulation; - the graph shows the source delivering all the Active and Reactive Power consumed by the load and the line and these are the characteristics of the line and load.

  Given that:

$$Z = R + j\omega L$$

Equation 6-1

$$Z_{Line} = (5 + j2.1991)\Omega$$

And

$$S_{Load} = (1.5 + j1.2) \times 10^6 \text{VA}$$

We can find the impedance for the load, knowing that the above mentioned capacity is function of voltage, in SimPowerSystems®:

$$Z_{Load} = \frac{(V_{Load})^2}{S_{Load}}$$

Equation 6-2

$$Z_{Load} = \frac{\left(\frac{33 \times 10^3}{\sqrt{3}}\right)^2}{(1.5 - j1.2) \times 10^6}$$

$$Z_{Load} = (147.561 + j118.049)\Omega$$

Now we can find the total amount of Active and Reactive Power delivered to the load and line;

$$S_{total} = \frac{V^2}{Z_{Load} + Z_{Line}}$$

Equation 6-3

$$S_{total} = \frac{\left(\frac{33 \times 10^3}{\sqrt{3}}\right)^2}{(147.561 + j118.049) + (5 + j2.1991)}$$

$$S_{total} = \frac{\left(\frac{33 \times 10^3}{\sqrt{3}}\right)^2}{(152.561 + j120.248)}$$

$$S_{total} = (1.4676 - j1.1568)\text{MVA}$$

$$P_{total} = 1.4676\text{MW}$$

$$Q_{total} = -1.1568\text{MVAr}$$

Figure 6-2 also shows the Power Factor angle for the power delivered by the source between 20 ms and 40 ms as:

$$\theta = \tan^{-1}\left(\frac{Q_{total}}{P_{total}}\right)$$

Equation 6-4

$$\theta = \tan^{-1}\left(\frac{-1.1568}{1.4676}\right)$$

$$\theta = -38.245°$$

The above value of Active and Reactive Power and Power Factor angle is clearly seen delivered to the load and line within the 20 ms to 40 ms interval.

As previously mentioned, the STATCOM is synchronised to the grid by using a Phase Lock Loop (PLL) which also requires 1 cycle (20 ms at 50 Hz) to operate and for this reason a firing block has been designed to prevent the STATCOM from firing for the first 40 ms of the simulation. The extra 20 ms from its minimum requirement has been put in place to assist in the analysis of before and after compensation scenarios in the simulation.

- 40 ms to 250 ms of simulation; - the graph shows a transient period which is due to the response of the STATCOM to the required power that needs to supply to its point of connection (the load).

- 250 ms to 500 ms of simulation; - the graph shows the amount of Reactive Power now supplied by the source after the STATCOM has stabilised its operation. It also shows the Power Factor angle of the source, showing that the source has a Power Factor close to 1 (theta close to 0°), as most of the Reactive Power is delivered to the load by the STATCOM.

While the above mentioned results are clear, it is important to note that in Figure 6-2 the results are from the source (grid) perspective.

The results on how the STATCOM responds in this scenario are depicted in Figure 6-3 and it also shows the 40 ms delay from the start of the simulation to the STATCOM's IGBT firing start.

Furthermore, it can be seen that the STATCOM after the initial oscillatory interval, once it gets back to steady-state, it only supplies the Reactive Power to the load, as its Active Power output is 0MW and the Power Factor angle is -90° confirming Capacitive Reactive Power supply to the load.

Another important factor to note from the model validation results is that steady-state the STATCOM only provide a portion of the overall Reactive Power previous calculated ($Q_{total} = -1.1568\text{MVAr}$) and this is due to the tuning of the model to only supply enough Reactive Power for the load alone, therefore imposing that the source (grid) supplies the remaining Reactive Power due to be consumed by the line.

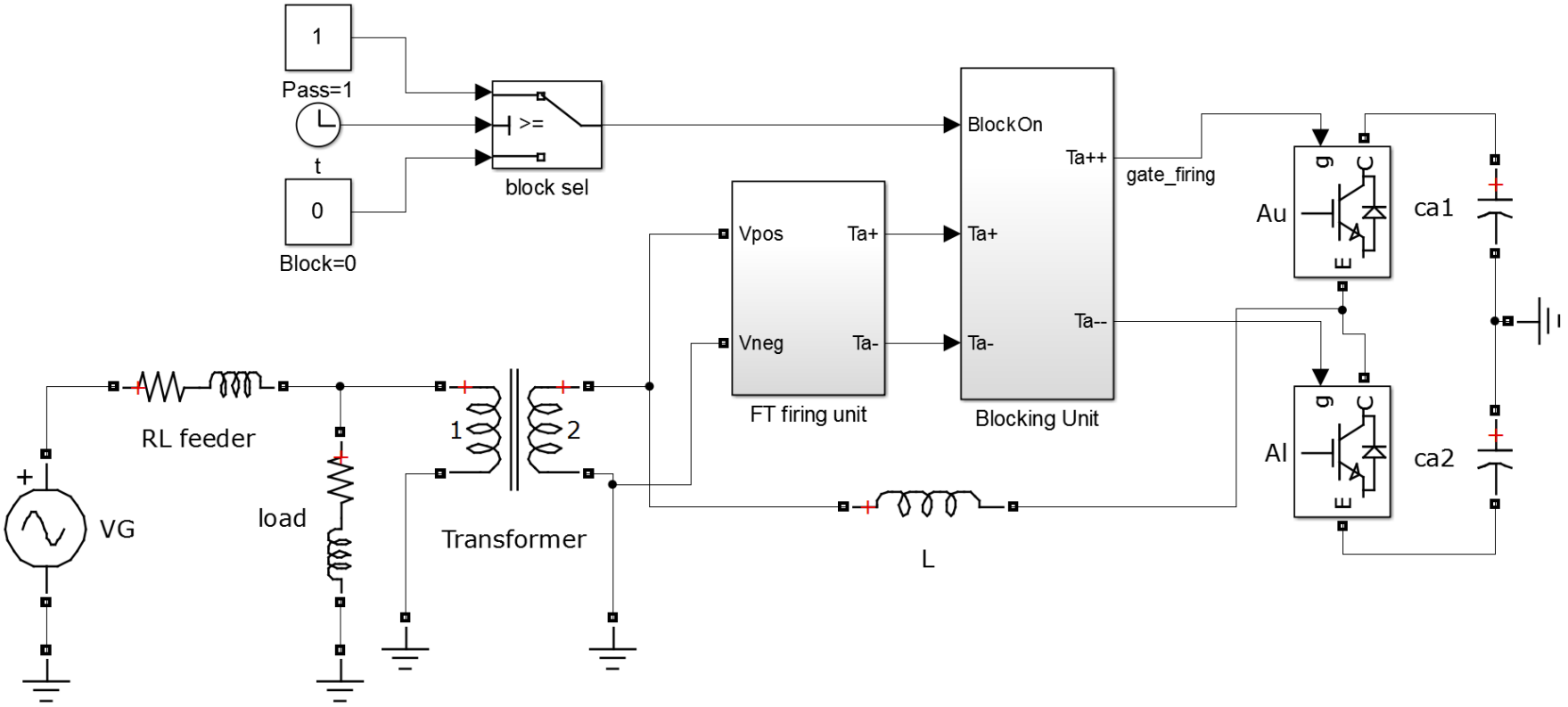

Figure 6-1 - Single phase STATCOM model

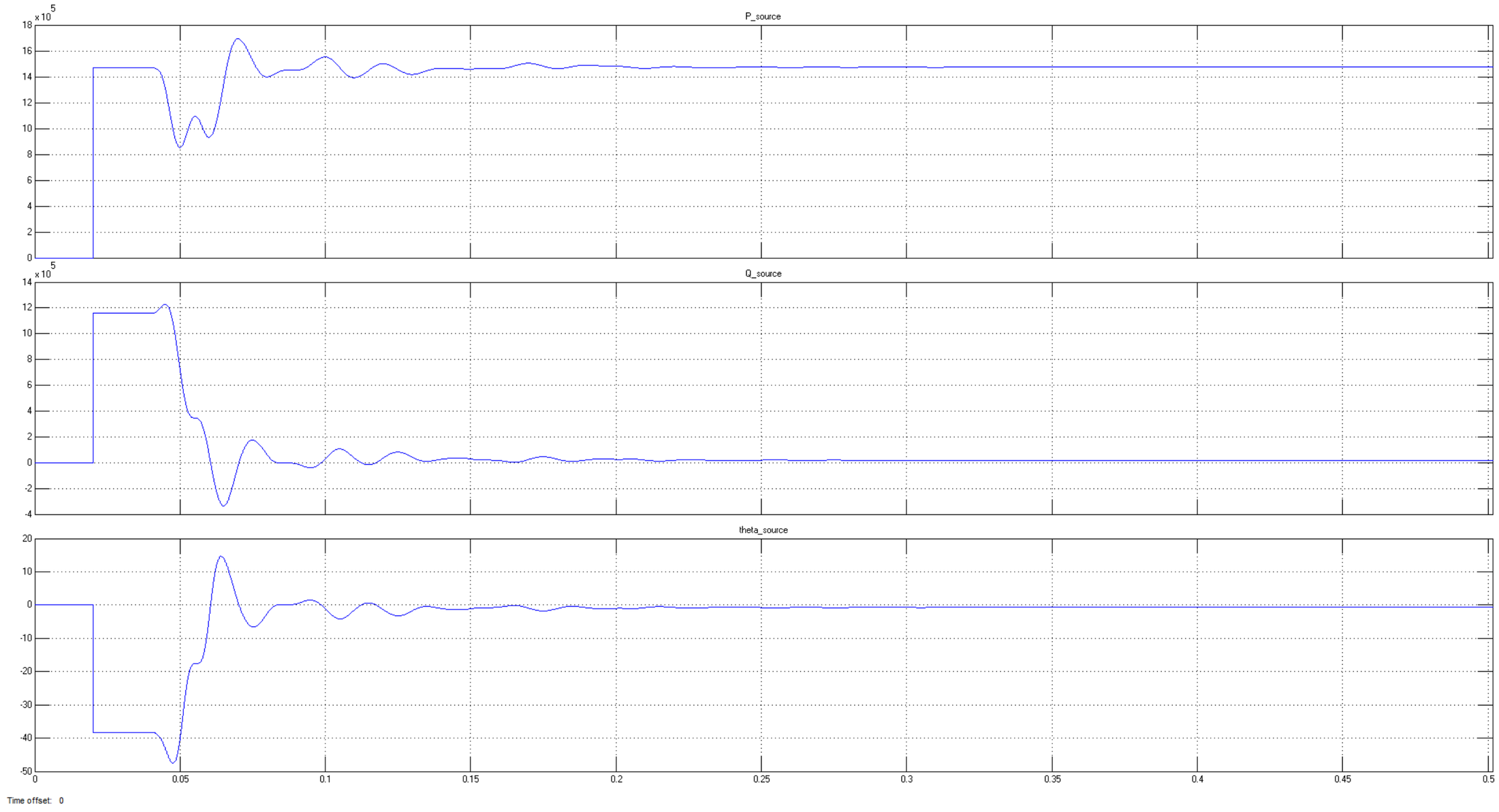

Figure 6-2 - Active and Reactive Power and Power Factor angle (grid perspective)

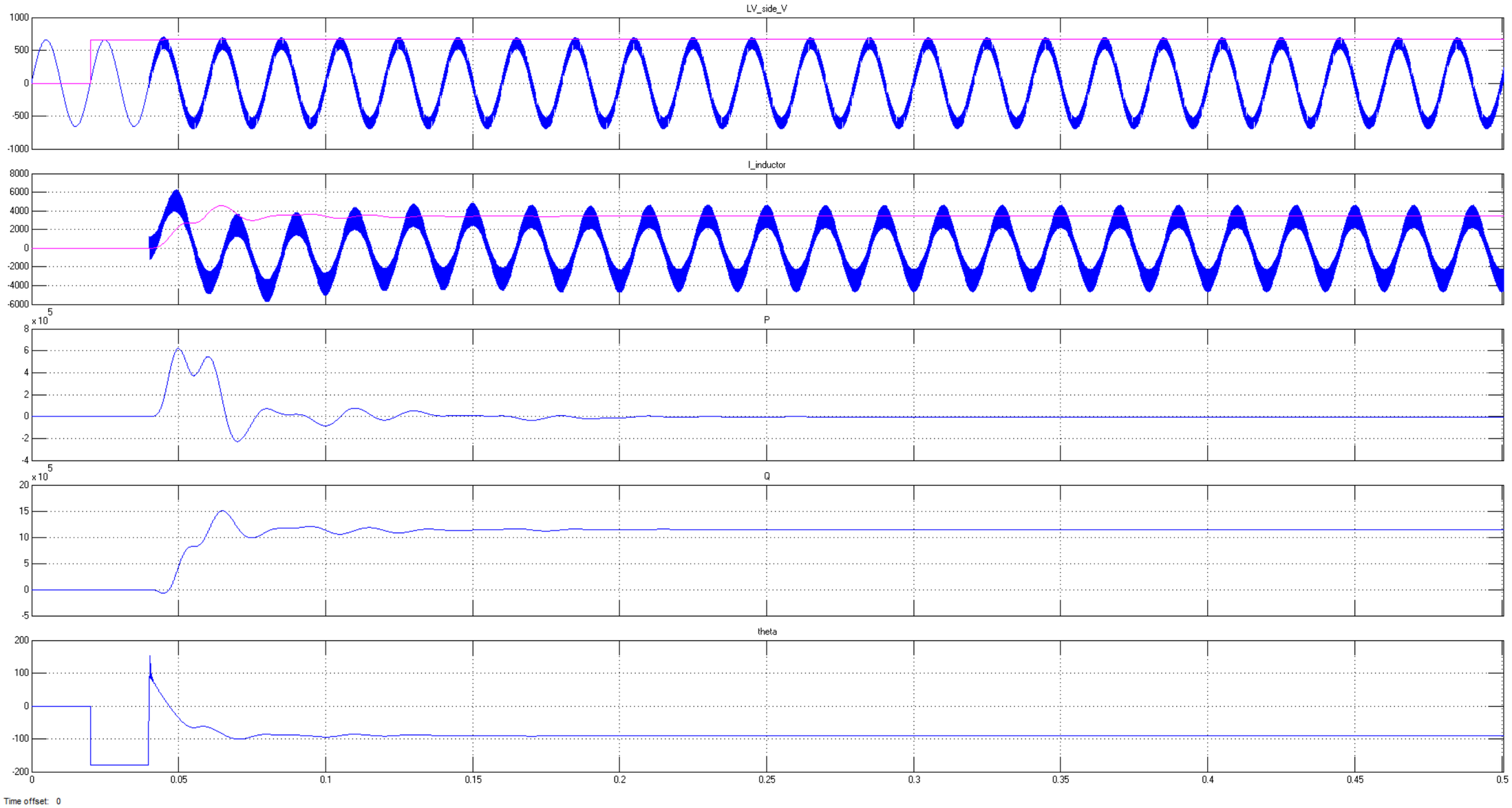

Figure 6-3 - Active and Reactive Power and Power Factor angle (STATCOM perspective)

6.2 ACTIVE POWER FLOW vs. PHASE SHIFT

The question at the core of this analysis is: given that we can calculate a theoretical active power flow out of the STATCOM using

$$P = \frac{|V_G||V_S|}{\omega L_S}\sin(\delta)$$

Equation 6-5

then how is this active power flow achieved in practice during the switching of the converter. Answering this question in turn allows us to explain how the DC bus voltage can be regulated by the control system and identify possible causes for excursions in the DC bus voltage.

To answer these questions, we need to consider what will happen when we introduce a phase shift (δ) between the grid voltage and the fundamental of the STATCOM switched output voltage. This can be readily achieved by introducing a phase shift to the modulating signal used to generate the IGBT firing pulses.

In practice, for a 2-quadrant reactive power support STATCOM, the modulating signal is phase locked to the grid voltage (on the converter side of the current steering reactor) to allow the control system to synchronise the STATCOM output voltage. The control system can also regulate the DC bus voltage by introducing an active power component to the STATCOM output. In effect this is achieved by the introduction of a phase shift between the grid voltage and the fundamental of the STATCOM output voltage.

To simulate a phase shift between the STATCOM and grid voltages we can readily introduce a phase shift to the modulating signal which will in turn adjust the firing pulses (assuming a fixed carrier signal). In practice when the STATCOM is operating in a steady state condition the introduction of this phase shift will be performed by the DC bus control loop to maintain a

constant DC bus voltage. In a perfect system this would not be required but due to losses, imperfections in the control system and network variations the control system must continuously regulate the active power component to regulate the DC bus. This also leads us to two conditions which can occur which will affect the DC bus voltage these are;

- The system = grid and the STATCOM can be considered to be operating in a steady state condition and the STATCOM DC bus control loop introduces a phase shift to increase or decrease the DC bus voltage.

- There is a system transient resulting in a change in the grid voltage magnitude and phase.

In terms of average active power flow into or out of the STATCOM these two conditions could be considered identical with regards to the effect of introducing a phase shift between the STATCOM fundamental and grid voltages.

Of course doing this would not include the effect of the grid voltage magnitude change but let us assume that we can neglect this effect for now so that we can focus on the effect of the phase shift. In practice this simplification may be reasonable if we assume that the grid voltage magnitude change is not too severe and that the STATCOM also acts to stabilise the grid voltage magnitude. The question then is, if we study just one of the above scenarios will this explain the effect of the phase shift for both cases?

Unfortunately, the answer is no if we are interested in what happens at the switching level. Whilst it will be shown that the net effect on active power flow of introducing the phase shift on the grid or STATCOM side is the same, we will see that how this is physically achieved differs when we consider the operation of the power electronics over a switching period. This

is an important outcome of this analysis as this difference is not explained by theoretical or high level power flow equations.

6.2.1 STEADY-STATE OPERATION

First we will consider the case where the grid and the STATCOM can be considered to be operating in a steady state condition and the STATCOM DC bus control loop introduces a phase shift to increase or decrease the DC bus voltage. As stated previously this scenario can be modelled by the introduction of a phase shift to the modulating signal. Unfortunately, this will also introduce an unwanted change to the reactive power output. If we recall the theoretical equation for the reactive power output of the converter

$$Q = \frac{|V_G|}{\omega L_S}[|V_S|\cos(\delta) - |V_G|]$$

Equation 6-6

we can see that for a change in δ we will also get a change in Q. Fortunately as the Q equation uses the *cosine* of the phase shift we know that the rate of change of Q for a small change in δ about δ=0 will be small (whereas the active power equation uses a sin(δ) term which has a maximum rate of change around δ=0). This means that provided we keep δ small we can either neglect the change in Q or we can correct for the change in Q to eliminate this additional variable.

To allow for the general case the simulation code performs a correction to the modulation ratio to maintain a fixed Q output. This correction is calculated as follows;

Given that we can approximate the STATCOM voltage $|V_S|$ using $|V_S| \approx m_a \frac{V_d}{2\sqrt{2}}$ then the change in Q with phase angle will be determined by the value of

$$m_a \frac{V_d}{2\sqrt{2}} \cos(\delta)$$

Equation 6-7

For a fixed DC bus the value for $\frac{V_d}{2\sqrt{2}}$ will be constant and independent of changes in δ. Thus to maintain a constant Q output we need to make

$$m_{a\_1} \cos(\delta_1) = m_{a\_2} \cos(\delta_2)$$

Equation 6-8

where the subscripts 1 and 2represent the values for two consecutive simulations. This means that given we run the first simulation using a modulation ratio of m_{a_1} and phase shift of δ_1 then a second simulation with a phase shift of $\delta_2$will have the same Q output provided

$$m_{a\_2} = m_{a\_1} \times \frac{\cos(\delta_1)}{\cos(\delta_2)}$$

Equation 6-9

It should also be acknowledged that whilst we can calculate a new modulation index to maintain the Q output we must also ensure that $m_{a\_2} \leq 1$ so that we remain an under-modulated system. The m_{a_2} equation derived above also allows us to define an upper limit for δ_2. That is, if we define the operation of the STATCOM to be a PWM system using "under modulation" then we know that $m_a \leq 1$. From our m_{a_2} equation we can ensure that this condition will be met provided that

$$\cos(\delta_2) \leq m_{a\_1} \cos(\delta_1)$$

Equation 6-10

Thus the upper limit for δ_2 is given by

$$\delta_2 \leq \cos^{-1}\left(m_{a\_1}\cos(\delta_1)\right)$$

Equation 6-11

Plots of the normalised inductor voltage and inductor current for δ_2= limit and δ_2 > limit are shown below.

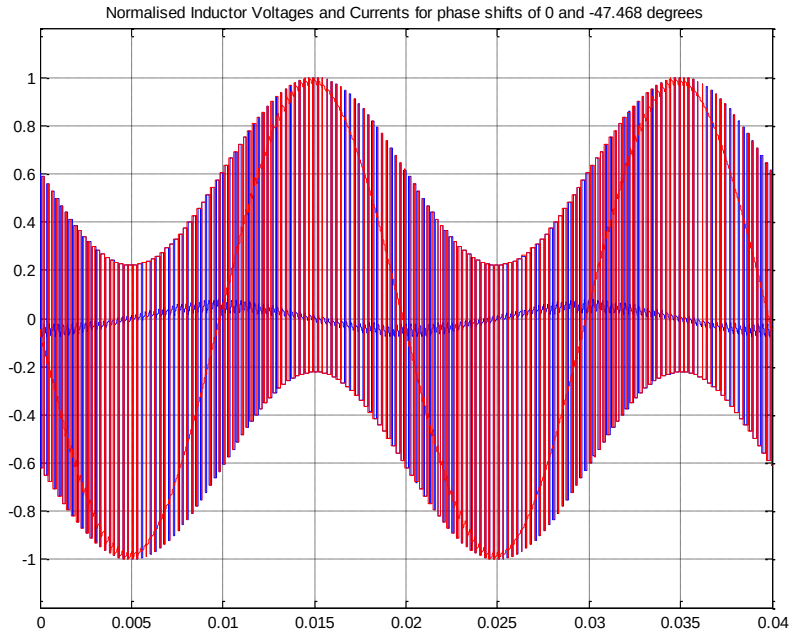

Figure 6-4 - Normalised inductor current and voltage (0° to -47.468°)

Here blue is for $\delta = 0$ and red for $\delta = limit\ value$= -47.468° for the chosen STATCOM parameters and initial modulation ratio.

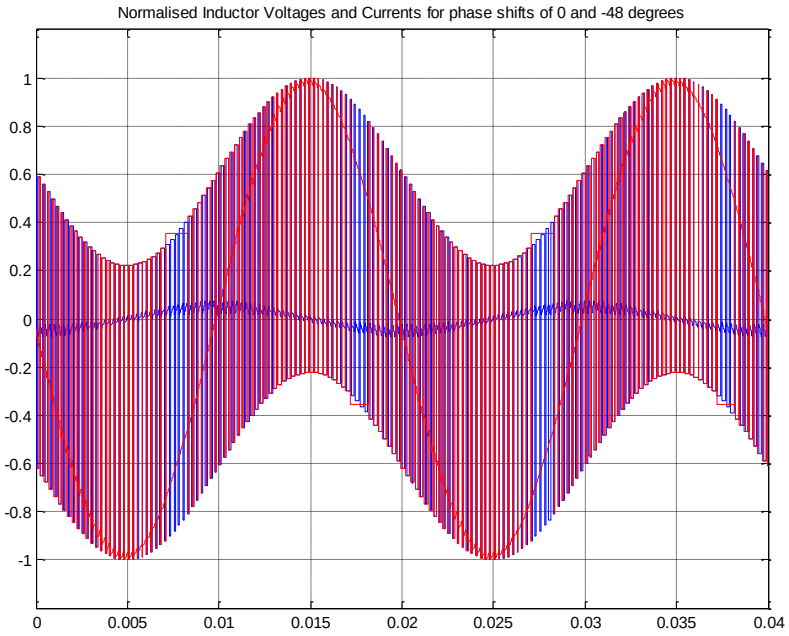

Figure 6-5 - Normalised inductor current and voltage (0° to -48°)

Again blue is for $\delta = 0$ and red for $\delta > limit\ value$= -48° for the chosen STATCOM parameters and initial modulation ratio. We can clearly see the change in the switching pulses for $m_a > 1$ at times 8 ms and 28 ms.

6.3 CURRENT STEERING REACTOR

Before we can start analysing the inductor voltage and current for different phase shifts we first need to clarify our understanding of the inductor voltage. The plots of the inductor voltage clearly show that while the inductor voltage is made up of switched $\pm V_{d.c.bus}$ pulses it also has a sinusoidal envelope which is defined by the grid voltage. This can clearly be seen from the inductor voltage equation derived earlier and repeated here

$$v_L(t) = \pm\frac{V_d}{2} - v_G(t)$$

Equation 6-12

This equation shows that the inductor voltage will be bound by the limits $+\frac{V_d}{2} - v_G(t)$ and $-\frac{V_d}{2} - v_G(t)$. When we talk about the inductor voltage there are in fact three components which we could be referring to;

- The instantaneous value = pulsed or switched voltages
- The fundamental of the voltage = 50 Hz voltage which by definition leads the fundamental of the inductor current by 90°
- The inductor voltage envelope which is defined by the negative of the grid voltage.

As we are interested in the phase relationship between the inductor current and the grid voltage from here onwards we will refer to the inductor voltage envelope in terms of the grid voltage unless otherwise stated. It should also be noted that whilst the inductor voltage envelope is defined by the negative of the grid voltage we have also defined the inductor current as positive when flowing from the STATCOM into the grid.

This means that we can directly compare the phase shift of the two values without having to correct for sign differences (that is they are both negatives with respect to the grid voltage and thus we do not have to consider the sign differences). A plot of the inductor voltage with these limits overlayed is shown below for $\delta = 0$ and $\delta = -10°$.

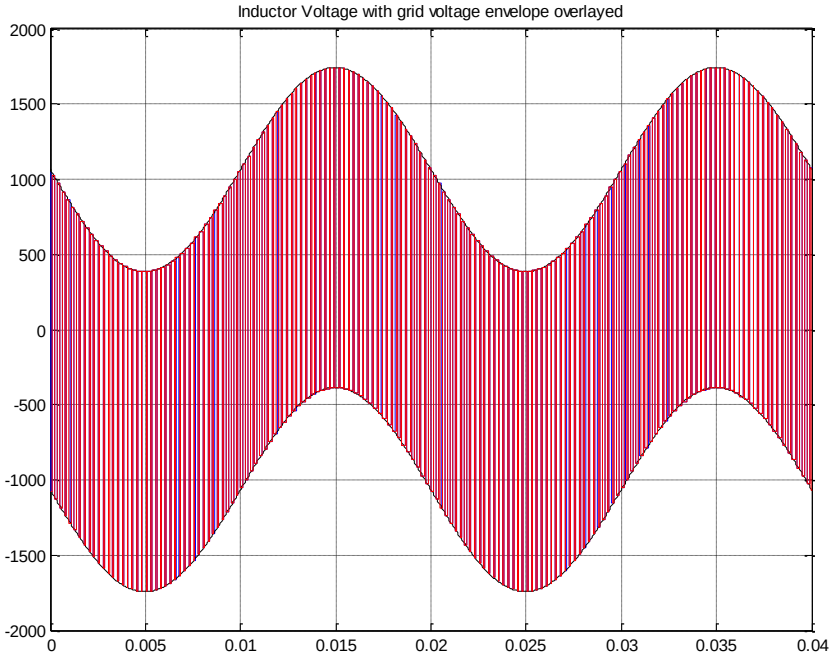

Figure 6-6 - Inductor voltage with grid voltage overlay

Here blue is for the inductor voltage for $\delta = 0$ and red is for $\delta = -10°$. If we look closely at the inductor voltage envelope we can see that the stepped DC voltage is equal to the envelope voltage at the middle of the step period. This is the consequence of applying the assumption that the grid voltage is fixed over the step period. A zoomed in plot to show this is shown below.

It should also be noted that the voltage envelope is the same for the two phase angles, this is because it is the STATCOM voltage which has been phase shifted and we can see from the inductor voltage equation this phase shift will not affect the inductor voltage envelope. This is a very important point as we will see when we consider the effect of applying a phase shift to the grid voltage as opposed to the STATCOM voltage.

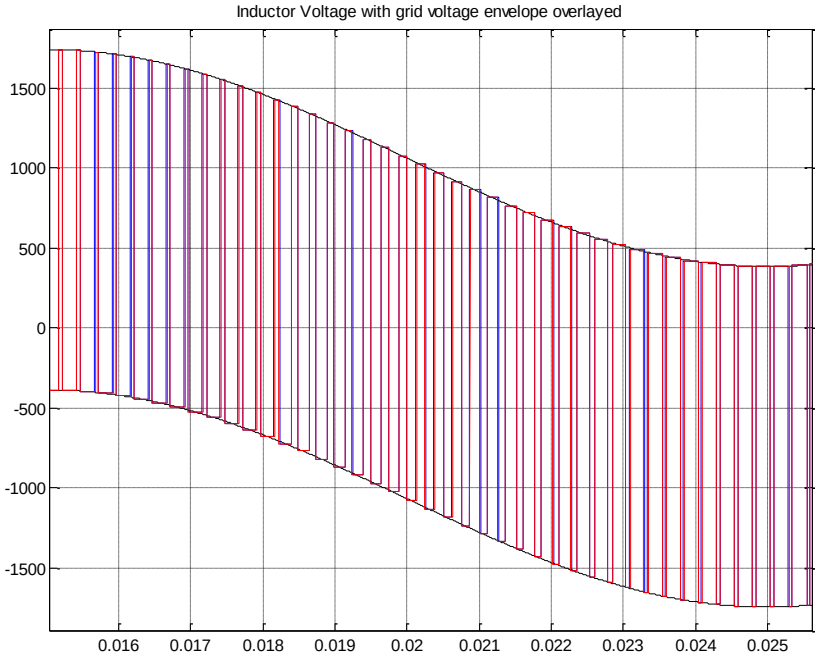

Figure 6-7 - Inductor voltage with grid voltage overlay (zoomed view)

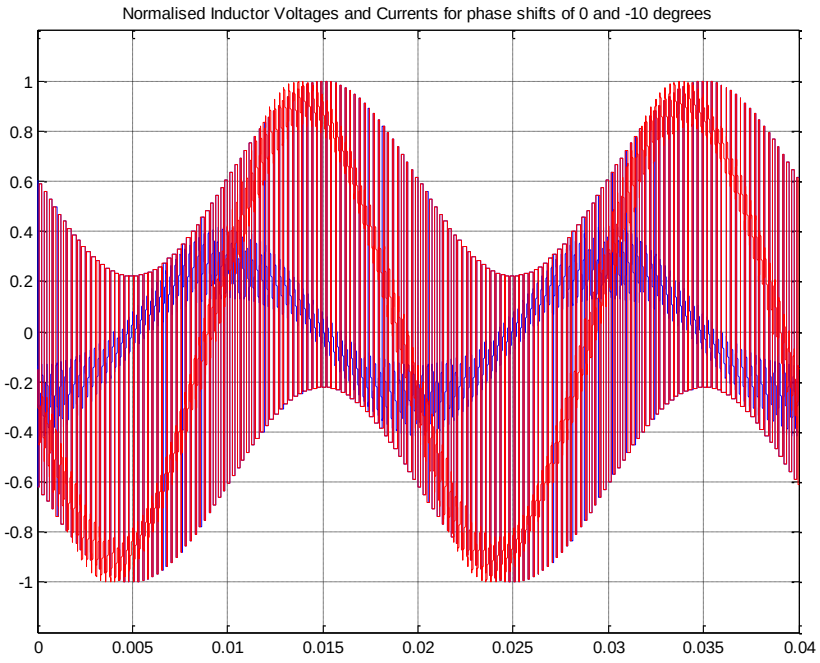

Figure 6-8 - Normalised inductor voltage and current for phase shift (0° to -10°)

Now that we can calculate valid results for our defined operating boundaries and we have a clear understanding of the inductor voltage behaviour we can investigate the behaviour of the inductor voltage and currents for different phase shifts between the grid and STATCOM voltages. Plots of the normalised inductor voltages and currents for $\delta_1 = 0$ and $\delta_2 = -10°$ whilst maintaining a fixed Q output and an "under-modulated" system are shown in Figure 6-9.

Here the normalised inductor current and voltage for $\delta = 0$ are shown in blue and for $\delta = -10°$ in red. The reason we normalised the values is to allow them to be overlayed onto the one plot whilst maintaining visibility of all variables.

Our previous analysis of the current flow entering the converter identified a direct relationship between capacitor charging and discharging with the inductor current. We have also shown from a theoretical viewpoint that the active power flow into the STATCOM can be described in terms of the inductor current magnitude and its phase relationship with the grid voltage.

As shown in the above figure, for $\delta < 0$ we have an increase in the inductor current magnitude and the phase shift between the current and the grid voltage is tending towards zero. While this is expected and in fact predicted by the active power equation we need to look more closely at what has made this happen in terms of the switching period. A zoomed in plot of the normalised current and voltage is shown below.

As we can see from the plot below, it is difficult to see a clear reason for the increased current magnitude and phase shift. To provide a better visual representation for our investigation a zoomed in plot of the normalised voltages and currents for $\delta = 0$ and for $\delta = -40°$ is shown below. Here we have zoomed in around the inductor current negative to positive transition zero crossing.

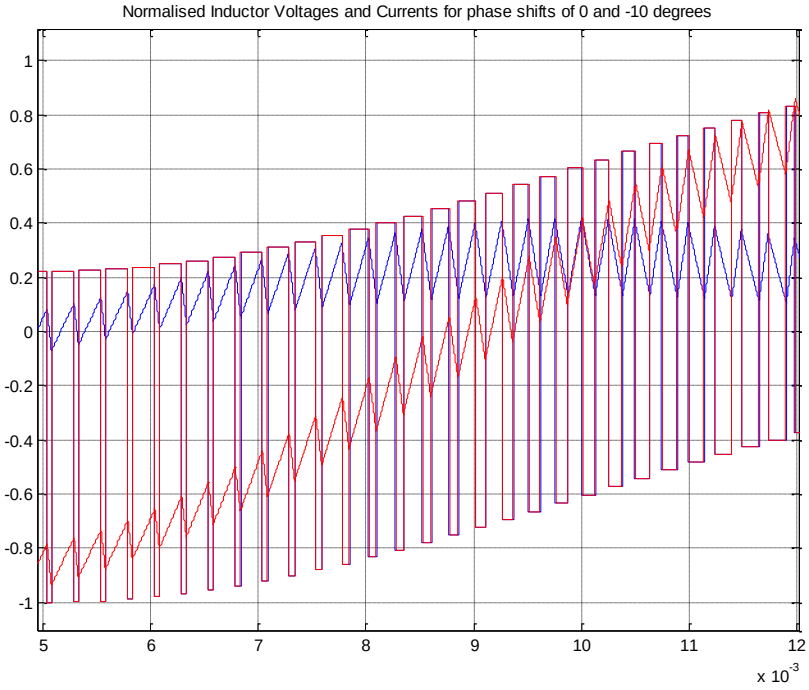

Figure 6-9 - Normalised inductor voltage and current for phase shifts of 0° and -10° – (zoomed view)

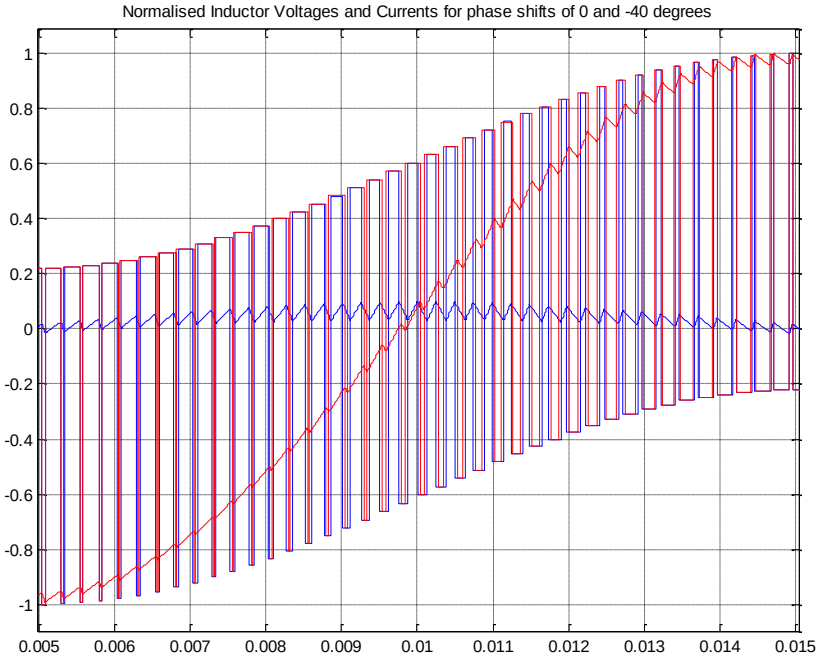

Figure 6-10 - Normalised inductor voltage and current for phase shifts of 0° and -40° – (zoomed view)

Here we can see that the positive voltage pulse width for $\delta = -40°$ (shown in red) is wider than that for $\delta = 0°$. Below is a further zoomed in plot of the same figure.

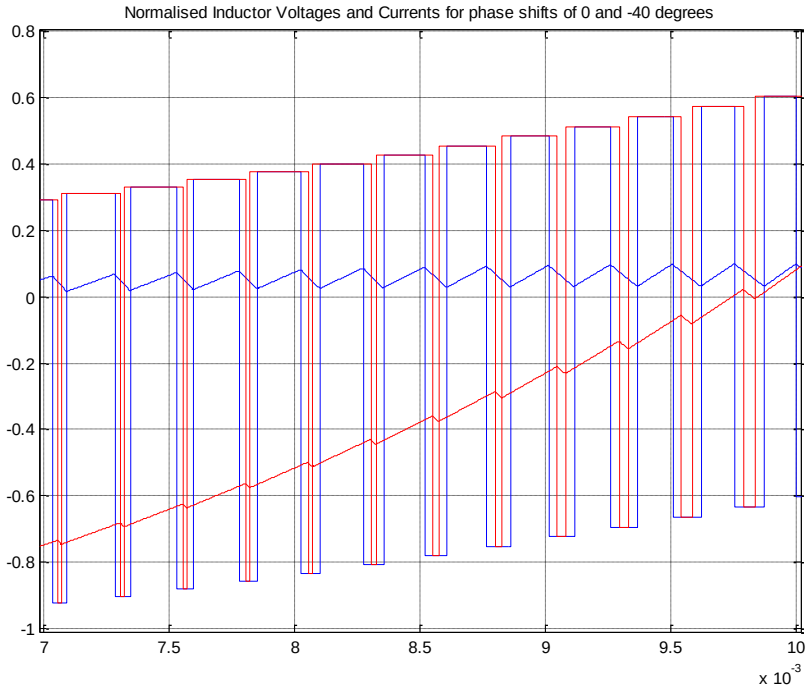

Figure 6-11 - Normalised inductor voltage and current for phase shifts of 0° and -40° – (zoomed view)

From this plot we can clearly see that for $\delta = -40°$ (shown in red) the positive pulse width has become wider and the negative pulse width has become narrower. If we recall that the inductor current can be approximated as a series of linear ramps of slope given by

$$\frac{1}{L}\left(\pm\frac{V_d}{2} - \tilde{V}_G\right) \approx \frac{v_{inductor}}{L}$$

Equation 6-13

then it is easy to see that an increase in the positive voltage pulse width will cause an increase in the change in current as it ramps in the positive direction. Conversely, a reduction in the negative voltage pulse width will cause a reduction in the change current as it ramps in the negative direction.

This explains why the inductor current with the introduction of a phase shift climbs more rapidly during the positive switch period and falls at a slower rate during the negative switch period. The net result of this is an overall increase in the magnitude of the inductor current when a phase shift is introduced.

For completeness it should also be noted that there must be an equivalent behaviour in the negative going direction of the inductor current. That is, in order to reach a symmetrical negative peak value of inductor current the positive voltage pulse width for a phase shifted STATCOM voltage must be shorter in duration and the negative voltage pulse width must be greater during the negative switch period. This is shown in the zoomed in plot of the normalised inductor voltages and currents below.

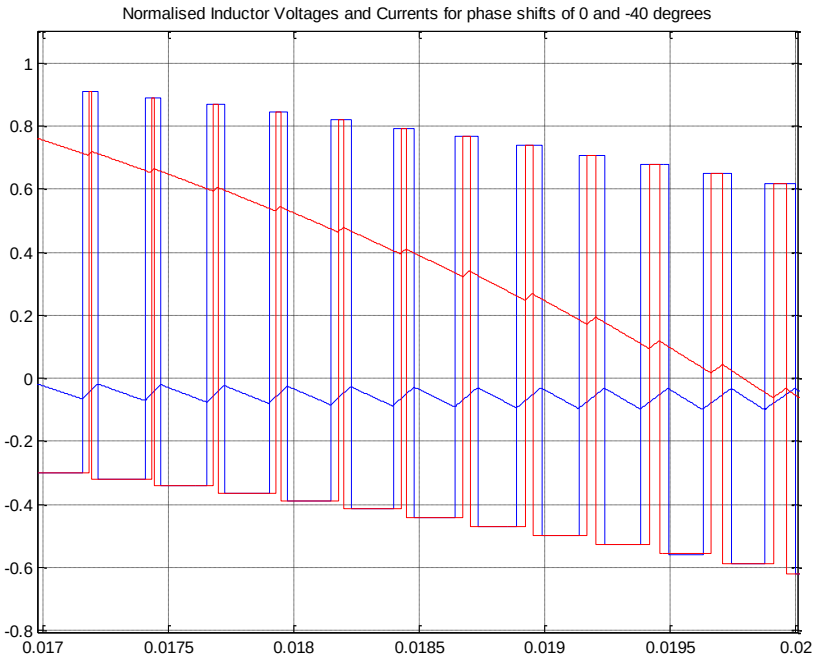

Figure 6-12 - Normalised inductor voltage and current for phase shifts of 0° and -40° – (zoomed view)

In essence this explains how the change in inductor current magnitude is achieved during the switch pulses. If we now go back to the basics behind controlling the magnitude of a PWM voltage (which we discussed earlier) and we use this information in conjunction with the fact that for an

increasing value of active power, we needed to increase the magnitude of the modulation index. It becomes apparent that the increase in m_a will result in wider pulses during the voltage peak values. This in turn produces the increase in current magnitude as described above. In addition, there will also be a phase shift of the firing pulses to align with the phases shifted modulating signal. The figure below shows the negative of the normalised modulating signal overlayed on the normalised inductor voltages and currents.

The reason the modulating signal has been shown as the negative of its actual value is so that we can see it amongst the other signals and even though inverted the signal still shows the behaviour we are interested in. If we compare the modulating signals, which define the location of the switching pulses, with the inductor current we can see that at $\delta = 0$ the peak of the modulating signal is in phase with the zero crossing of the inductor current.

We would expect this as at $\delta = 0$ the inductor voltage will be in phase with the STATCOM and grid voltages and the inductor current will have a 90° phase shift to these voltages. For $\delta = -40°$ we can see that the peak of the modulating signal is now phase shifted such that it no longer aligns with the inductor current zero crossing. This phase shift will result in a phase shift of the firing pulses which form the peak of the STATCOM voltage waveform (that is the longer duration pulses) away from the inductor current zero crossing.

The net effect of this being that we have more longer-duration pulses during the current transition from its negative to positive or positive to negative peak values. As shown previously this causes an increase in the resultant ramp rate of the current. As a consequence of this we get an increase in the current magnitude and a phase shift in the current.

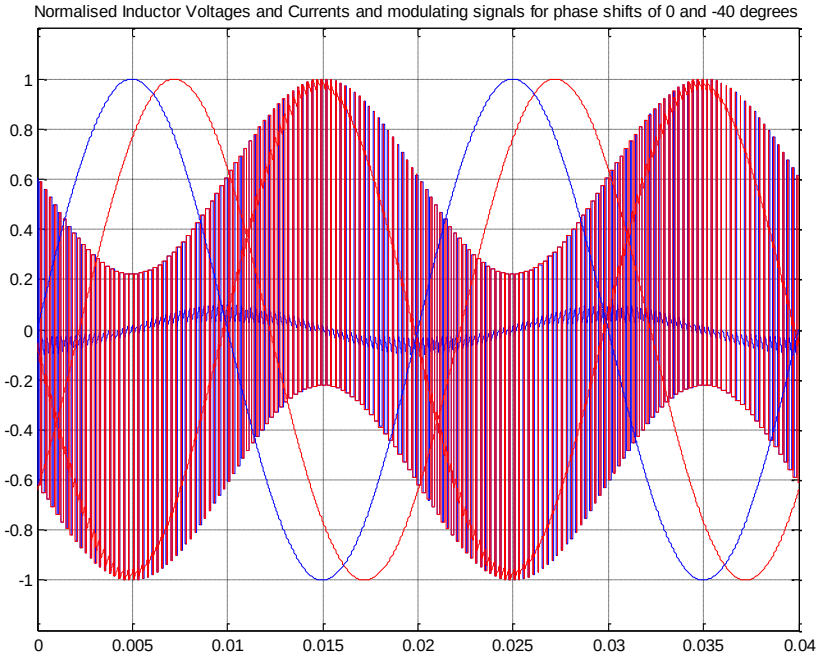

Figure 6-13 - Normalised inductor voltages, currents and modulating signals for phase shift of 0° and -40°

An alternate way of explaining this would be to say that at $\delta = 0$ the longer duration pulses which form the switched voltage peak are symmetrical about the inductor current zero crossing. For $\delta \neq 0$ these pulses are shifted so that they are no longer symmetrical around the current zero crossing.

The result of this shift is increased resultant ramp rates for the current which causes an increase in current magnitude and a phase shift. The relative phases shift behaviour between the inductor current and the switching pulses is shown below.

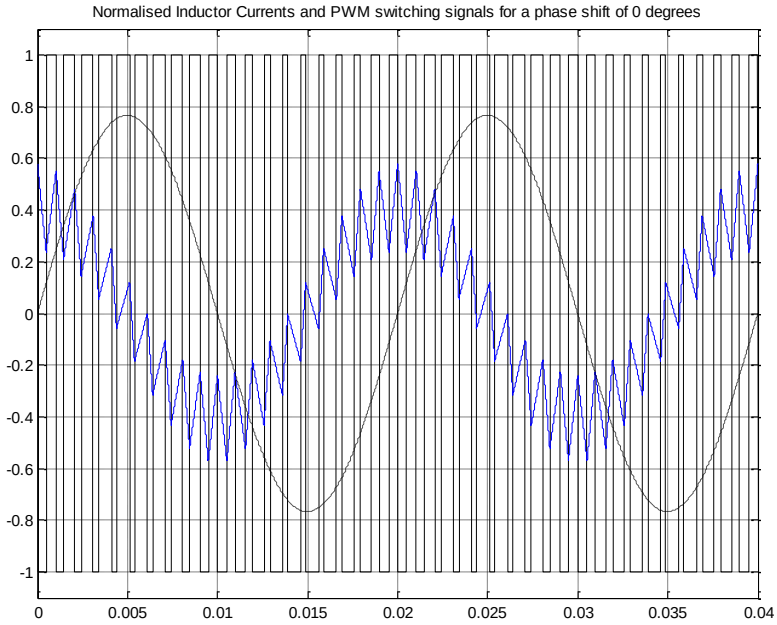

Figure 6-14 - Normalised inductor current and PWM switching signals (no phase shift)

Here we have the results for $\delta = 0$ and we can see that the widest pulses (which represent that peaks of the STATCOM voltage waveform) occur symmetrically around the inductor current zero crossing.

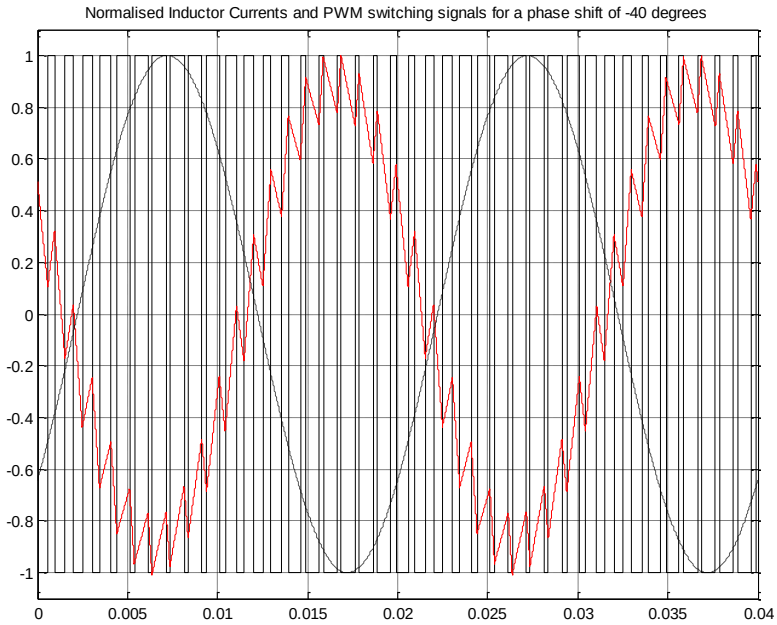

Figure 6-15 - Normalised inductor current and PWM switching signals (-40° phase shift)

Here we have the results for $\delta = -40°$ and we can see that the widest positive pulses occur before the inductor current zero crossing for the current transition from its negative to its positive peak and the widest negative pulses occur before the inductor zero crossing for the current transition from its positive peak to its negative peak.

This behaviour is not surprising if we consider that the limits for practical operation of the converter are $-\frac{\pi}{2} \leq \delta \leq \frac{\pi}{2}$. We can now see that at $\delta = \pm\frac{\pi}{2}$ the longest duration pulses will occur symmetrically around the peak values of the inductor current. This would result in a current of maximum peak amplitude and in phase with the grid voltage.

6.4 NETWORK TRANSIENTS AND EFFECTS

We will now consider the case where there is a system transient resulting in a change in the grid voltage magnitude and phase. To simulate what happens under these conditions we will apply a negative phase shift to the grid voltage which allows us to leave the firing pulses of the converter unchanged whilst introducing the required phase shift between the grid and STATCOM voltages.

As discussed in the previous analysis, we need to maintain a constant Q output as we vary the phase angle for our analysis. To do this we will use the same correction calculation for the modulation ratio as we did for the previous studies. The results of simulating for $\delta_1 = 0$ and $\delta_2 = -10°$ whilst maintaining a fixed Q output and applying the phases shift to the grid voltage are shown below.

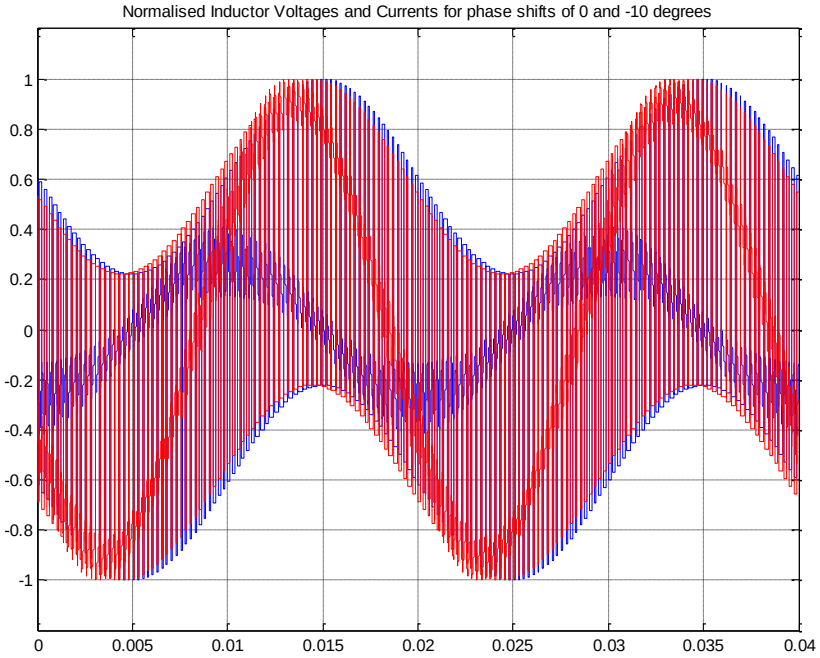

Figure 6-16 - Normalised inductor voltages and currents for phase shift of 0° and -10°

Here the normalised inductor current and voltage for $\delta = 0$ are shown in blue and for $\delta = -10°$ in red. Note that these values have been normalised to allow them to be overlayed onto the one plot.

These results show that there is a phase shift in the inductor voltage envelope. If we recall that the inductor voltage is defined and is repeated below for convenience:

$$v_L(t) = \pm\frac{V_d}{2} - v_G(t)$$

then it becomes apparent that when a phase shift is introduced to the grid voltage we will have a phase shift in the inductor voltage envelope. In our previous analysis we did not have this effect as it was the STATCOM voltage which was phase shifted and the grid voltage remained unchanged. A plot of the inductor voltage with the limits $+\frac{V_d}{2} - v_G(t)$ and $-\frac{V_d}{2} - v_G(t)$ is shown below for $\delta = 0$ and $\delta = -10°$.

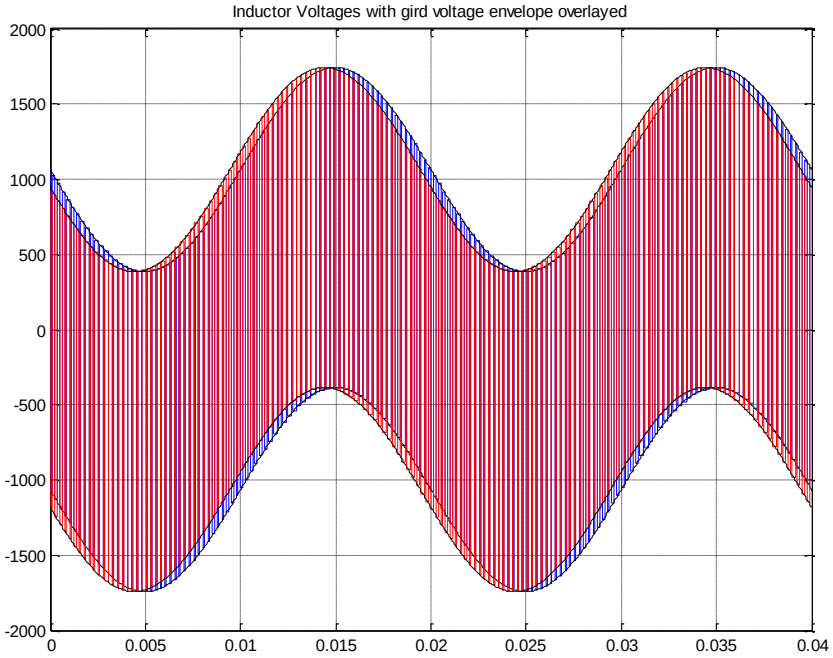

Figure 6-17 - Inductor voltage with grid voltage envelope

Here blue is for the inductor voltage for $\delta = 0$ and red is for $\delta = -10°$. If we look closely at the inductor voltage envelope we can see that the stepped DC voltage is equal to the envelope voltage at the middle of the step period. As stated previously, this is due to the assumption that the grid voltage is fixed over the step period. A zoomed in plot to show this is also shown below.

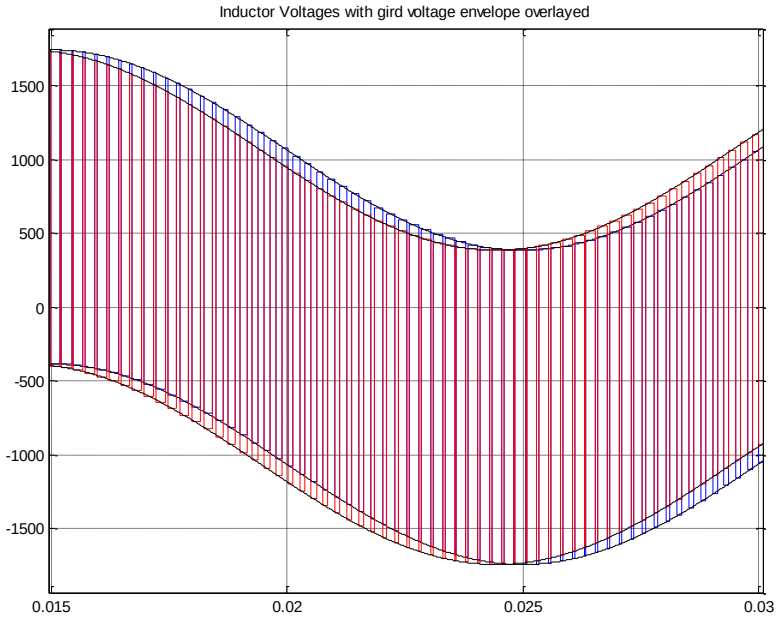

Figure 6-18 - Inductor voltage with grid voltage envelope (zoomed view)

For comparison the inductor voltage using the exact grid voltage (that is at the simulation time step) is also shown below. Here we can see that the inductor voltage exactly follows the grid voltage envelope.

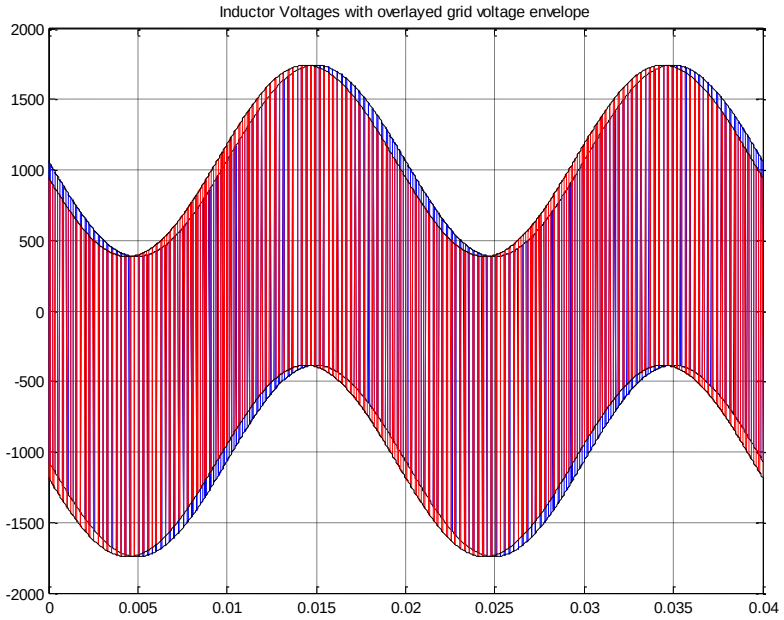

Figure 6-19 - Inductor voltage with grid voltage envelope

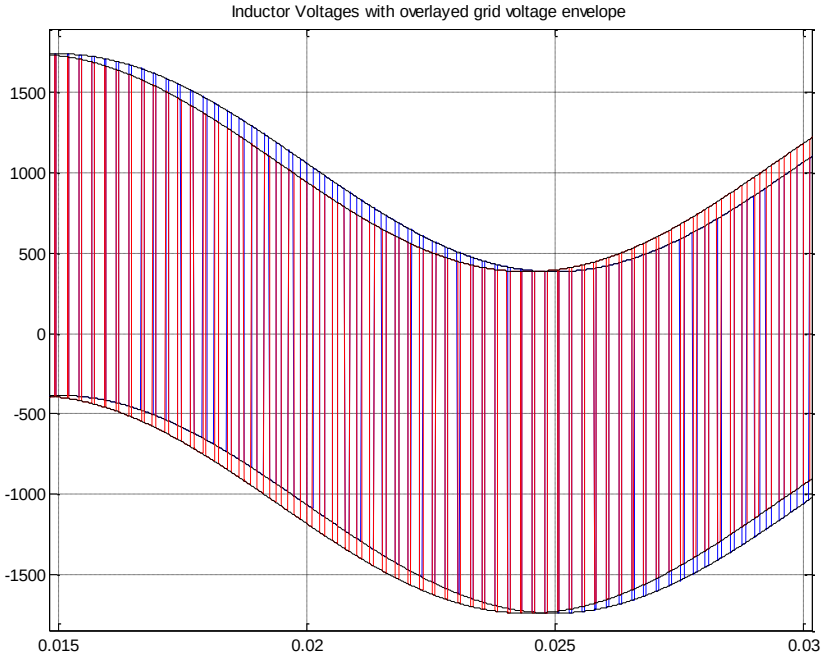

Figure 6-20 - Inductor voltage with grid voltage envelope (zoomed view)

Returning to our analysis of the inductor current, we have seen and explained the direct relationship between capacitor charging and discharging in terms of the inductor current. We have also shown from a theoretical viewpoint that the active power flow into the STATCOM can be described in terms of the inductor current magnitude and its phase relationship with the grid voltage. So the question then becomes, what is the effect of the grid phase shift on the inductor current? The figure below shows a plot of the normalised inductor voltages and currents for $\delta = 0$ and $\delta = +10°$.

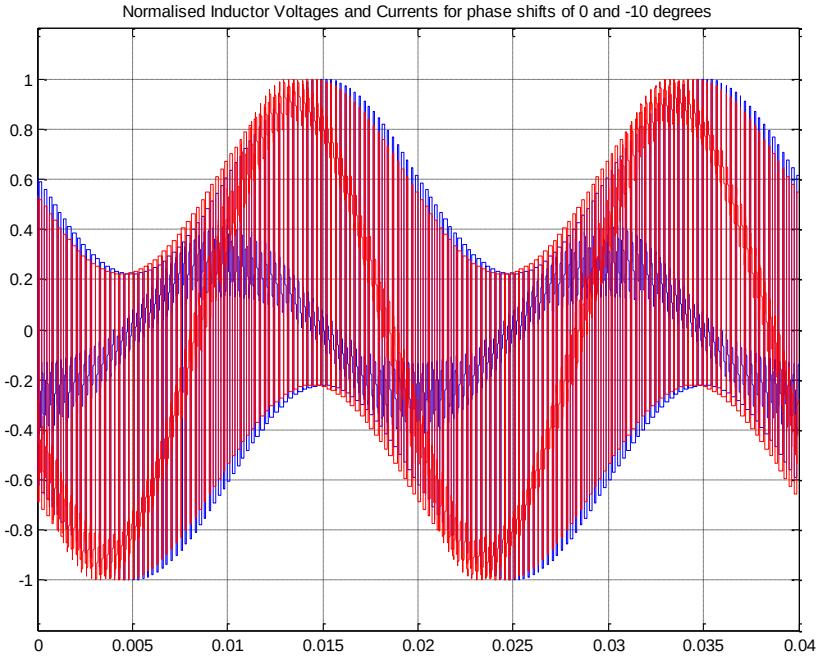

Figure 6-21 - Normalised inductor voltage and current for phase shift of 0° to -10°

We can clearly see that the phase shift between the grid voltage inductor current (ϕ) for $\delta < 0$ tends toward zero as $\rightarrow -\frac{\pi}{2}$. This behaviour will result in an increase in active power flow into the converter. This is not surprising based on our previous theoretical analysis.

Running the simulation for $\delta = 0$ and $\delta = +10°$ (see figure below) we can see that for $\delta = +10°$ the phase shift between the inductor voltage and current has grown to be >90°. This is also to be expected as for $\delta = +10°$ there will be net active power flow from the STATCOM to the grid.

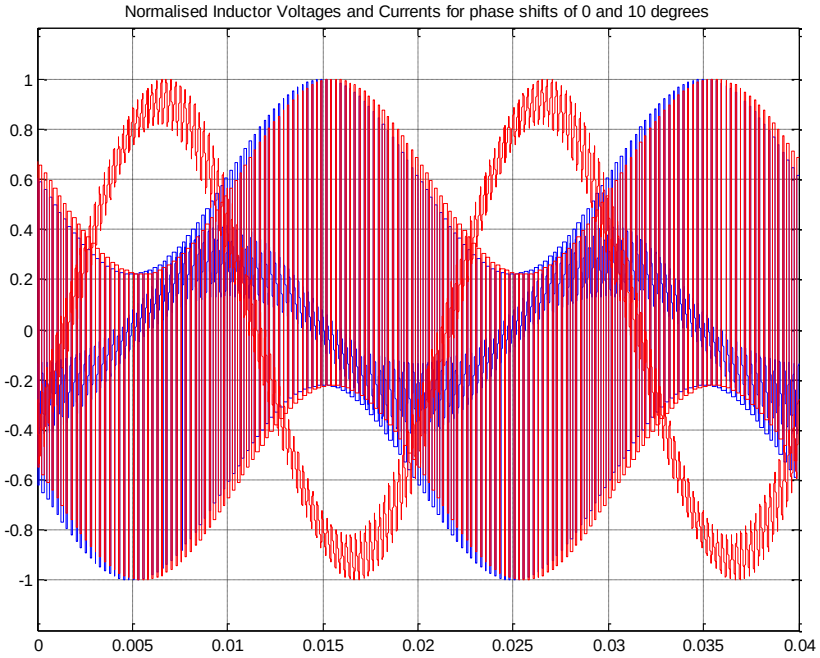

Figure 6-22 - Normalised inductor voltages and currents for phase shifts of 0° and 10°

Returning to our results for phase shifts of $\delta = 0$ and $\delta = -10°$, another key point to note is the increase in the inductor current magnitude. To remove any confusion about the normalising of the previously shown results the results are shown again below without normalisation.

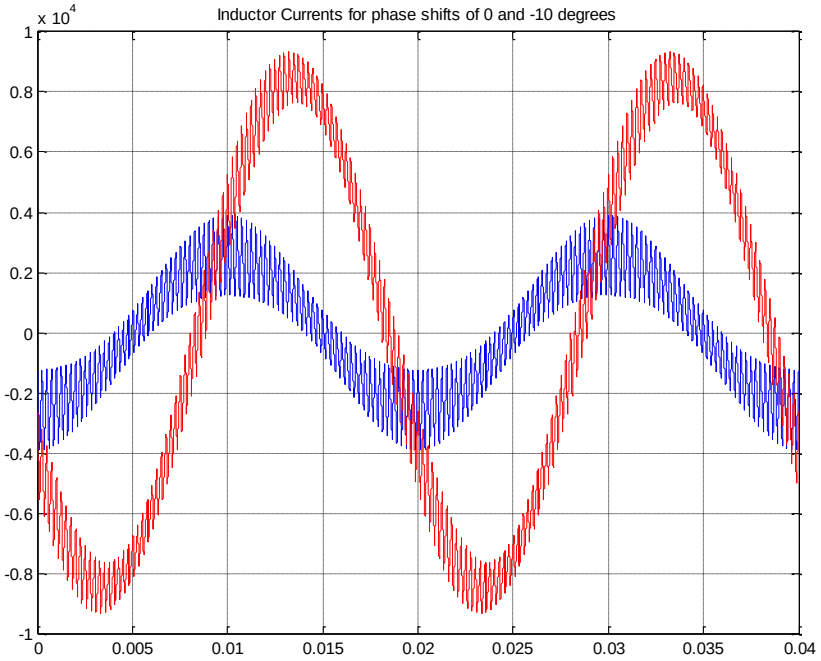

Figure 6-23 - Inductor current for phase shifts of 0° and -10°

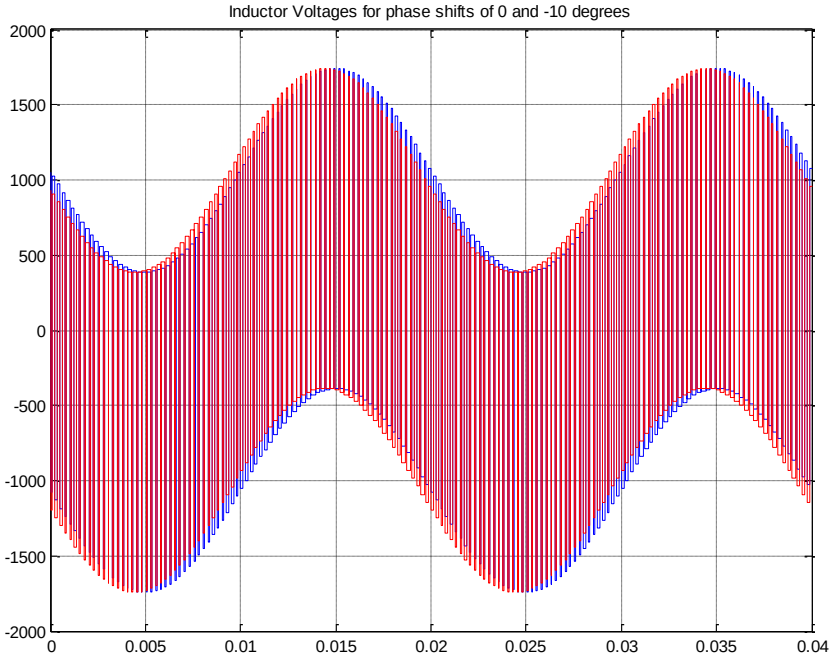

Figure 6-24 - Inductor voltages for phase shifts of 0° and -10°

Here we can see that there is a significant increase in the inductor current magnitude for $\delta = -10°$ compared to that at $\delta = 0°$. To explain how the phase shift and increase in current magnitude occurs in terms of the power electronic switching cycles we need to look closely at the inductor voltage for the two phase shifts. The figure below shows the normalised waveforms zoomed in around the inductor current negative to positive transition zero crossing.

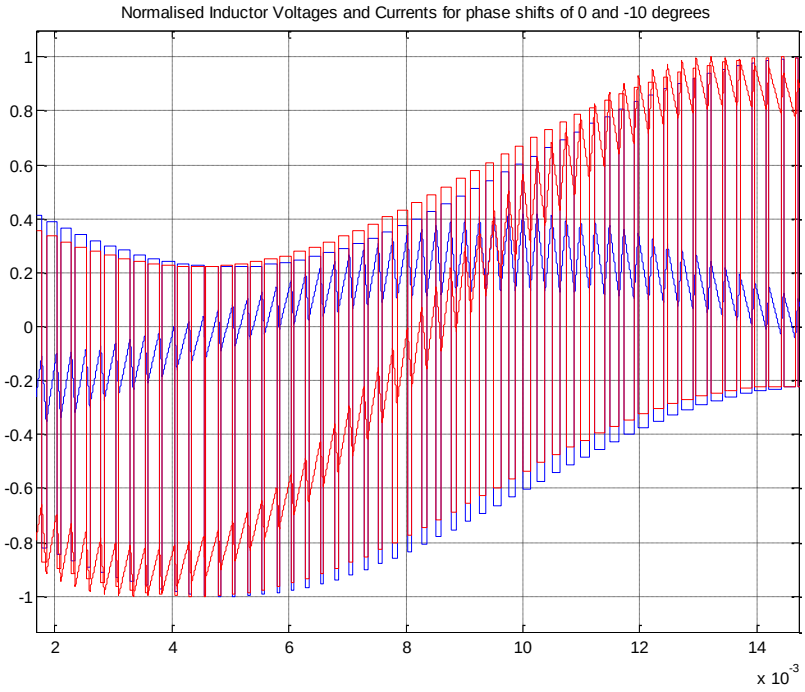

Figure 6-25 - Normalised inductor voltages and current for phase shifts of 0° and -10°

Looking at the inductor voltage it can be seen that with the negative phase shift (shown in red for $\delta = -10°$) the positive side voltage steps in the inductor voltage are greater in magnitude than they were at $\delta = 0°$ (in blue) and smaller for the negative side voltage steps. If we recall that the inductor current can be approximated as a series of linear ramps of slope given by:

$$\frac{1}{L}\left(\pm\frac{V_d}{2} - \tilde{V}_G\right) \approx \frac{v_{inductor}}{L}$$

Equation 6-14

It is then easy to see that an increased inductor voltage over a switch period will cause an increase in the change in current for the same switch period. Conversely, a reduction in the inductor voltage over a switch period will cause a reduction in the change in current for the same switch period.

We can also see that the switching pulse width has remained relatively constant which allows for direct comparison of the results for differing phase shifts (in reality the switching pulse width will have changed due to the required change in the modulation ratio to maintain a constant Q output but this has obviously not been significant for the given phase shift).

This explains why we see an inductor current with the introduction of a phase shift which climbs more rapidly during the positive switch period and falls at a slower rate during the negative switch period. The net result of this is an overall increase in the magnitude of the inductor current when a phase shift is introduced.

For completeness it should also be noted that there must be an equivalent behaviour in the negative going direction of the inductor current. That is, in order to reach a symmetrical negative peak value of inductor current the inductor voltage for a phase shifted STATCOM voltage must be less during the positive switch period and greater during the negative switch period. This is shown in the plot of the normalised inductor voltages and currents below.

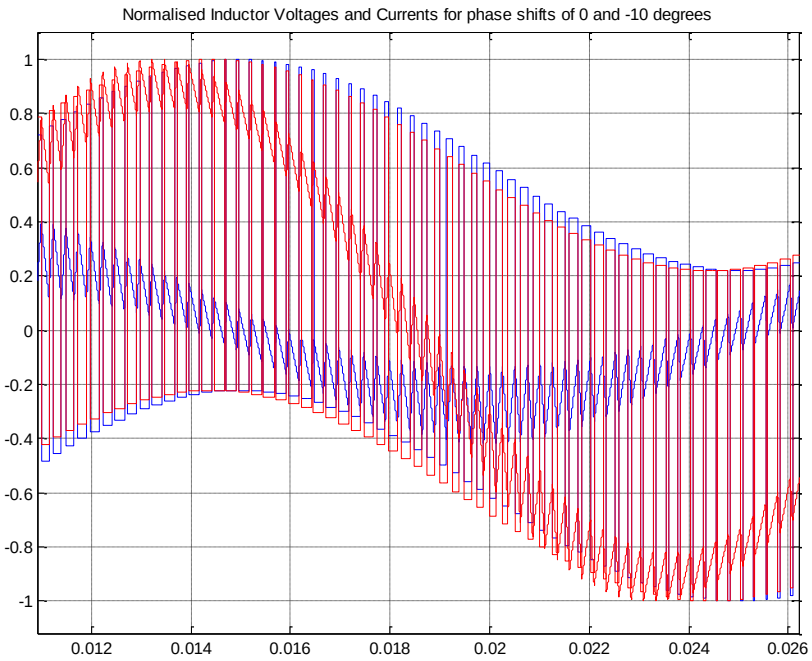

Figure 6-26 - Normalised inductor voltages and current for phase shifts of 0° and -10°

Comparing the difference in inductor voltages and currents for phase shifts of $\delta = -10°$ and $\delta = +10°$ it can be seen that in both cases it is the changes in the inductor voltage which cause the increase in the inductor current magnitude. The difference being the location of the voltage changes due to the phase shift sign with respect to the inductor voltage waveform. Plots for the normalised inductor current and voltage for the two cases are shown below for direct comparison.

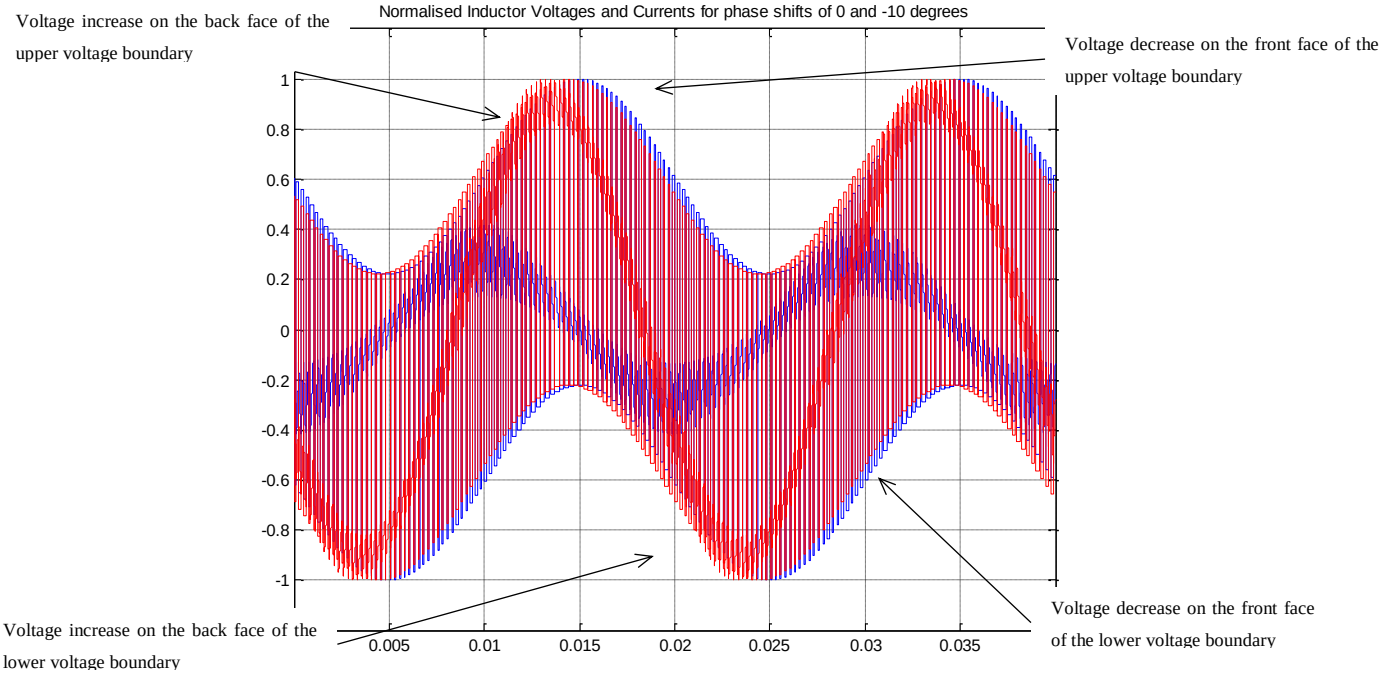

Figure 6-27 - Normalised inductor voltages and current for phase shifts of 0° and -10°

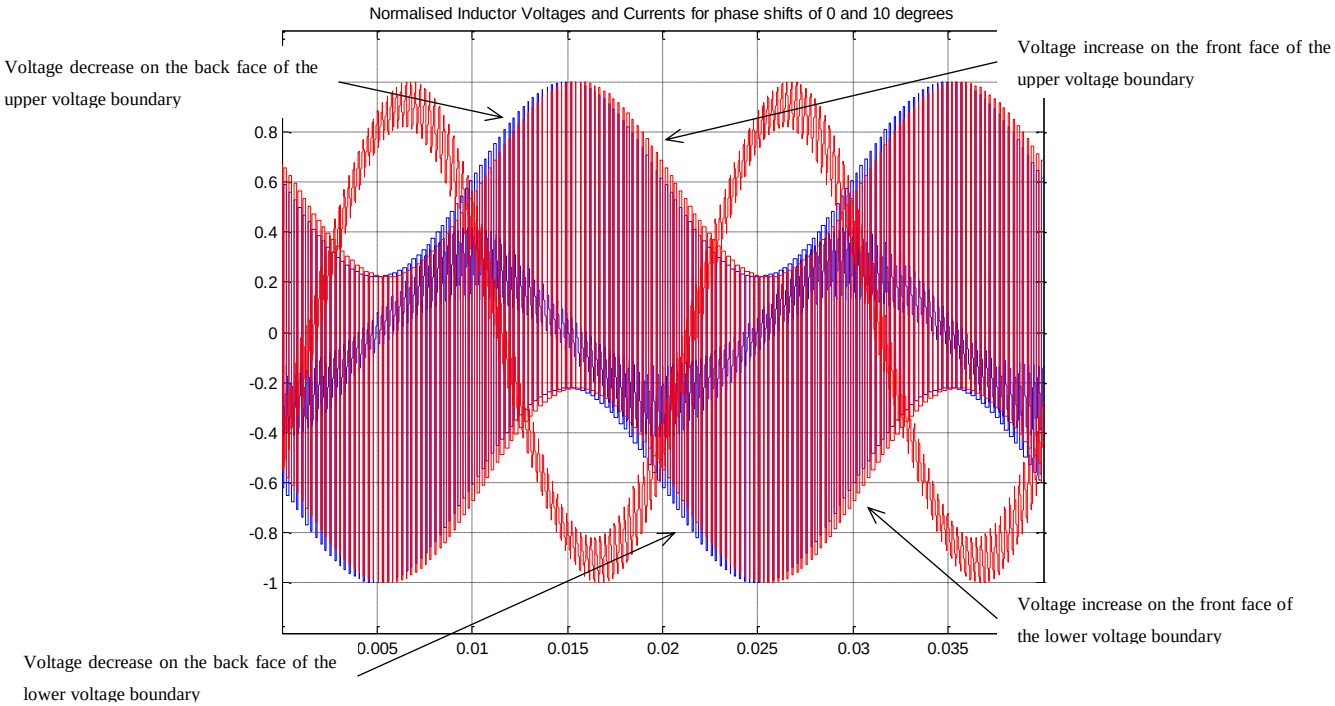

Figure 6-28 - Normalised inductor voltages and current for phase shifts of 0° and 10°

The differences caused by introducing a phase shift to the grid voltage can be summarised as follows;

Table 6-1 – Tabulated results for the introduction of phase shift to grid voltage

Inductor voltage waveform location	Negative phase shift	Effect on i_L	Positive phase shift	Effect on i_L
front face upper boundary	decreased voltage on positive pulse	reduced ramp in the positive direction	increased voltage on positive pulse	increased ramp in the positive direction
back face upper boundary	increased voltage on positive pulse	increased ramp in the positive direction	decreased voltage on positive pulse	reduced ramp in the positive direction
front face lower boundary	decreased voltage on negative pulse	reduced ramp in the negative direction	increased voltage on negative pulse	increased ramp in the negative direction
back face lower boundary	increased voltage on negative pulse	increased ramp in the negative direction	decreased voltage on negative pulse	reduced ramp in the negative direction

Just as was the case for our previous analysis, these results are not surprising in terms of creating a change in the active power flow and align with what we saw during our theoretical analysis.

If we now compare our observations for the two cases we studied above we can see that the net result of introducing a phase shift, whether it be on the STATCOM switched voltage or the grid voltage, we get the same result in terms of the changes to the inductor current.

What is important about this outcome is that this shows that the net effect on the DC bus voltage (or the charging or discharging the capacitors) will be the same for both cases. However, as we have seen, the exact way in which this is achieved is different for the two scenarios.

6.5 INSTANTANEOUS POWER

Before we move on from our analysis of the inductor current there is one more simple calculation we can perform to verify that the active power flow

is the same independent of the side of the current steering reactor in which the phases shift is introduced. This calculation is of course for the instantaneous power flow to/from the converter. The power calculation can be performed on either side of the current steering reactor using the well-known equation for instantaneous power;

$$p(t) = v_{grid}(t) \times i_{inductor}(t)$$

Equation 6-15

$$p(t) = v_{STATCOM}(t) \times i_{inductor}(t)$$

Equation 6-16

It should be noted that while these two equations will not give the same instantaneous values they will have the same value when averaged over one period of the grid voltage. Below are plot of the instantaneous power calculated on either side of the reactor for varying phase shifts and calculation approximations.

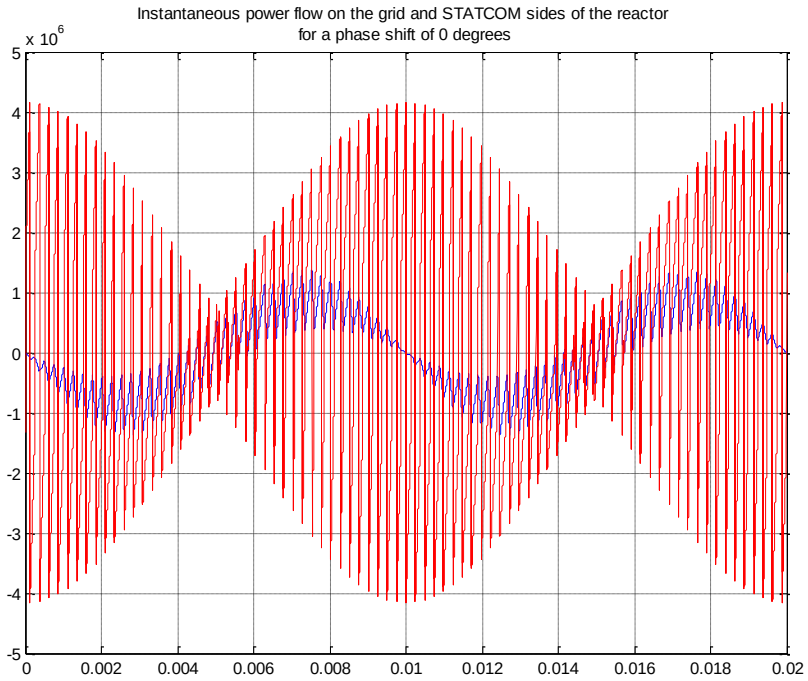

Figure 6-29 - Instantaneous power flow (no phase shift)

Here the calculation has been performed using the approximation of constant grid voltage over the switch period and with the phase shift applied to the STATCOM voltage. The grid side power is shown in blue and the converter side in red. Below is that same calculation with the phases shift applied to the gird side.

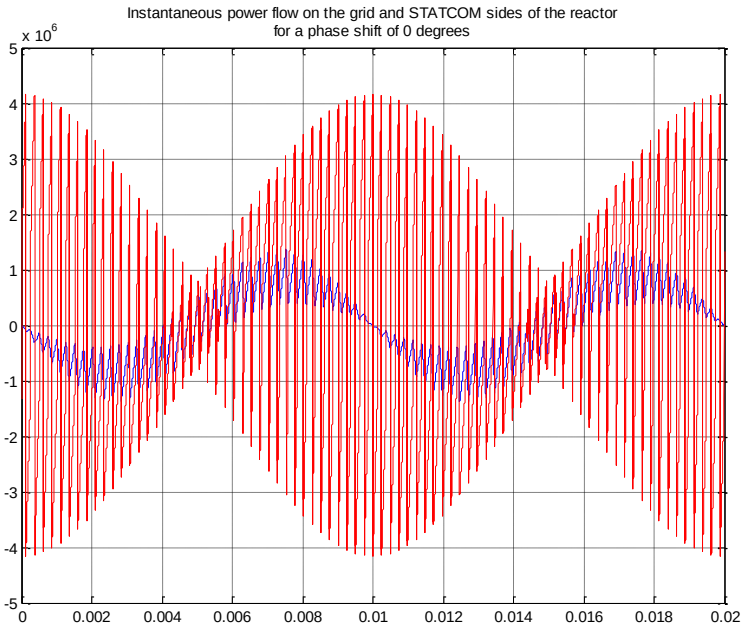

Figure 6-30 - Instantaneous power flow (no phase shift)

Comparing the two above plots we can see that they are almost identical. For completes the below plot has been calculated without the assumption of constant grid voltage over the switching period.

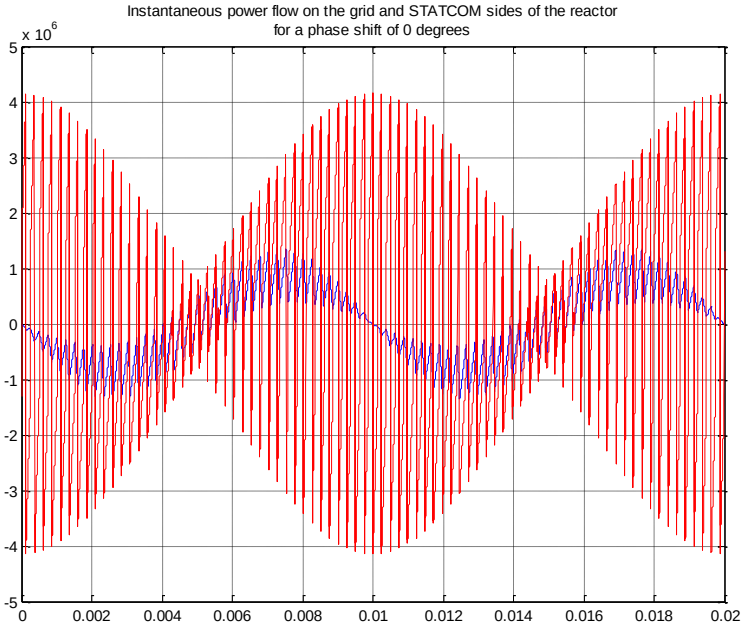

Figure 6-31 - Instantaneous power flow (no phase shift)

Again these results almost identical to that calculated above. Below is a plot of the instantaneous power for $\delta = -10°$.

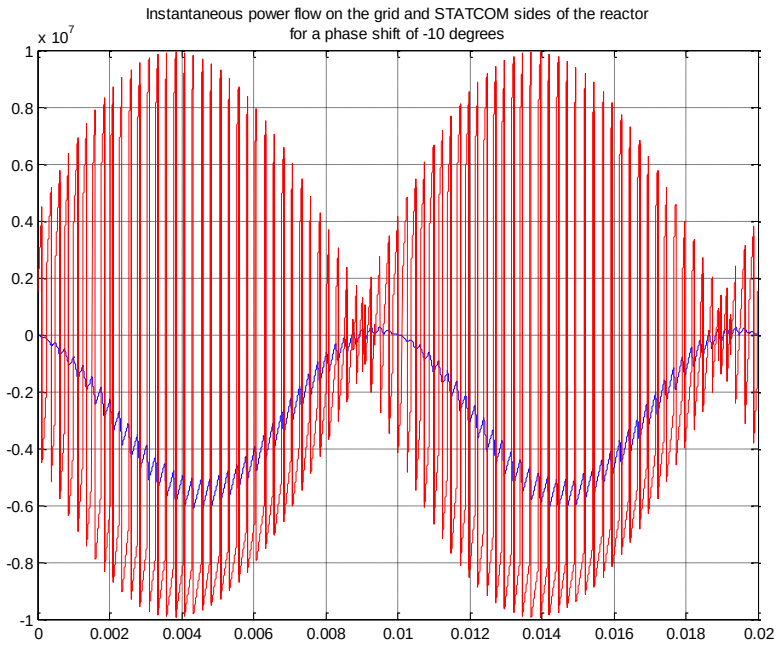

Figure 6-32 - Instantaneous power flow (-10° phase shift)

We can clearly from the plot of the grid side instantaneous power that there is a resultant negative power flow = active power flowing into the converter for $\delta = -10°$. This is somewhat more difficult to see in the plot for the converter side. Of course having calculated the instantaneous power flows we can also calculate the average power P using;

$$P = \frac{1}{T}\int_0^T p(t)\,dt$$

Equation 6-17

Note that the simulation based on no grid voltage averaging seems more accurate when calculating the average power flow.

6.6 DC BUS BEHAVIOUR

Now that we have satisfied ourselves that regardless of the exact mechanism which occurs at the switching level we get the same net effect on the inductor current for the introduction of a phase shift we can use the calculated inductor current to investigate the effects on the DC bus voltage.

We can with confidence say that for an increasing inductor current magnitude and a reducing phase shift between the inductor current and the grid voltage there will be an increase in the active power flow. To demonstrate this in terms of the DC bus voltage behaviour we will use the calculated inductor current to calculate the instantaneous charge flowing to/from the capacitor and thus determine the effect of the phase shift on the charge/discharge of the DC bus capacitors. The charge flowing into the capacitor can be found using;

$$i = \frac{dq}{dt}$$

Equation 6-18

$$\Longrightarrow q = \int i\, dt$$

Equation 6-19

Numerically we implement this equation as

$$q_{n+1} = q_n + (i \times \Delta t)$$

Equation 6-20

where i is the average current of the time period Δt. We can also use the well-known equation $i = C\frac{dv}{dt}$ to calculate the change in capacitor voltage based in the inductor current as;

$$\Delta V_{cap} = \frac{1}{C}\int_{t1}^{t2} i\, dt$$

Equation 6-21

which we numerically implement as

$$v_{n+1} = v_n + \frac{1}{C}(i \times \Delta t)$$

Equation 6-22

As per previous discussions we summarise the capacitor charging states as:

Table 6-2 – Capacitor changing states

Inductor current	Device state	Inductor current behaviour	Device conducting	Net effect
$i_L > 0$	IGBT upper 'on' & lower 'off	positive slope	IGBT upper	Discharge C_1
$i_L > 0$	IGBT upper 'off' & lower 'on'	negative slope	Diode D2	Charge C_2
$i_L < 0$	IGBT upper 'on' & lower 'off	positive slope	Diode D1	Charge C_1
$i_L < 0$	IGBT upper 'off' & lower 'on'	negative slope	IGBT lower	Discharge C_2

The instantaneous charge flow and resultant capacitor voltages have been calculated for C_1 and C_2 for no phase shift between the STATCOM fundamental and the grid voltage and is shown in the figure below.

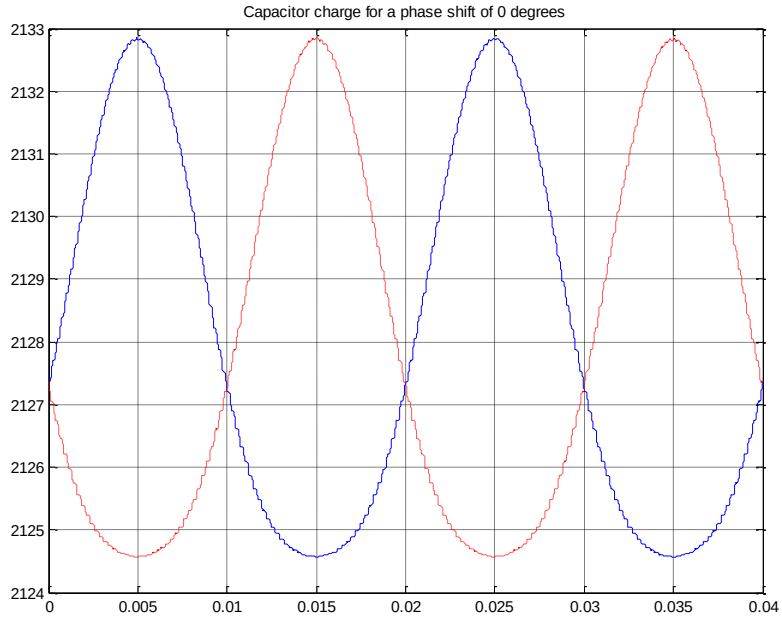

Figure 6-33 - Capacitor charge for 0° phase shift

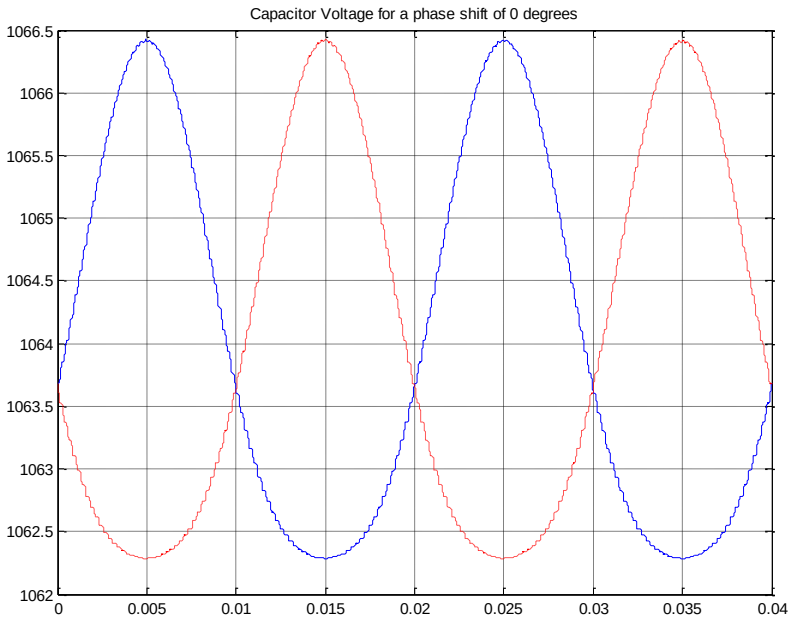

Figure 6-34 - Capacitor voltage for a phase shift of 0°

Here the initial capacitor charge and voltages have been set by the steady state DC bus voltages. That is, we have assumed a steady state voltage of 1064V which gives an initial charge state of 2128 Coulombs (for a 2F capacitor).

In addition to the capacitor voltage we can calculate the resultant DC bus voltage using the simple equation

$$v_d(t) = v_{C1}(t) + v_{C2}(t)$$

Equation 6-23

A plot of the DC bus voltage is shown below.

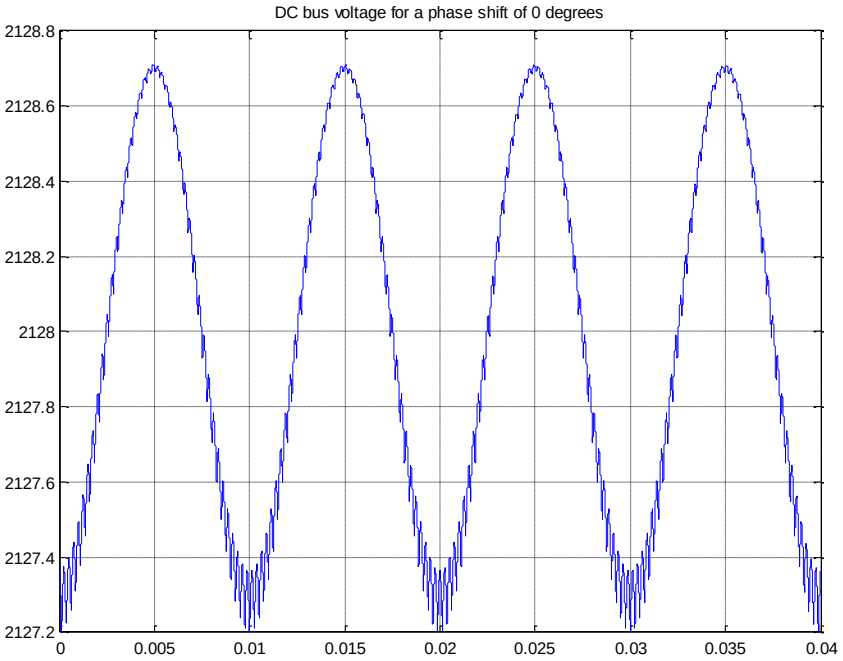

Figure 6-35 - DC bus voltage

From the plot of the DC bus voltage plot we can clearly see the 100 Hz ripple caused by the 180° phase shifted capacitor charging waveforms. It should also be noted that in calculating the capacitor charge, capacitor voltage and DC bus voltage values it has been assumed that the control

system is operating at steady state with the initial value for the voltage = target voltage for the capacitors. This is why we can see that the DC bus voltage has an average value of $2128V$.

To achieve this in our calculation we need to correct the average value of the calculated capacitor charge to make it equal to the initial or steady state value. This is achieved by integrating the charge over a period and then applying a correction to the calculated DC offset to make it equal to the steady state value. Once we have calculated the required offset we can then use this value as the initial condition for studies where $\delta \neq 0$.

If we look more closely at the capacitor voltage waveform we can see that it is composed of a piecewise series of parabolic followed by zero slope line sections. It can also be seen that as the charge of one capacitor charges (parabolic section) the charge on the other remain constant (zero slope section) and that the waveforms for the two capacitors are 180 degrees out of phase of each other.

This behaviour is explained by looking at Table 6-2 which details the charge and discharge states for the capacitors based on the instantaneous polarity of the inductor current and the state of the IGBTs. For example, we can see that for $i_L < 0$ capacitor charges for when the upper IGBT is in the 'on' state and remains in that state of charge when the upper IGBT is in the 'off' state. It does not discharge until the next half cycle when $i_L > 0$.

This behaviour can clearly be seen in the plot below.

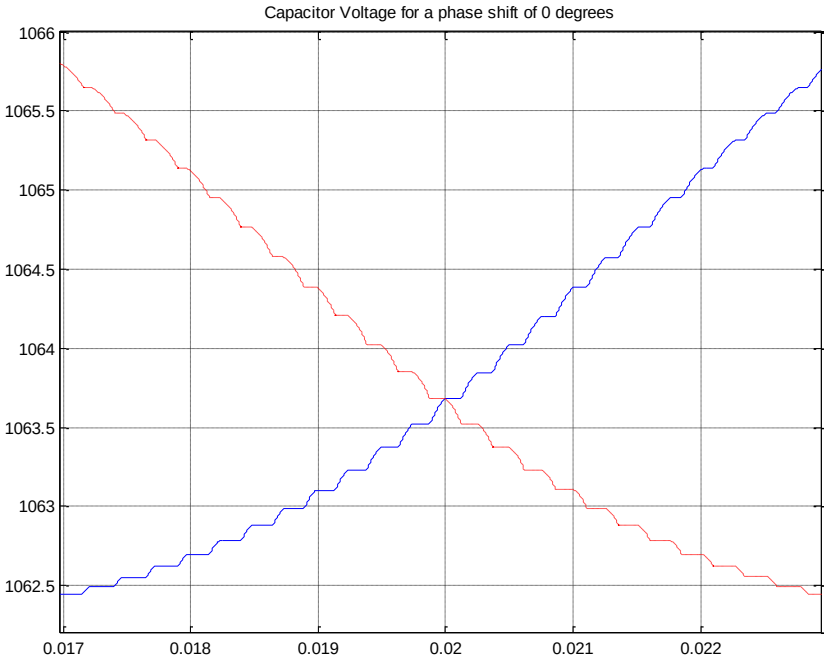

Figure 6-36 - Capacitor voltage for a phase shift of 0°

The 'parabolic' charging behaviour comes from the assumption of constant grid voltage over the switch period. This means that the current over the switch period will be a linear ramp which we can express as

$$i_{switch_{period}}(t) = kt$$

Equation 6-24

and thus

$$V_{cap}(t) = \frac{1}{C}\int i\,dt = \frac{1}{C}\int kt\,dt = \frac{k}{2C}t^2$$

Equation 6-25

which describes a parabolic form. It should be noted that if we did not make the assumption of constant grid voltage over the switch period then the

general form of the capacitor voltage waveform during the charge/discharge periods would be given by

$$V_{cap}(t) = \frac{1}{C}\int i\,dt = \frac{1}{LC}\int \left\{\pm\frac{V_d}{2} - \hat{V}_G sin(\omega t)\right\} dt$$

Equation 6-26

$$\Longrightarrow V_{cap}(t) = \pm\frac{V_d}{2}t + \frac{\hat{V}_G}{\omega}cos(\omega t)$$

Equation 6-27

which represents the sum of a linear ramp and a curve defines by the *cosine* term. It can be shown that our approximation closely follows this behaviour. The plot below shows a section of the capacitor charging voltage calculated using the two calculation methods (blue = using the approximation and red = using the time varying grid voltage). As we can see there is very little difference between the two.

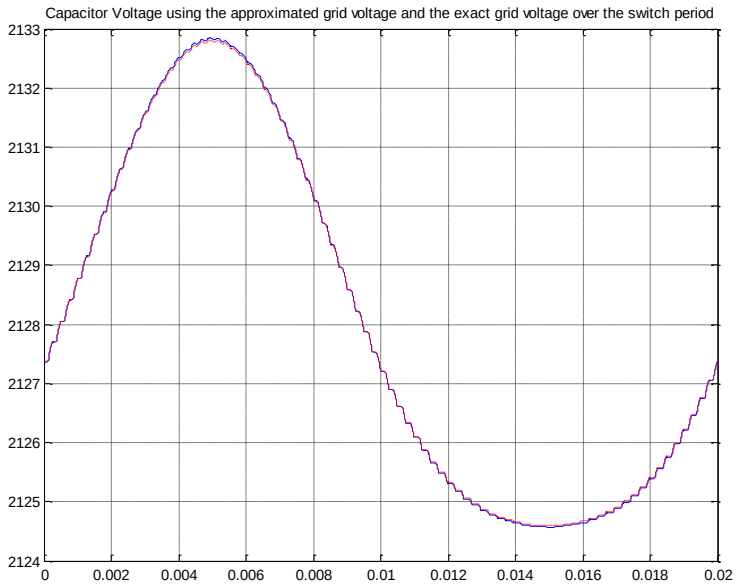

Figure 6-37 - Capacitor voltage using approximated and exact grid voltage

A zoomed in plot of the DC bus voltage is also shown below. As would be expected, the voltage waveform is composed of a series of piecewise parabolic sections which are comprised of the charge and discharge sectors of the two capacitors.

It should be noted that there is no section of constant voltage as we saw in the individual capacitor voltage waveforms. The reason for this is the alternate switching of the upper and lower IGBTs. That is, as we saw for the individual capacitor voltages, when one capacitor has a static voltage (or charge) the other is charging or discharging. The result on the overall bus voltage is a constantly changing instantaneous bus voltage.

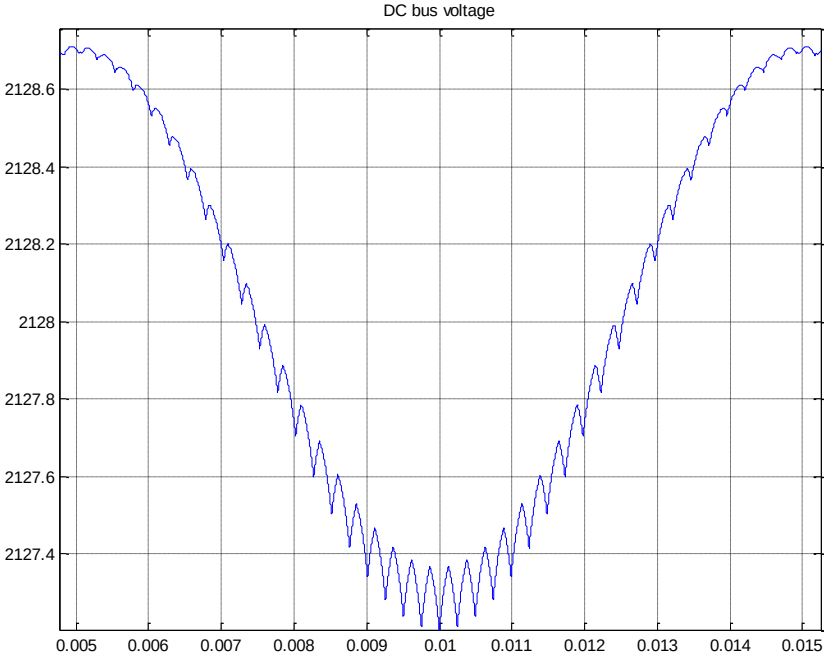

Figure 6-38 - DC bus voltage (zoomed in view)

To show the effect of active power flow into the converter the capacitor charge, capacitor voltage and DC bus voltage plots are shown below for a -1° phase shift between the grid voltage and the STATCOM fundamental voltage.

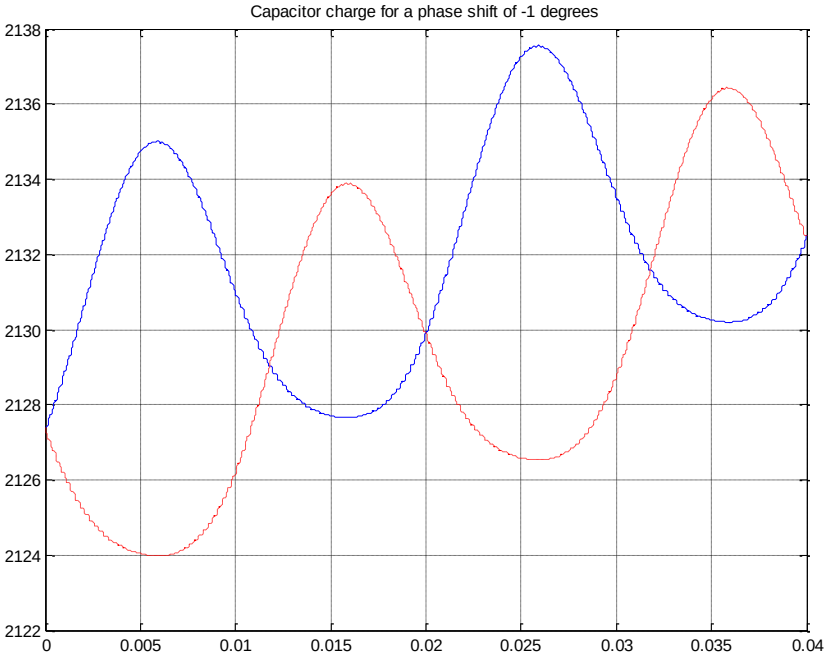

Figure 6-39 - Capacitor change for a phase shift of -1°

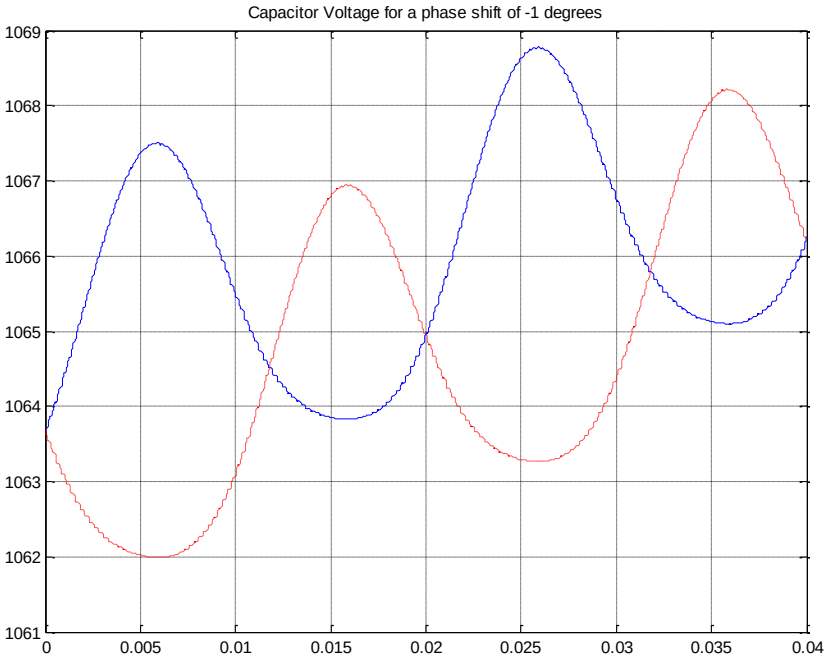

Figure 6-40 - Capacitor voltage for phase shift of -1°

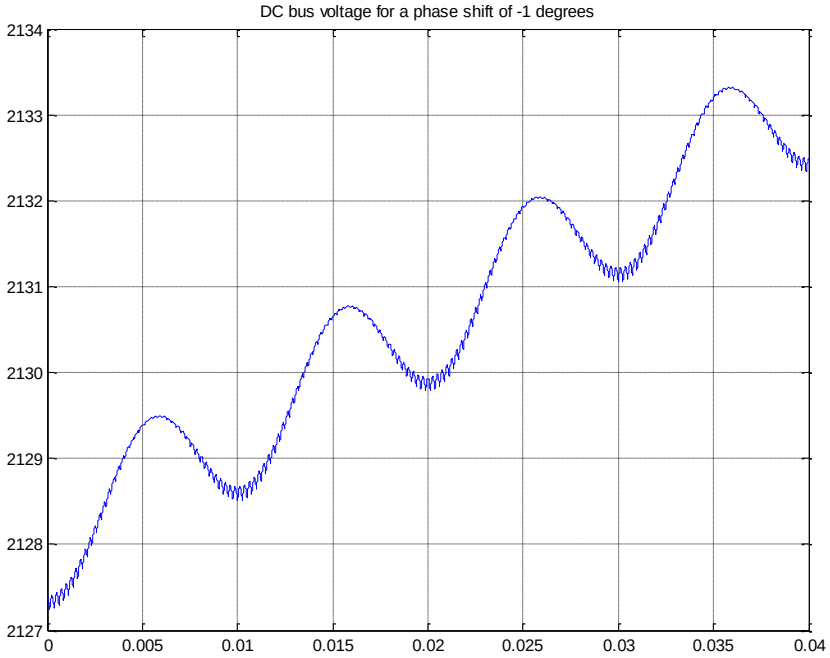

Figure 6-41 - DC bus voltage for a phase shift of -1°

As expected for a lagging phase shift there is a resultant increase in capacitor charge and voltage which results in an increasing DC bus voltage.

If we now compare these results with the theoretical prediction for the voltage change based on the active power equation;

$$\Delta V = -V_1 + \sqrt{V_1^2 + \frac{2P \times \Delta t}{C}}$$

Equation 6-28

for $V_1 = 2128V, C_{cap} = 2F$ and thus the bus capacitance is $C = 1F$, $\Delta t = 40 \times 10^{-3}$ (as the simulation shown above is over 2 cycles of the grid frequency) and

$$P = \frac{|V_G||V_S|}{\omega L_S}\sin(\delta) = \frac{|V_G|\left(m_a\frac{V_d}{2}\times\frac{1}{\sqrt{2}}\right)}{\omega L_S}\sin(\delta)$$

Equation 6-29

$$P = \frac{480\left(0.676\times\frac{2128}{2\sqrt{2}}\right)}{2\times\pi\times 50\times 50\times 10^{-6}}\sin(1°) = 2.7124\times 10^5$$

Which gives a change in voltage of:

$$\Delta V = -2128 + \sqrt{2128^2 + \frac{2\times 2.7124\times 10^5\times 40\times 10^{-3}}{1}} = 5.0924V$$

We must of course remember that this voltage represents the change in the bus voltage which would be equally split across the two series connected capacitors. That is, the capacitor voltage change predicted is 2.5462V which aligns with the calculated values above.

Note – it is important to remember that the voltage change predicted is the average voltage as the bus voltage is itself sinusoidal in nature.

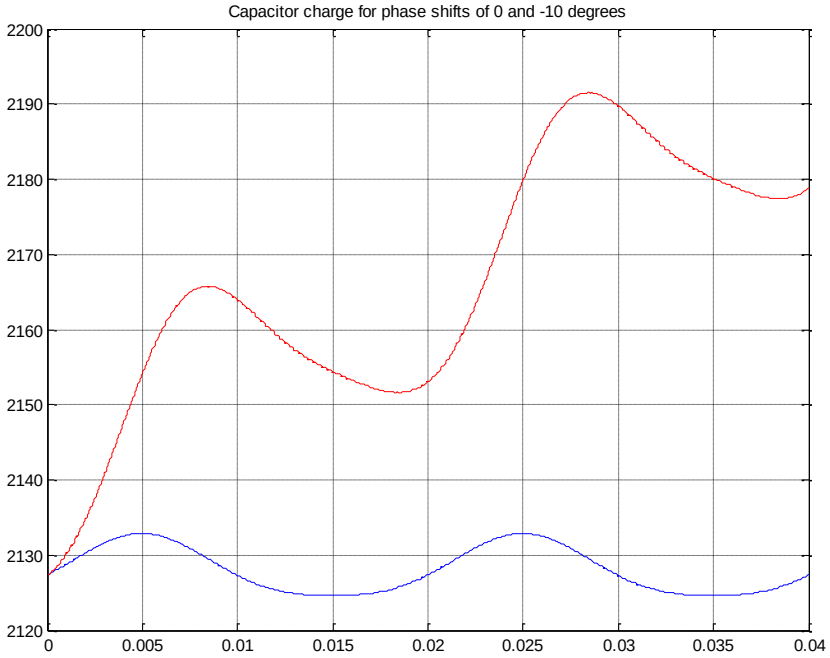

Figure 6-42 - Capacitor charge for phase shifts of 0° and -10°

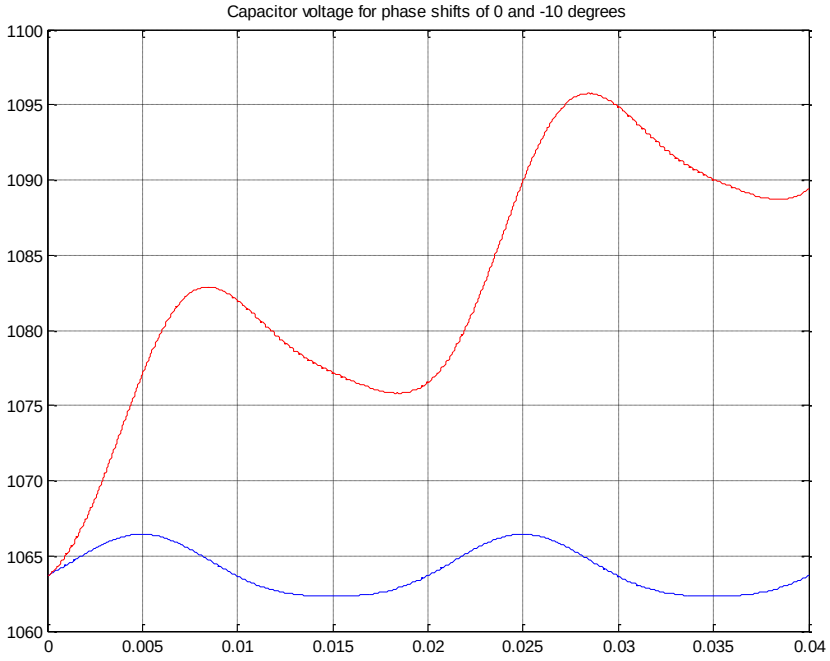

Figure 6-43 - Capacitor charge for phase shifts of 0° and -10°

Here we can see that for $\delta < 0$ while the over charge (and thus voltage) increases the depth of discharge is in fact greater than that for $\delta = 0$. We can also see from theses plots that the charge and discharge times are the same. This is probably more evident from the fact that independent of the phase angle the frequency of the charge and voltage cycles must remain the same and equal to the grid frequency.

The conclusion we can draw from this is that while the discharge rate is greater for $\delta < 0$ the increases in the charge rate is even greater. This means that whilst the diode conduction times are unchanged, the net increases in capacitor charge comes from an increase in the resultant current which flows during the conduction time.

6.7 NETWORK TRANSIENTS

The next point of this analysis is to assess what happens within the STATCOM as a network transient occurs. A three phase STATCOM such as the one installed at St. George Substation could be subject to a number of network transient scenarios and a number of power system protection related operations can cause the STATCOM to react.

The most common types of power system protection faults are the following:

- Single Phase to Ground (Ph-E) fault: Where ***only one*** of the phase conductors has direct or indirect conduction to the general mass of earth (e.g. Tree branch gets in contact with phase conductor, due to its proximity)

- Phase to Phase (Ph-Ph) fault: Where ***two conductors only*** become in contact with each other (e.g. Two conductors clashing during a storm or a tree branch falling across two conductors, but **not** providing a path to the general mass of earth)

- Three Phase (3Ph) fault: Where ***all three (3) conductors*** become ***simultaneously*** in contact with each other (e.g. All three conductors simultaneously clashing during a storm or a tree branch falling across all three conductors simultaneously)

- Phase to Phase to ground (Ph-Ph-E) fault: Where two of the conductors become in contact with each other and a path of to the general mass of earth is simultaneously established (e.g. A three branch - ***still attached to a tree*** clashes with two conductors providing a path for a portion of the fault current to be injected into the general mass of earth)

The protection to the above mentioned faults is managed by the protection system of the network portion under fault, however, as a result of operation of the protection system, commonly load rejection occurs and as a consequence the STATCOM will sense changes in phase and / or voltage magnitude between itself (V_S) and the grid (V_G).

The above is a reasonably common occurrence in any electrical network, but what is interesting about the St. George Substation is the fact that due to its location with the Ergon Energy network and the configuration of the system, St. George has what is considered a "weak" feeder. This "weak" characteristic of the radial supply at St. George is due to its reasonably high Thevenin equivalent impedance which diminishes its capacity to supply fault current when a fault occurs.

This lack of capacity of the feeder causes a reasonable amount of voltage changes should a fault occur around this part of the electrical network and any load rejection around the Substation could cause network transients which will affect the operation of the STATCOM.

Let's now remind ourselves that the STATCOM at St. George Substation is a three phase device and the model developed during this project is a single phase STATCOM. The reason why this is important is that, there are only a limited number of scenarios which could be considered for a network

transient within this model. While there are a number of scenarios which could be simulated, the following scenario has been chosen and the argument for this choice is supported as follows:

Let's assume that a fault occurs within the first couple of transmission towers just outside St. George Substation's boundary and this fault is a Phase to Ground (Ph-E), as this is a single phase system and it is the only type of line fault that is possible in this system.

The simulation for this fault is done over a $1{,}000ms$ period and is comprised of purely resistive fault impedance $Z_f = 1\Omega$ on the active conductor to ground.

The philosophy of operation of this simulation is as follows:

- Much like in the previous simulations, there is a delay in the initial operation of the STATCOM (40ms)
- After this initial period, the STATCOM starts to operate and falls into steady-state within the first 200ms (supplying all the Reactive Power needed by the load)
- For the purpose of the analysis, there is a wait period of another 100ms, then an 1Ω fault is applied to the active conductor and remains active for 5ms.
- It takes another 200ms for the STATCOM to recover into steady-state, where it operates until the end of the simulation.

The simulation results for the above described fault are depicted below:

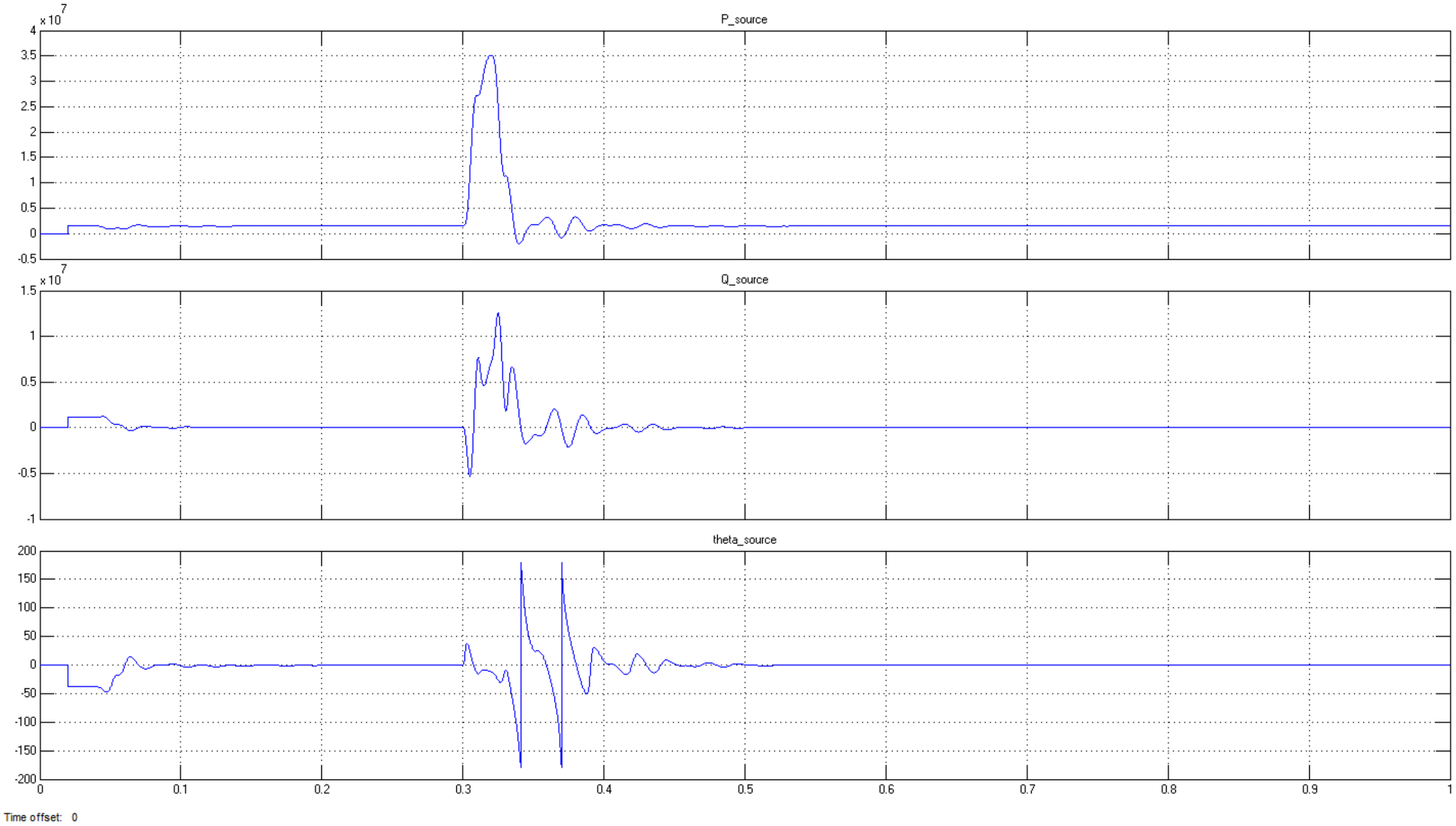

Figure 6-44 - Simulation results for fault condition (network perspective)

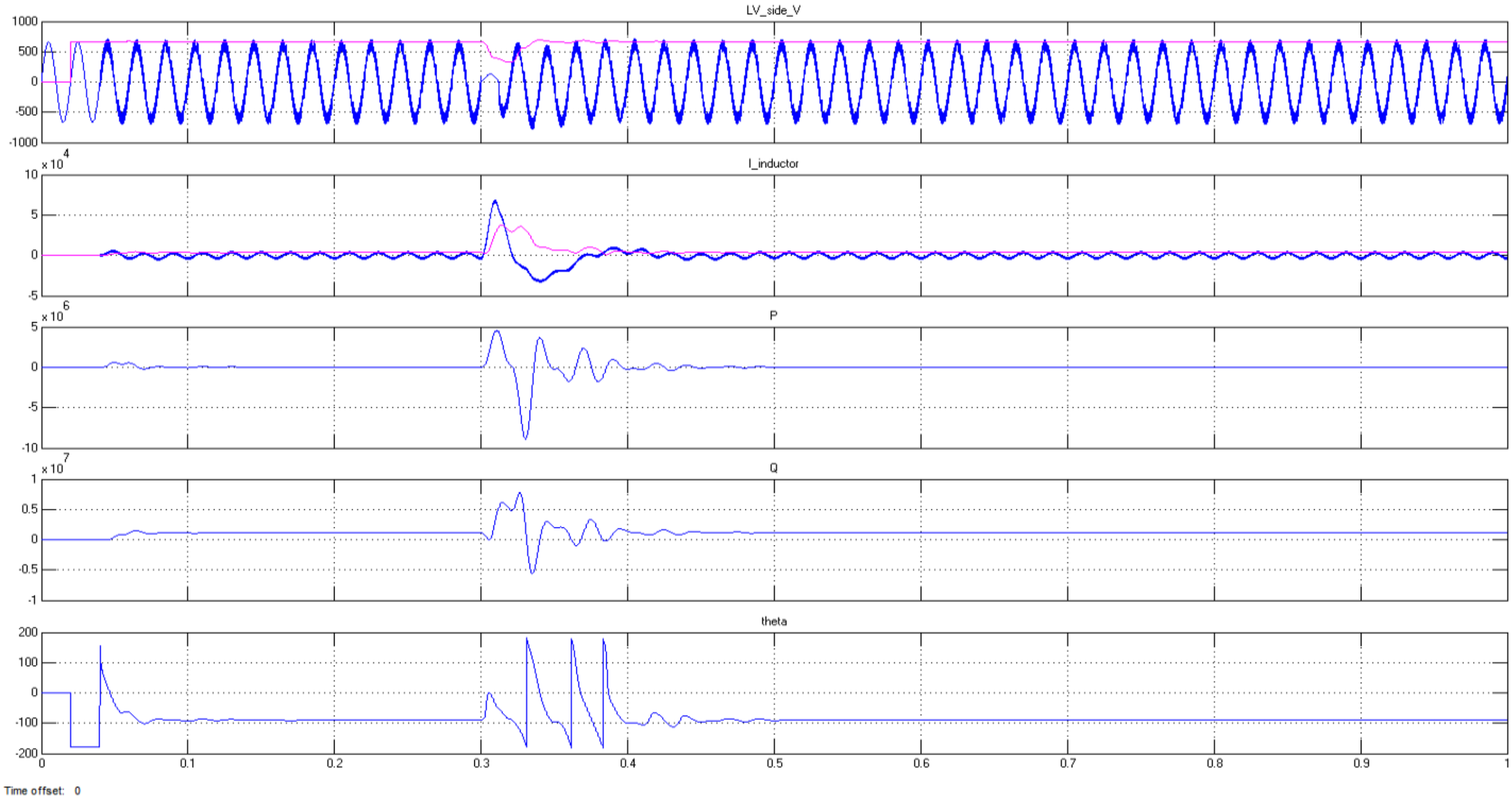

Figure 6-45 - Simulation results for fault condition (STATCOM perspective)

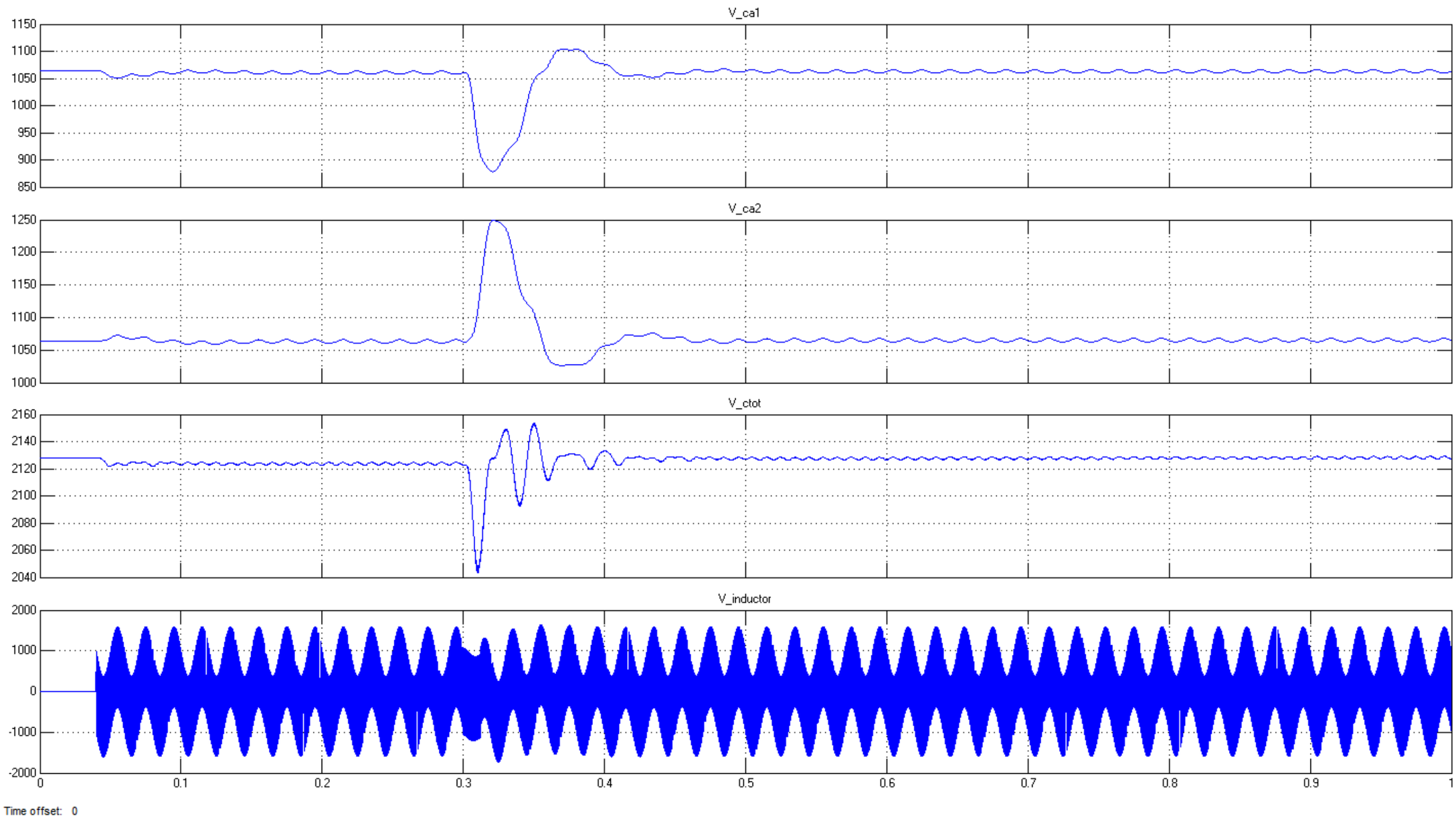

Figure 6-46 - Open-loop DC bus reaction to the fault

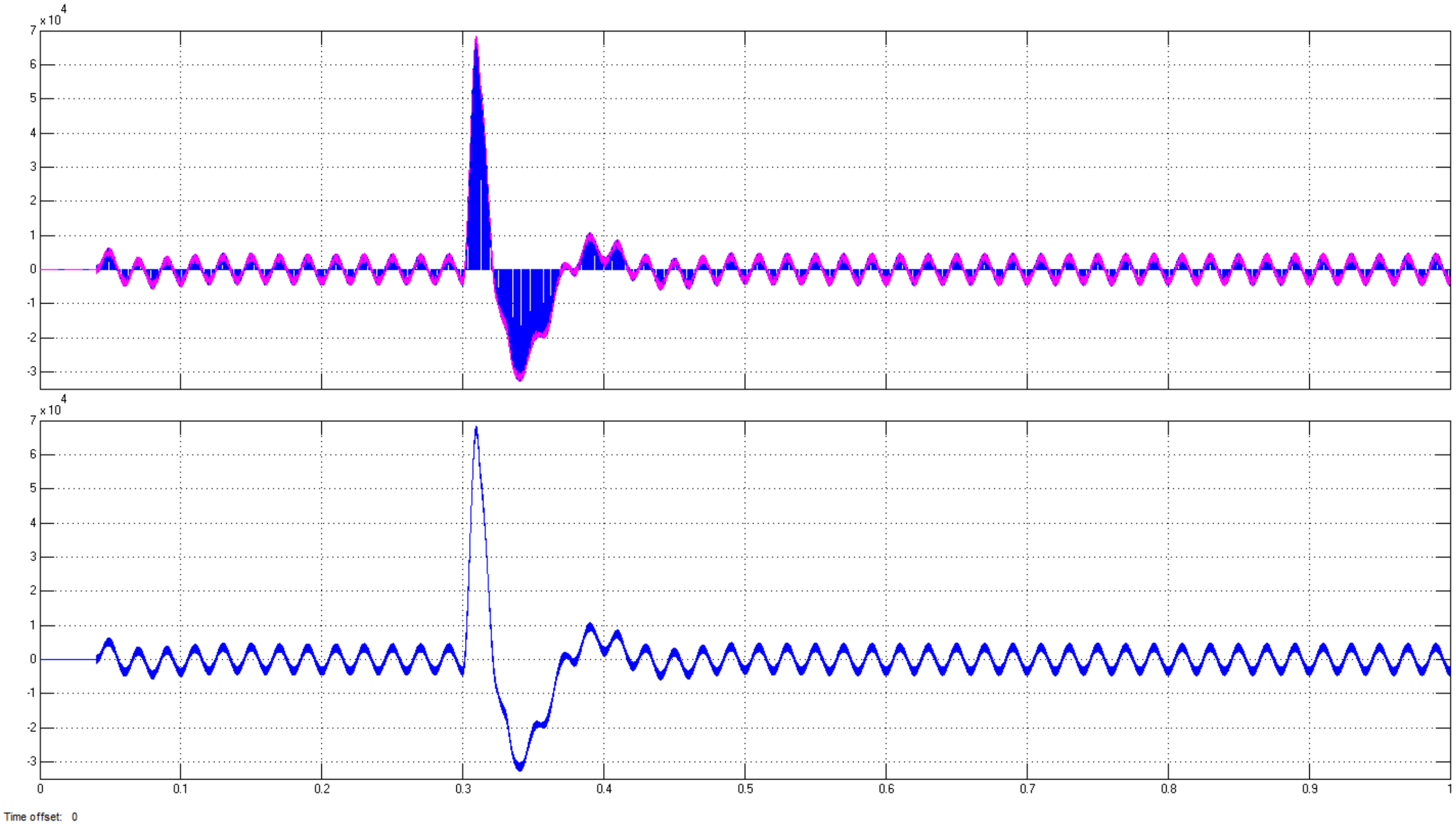

Figure 6-47 - IGBT plus diode currents and Inductor current

Remembering that we are considering an open-loop control system for this STATCOM model, we should also consider that any protection system would be too slow to operate within the fault period and for this reason the applied fault period is limited to 5ms.

The result of this simulation is shown in Figure 6-44 and this shows the electrical network's perspective into the fault, or how the network perceives the fault. During the fault period the network has to delivery around $35MW$ of Active Power to the fault. But we are able to see that after a transient period of around 200ms, the system is back into steady-state operation.

In Figure 6-45, we can clearly see the reaction of the STATCOM to the fault in the system and especially how this makes the STATCOM perceive a transient within the system. While the top graph shows how the inductor voltage drops due to the fault, we can see that level of current delivered by the STATCOM via the current steering reactor is in excess of $68kA$. Followed by the amount of Real and Reactive Power delivered by the STATCOM towards the fault.

Interestingly, in Figure 6-46, we see that even though the fault current delivered by the STATCOM is shown as of in excess of $68kA$ (Figure 6-45), as the fault has a reasonable short duration, the recovery of the open-loop DC bus is of reasonable effect. Also, while there is an unbalance of voltage in each capacitor from the DC bus this unbalance is reasonably symmetrical and allows the DC bus to recover from the fault within around 150ms.

Not surprisingly, Figure 6-47 shows that the level which the current magnitude reaches is also in excess of $68kA$, but it demonstrates the fast recovery of the STATCOM in this modelled scenario is theoretically possible.

Overall this simulation shows that even in an open-loop configuration, the STATCOM is able to deal with a simple network transient and its DC bus is able to recover from that transient reasonably fast.

It is important to additionally mention that by implementing a control system to manage the DC bus within the model (such as the D-VAR® STATCOM's control system) would allow to cater for situations when the DC bus becomes unsymmetrical to a greater level than the one modelled within this project and would be of great value if implemented in a three phase model of any future works.

7 CONCLUSION

Based on the above finding a number of conclusions are drawn in regards to the operational capabilities of the open-loop STATCOM model developed.

While the initial aim of this project was to create a three phase model of the STATCOM as the project progressed, it became clear that within the time restrictions enforced by the length of the project subjects (ENG4111 and ENG4112 – Research Project 1 and 2 respectively) it would not have been possible to achieve reasonable outcomes.

Additionally, the limitation of information imposed by AMSC's IP guidelines did not create an issue for the outcome of this project as the main interest was not to study the control system operational response for this STATCOM, but to study how the power-electronics systems act, react and operate. Although, knowledge of the control system philosophy would have been advantageous during the modelling process.

This dissertation provides insight in how an open-loop controlled single phase STATCOM operates and since the each of the DBR boards in imbedded within the three phase STATCOM further work needs to be done as to achieve more realistic results for the reasons why the DBR boards have failed in the D-VAR® STATCOM.

7.1 DC BUS ANALYSIS

It was found the regardless of the switching strategy operation (PWM), changes in charge of the DC bus are directly related only to the amount of Active Power delivered / absorbed by the STATCOM.

By changes the inductor current and angle between it and the grid voltage (ϕ) or Power Factor angle, will significantly change the amount by which the DC bus gets charged or discharged.

While ideally the STATCOM will be operating in a "purely Reactive" state (either inductive of capacitive), the losses within the STATCOM still have to be supplied by the network, otherwise unnecessary discharge of the DC bus will occur.

While in operation, if a certain amount of Active Power is flowing "towards" the STATCOM any surplus from the supply of losses within the STATCOM will charge the DC bus without the need of control system operation.

7.2 EFFECTS OF NETWORK TRANSIENTS ON DC BUS

Following the finds with respect to the DC bus and switching strategy, a number of simulations were done and these show that the modelled STATCOM has the ability to reasonably recover from the applied transient in the system without any major to its DC bus.

Considering the limitations of the model the simulation performed has shown that when a fault of 1Ω is placed on the equivalent transmission line for 5ms, upon the return to steady-state the DC is able to return to a reasonably close voltage value without the use of a control system for its regulation.

This return close to its nominal voltage value is attributed only to the changes in the ϕ (Power Factor angle), but a more comprehensive analysis will be of great advantage to achieve a more definitive answer to the effects of network transients in the DC bus voltage of the modelled STATCOM.

Also due it the DC bus capacitors configuration within the three phase model, the above results are inconclusive in regards to the real effect of transients in the D-VAR® STATCOM, but provide an helpful insight in the effects of the single phase model STATCOM used during this project.

8 SAFETY

This project is a theoretical assessment of the operational characteristics of the D-VAR® with particular attention to the DC bus voltage building and effects of system transient in the DC bus.

All the work to be performed during the delivery of this project will be performed in a domestic environment which presents hazards that should be managed and risks that should be mitigated, these include but are not limited to; slips, trips and falls, poor house-keeping and the like.

Furthermore, due to the nature of the approach used in this analysis, ergonomic hazards are present and need to be monitored closely and the correct methods should be used when carrying out the various tasks.

The tool used in the process of assessment of the risk is Table 8-1 – Risk Matrix (Protech Power):

Table 8-1 – Risk Matrix (Protech Power)

			CONSEQUENCE				
			1	2	3	4	5
			Negligible	Minor	Moderate	Significant	Severe
LIKELIHOOD	5	Very Likely	Medium (5)	Medium (10)	Med High (15)	High (20)	High (25)
	4	Likely	Low Med (4)	Medium (8)	Med High (12)	Med High (16)	High (20)
	3	Possible	Low (3)	Medium (6)	Medium (9)	Med High (12)	Med High (15)
	2	Unlikely	Low (2)	Low Med (4)	Medium (6)	Medium (8)	Medium (10)
	1	Very Unlikely	Low (1)	Low (2)	Low (3)	Low Med (4)	Medium (5)

The above risk matrix was developed by and is currently used by Protech Power, my current employer, and will be used during this project to assist in the risk assessment of the tasks undertaken during this project.

As with most risk assessment procedures, risk rating is to be carried out and re-assessment of the risk is to be carried out once implementation of control measures took place.

8.1 RISK RATING

- High risk activities (risk rating ≥20) – activity is not to go ahead, under any circumstance.

- Medium High risk activities (12 ≥ risk rating ≥ 19) – activity is not to go ahead, consultation with sponsor is to take place – re-assess.

- Medium risk activities (5 ≥ risk rating ≥ 10) – activity is not to go ahead, consultation with sponsor is to take place – re-assess.

- Medium Low risk activities (4 risk rating) – activity may go ahead, provided authorisation from sponsor has been granted and re-assessment of risk is completed periodically.

- Low risk activities (1 ≥ risk rating ≥ 3) – activity can go ahead without previous approval from sponsor – re-assessment of risk is completed periodically.

All activities through-out this project will be carried out following the above mentioned methodology of risk assessment, ensuring the safe completion of the project.

9 RESOURCES

The only resource requirement for the successful completion of this project is a current student license of MATLAB® and SimPowerSystems®, both MathWorks® software Applications, which I currently hold a license to R2013a version.

No other resource will be required as this is a purely theoretical project.

10 TIMELINE

This project timeline is based on the various deadlines imposed by the University of Southern Queensland for the successful completion of the project. The project consists of a number of critical tasks to achieve the aims of this project. Table 10-1 shows these tasks with expected completion dates.

Table 10-1 – Project timeline description table

Task number	Task Description	Estimated Completion Date
1	Project proposal submission	11/03/2015
2	Project Specification	18/03/2015
3	Literature Review	25/05/2015
4	Preliminary Report *(extension granted by Chris Snook)*	10/06/2015
5	Complete MATLAB® SimPowerSystems model	26/06/2015
6	Perform analysis of model to describe power electronics principles of the DC bus control within D-VAR®	31/07/2015
7	Investigate the effects of transients in the network and DC bus voltage	07/08/2015
8	Suggest possible issues and solutions which may allow DC bus voltage to be built in transient system conditions	14/08/2015
9	Finalise partial draft dissertation	12/09/2015
10	Partial draft dissertation	16/09/2015
11	Apply suggestions given by supervisor following partial draft dissertation assessment	26/10/2015
12	Dissertation Submission	29/10/2015

Following the successful submission of this preliminary report the following steps will be taken to ensure that the project is kept within the imposed time.

It is critical that each task is completed to a satisfactory level in order to proceed to the next step and this will guarantee a successful completion of the project within the available time.

This progress will be closely managed by constant communication between myself, the project supervisor (Dr Tony Ahfock – University of Southern Queensland) and the project sponsor, (Dr Andrew Hewitt – Ergon Energy).

11 REFERENCES

Ahfock, T. & Bowtel, L., 2006. *DC offset elimination in a single-phase grid-connected photovoltaic system.* Melbourne, AUPEC'.

American Super Conductor (AMSC), 2013. AMSC Corporate Overview. In: A. S. C. (AMSC), ed. MA: AMSC Voltage Stability and Transmission Technology Workgroup.

Australian Energy Market Commission, 2015. *National Electricity Rules Version 68.* [Online] Available at: http://www.aemc.gov.au/getattachment/5fcd7e63-b078-4ff8-a161-642f22fdde51/National-Electricity-Rule-Version-68.aspx [Accessed 23 February 2015].

Ekanayake, J. B. & Jenkins, N., 1996. A three-level Advanced Static VAr Compensator. *IEEE Transactions on Power Delivery,* 1 January, 11(1), pp. 540 - 545.

Gharedaghi, F., Jamali, H., Deysi, A. & Khalili, A., 2011. *Journal of Basic and Applied Scientific Research.* [Online] [Accessed 14 October 2014].

Hingorani, N. G. & Gyugyi, L., 2000. *Understanding FACTS - concepts and technology of flexible AC transmission systems.* Unknown ed. Delhi: John Wiley & Sons.

Krishna, B. V., 2014. Realization of AC-AC Converter Using Matrix Converter. *International Journal of Advanced Research in Electrical, Electronics and Instrumentation Engineering,* 3(1), pp. 6505 - 6512.

Marin, R. D., 2005. *Detailed analysis of a multi-pulse STATCOM.* [Online] Available at: http://www.gdl.cinvestav.mx/jramirez/doctos/doctorado/Predoctoral.pdf [Accessed 24 November 2014].

Mohan, N., Robbins, W. P. & Undeland, T. M., 1989. *POWER ELECTRONICS: Converters, Applications and Design.* unknown ed. New York: John Wiley & Sons, Inc..

Rashid, M. H., 1988. *Power Electronics - Circuits, Devices and Applications.* First Edition ed. New Jersey: prentice-Hall, Inc..

Shen, C., Yang, Z., Crow, M. L. & Atcitty, S., 2000. *Control of STATCOM with energy storage device.* [Online] Available at: http://ieeexplore.ieee.org.ezproxy.usq.edu.au/stamp/stamp.jsp?tp=&arnumber=847313
[Accessed 12 May 2015].

Siemens, 2015. *Wotonga SVC Plus Substation*, Mackay, Australia: Siemens.

Stevenson Jr., W. D., 1975. *Elements of Power System Analysis.* 3rd ed. New York: McGraw-Hill.

Vedam, R. S. & Sarma, M. S., 2009. *POWER QUALITY VAR Compensation in Power Systems.* Boca Raton, FL: CRC Press.

Wang, H. F., unknown. *Modelling STATCOM into Power Systems.* [Online] Available at: http://ieeexplore.ieee.org.ezproxy.usq.edu.au/stamp/stamp.jsp?tp=&arnumber=826734
[Accessed 20 May 2015].

12 APPENDIX

12.1 APPENDIX A – PROJECT SPECIFICATION

In July 2013 Ergon Energy commissioned its first STATCOM into the 66kV network at its St George substation. During the commissioning of the STATCOM and its first year of service there were a number of problems encountered which highlighted the need for Ergon Energy to develop its understanding of how the STATCOM operates to allow for ongoing fault finding and maintenance requirements.

Whilst the STATCOM is supported by the manufacturer and much of the detailed technical details of its operation remains proprietary information Ergon Energy engineering believes that in order to be able to support this device for its expected service life it is important to have a base level understanding of how the STATCOM operates.

The key objectives of this research project will be:

- Develop a mathematical single phase model of the St. George STATCOM
- Provide an explanation of how power electronic switching is performed in a STATCOM (with a focus on the strategy used in the Ergon Energy STATCOM)
- Perform an assessment on how the switching strategy influences the DC bus voltage within the STATCOM model
- Investigate the effects of system transients on the DC bus voltage

12.2 APPENDIX B – GENERATOR EQUATION DERIVATION

Consider the simplified system represented in Figure 12-1 below.

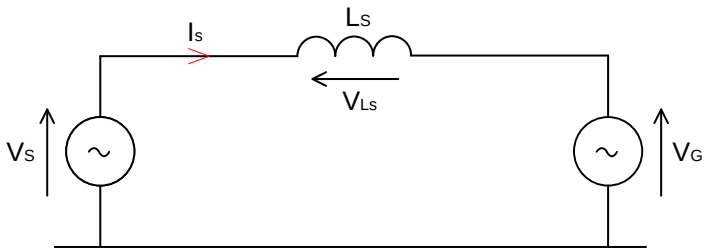

Figure 12-1 - STATCOM connected to the power network (equivalent circuit)

Where:

- V_S is STATCOM voltage,
- V_G is grid voltage and
- L_S is STATCOM inductance.

Taking the grid voltage as the reference voltage we can further define the STATCOM and grid voltage as:

$$V_S = |V_S| \angle \delta$$

Equation 12-1

$$V_G = |V_G| \angle 0°$$

Equation 12-2

Where $|V_G|$ and $|V_S|$ are the RMS values of the grid and STATCOM voltages respectively.

From which we can express the current *leaving* the STATCOM as:

$$I_S = \frac{V_{Ls}}{j\omega L_S} = \frac{|V_S|\angle\delta - |V_G|\angle 0}{j\omega L_S}$$

Equation 12-3

And thus we can express the power flow from the STATCOM into the network by deriving the following equations:

$$S = P + jQ = V_G I_S^* = \frac{|V_G||V_S|\angle - \delta - |V_G|^2\angle 0}{-j\omega L_S}$$

Equation 12-4

Through algebraic manipulation of Equation 6-12, the following equations are developed.

$$S = P + jQ = V_G I_S^* = \frac{|V_G||V_S|[\cos(\delta) - j\sin(\delta)] - |V_G|^2}{-j\omega L_S}$$

Equation 12-5

$$S = P + jQ = V_G I_S^* = \frac{|V_G||V_S|}{\omega L_S}\sin(\delta) + j\left[\frac{|V_G||V_S|}{\omega L_S}\cos(\delta) - \frac{|V_G|^2}{\omega L_S}\right]$$

Equation 12-6

That is:

$$P = \frac{|V_G||V_S|}{\omega L_S} sin(\delta)$$

Equation 12-7

and

$$Q = \frac{|V_G|}{\omega L_S} \times (|V_S| cos(\delta) - |V_G|)$$

Equation 12-8

It is important to note that the sign of both real and reactive power flow, shown in Equation 12-7 and Equation 12-8 represent the mode which the STATCOM is operating.

A change in $|V_G|$ due to changes in the system condition will also affect P and Q, it is also possible that the phase angle of $\overrightarrow{V_G}$ (recall that we assumed that $V_G = |V_G| \angle 0$) can change during a fault condition (or post fault) which will also affect the power flowing to/from the STATCOM.

The active power flow equation clearly shows that if the STATCOM voltage $V_S = |V_S| \angle \delta$ lags the grid voltage (that is $\delta < 0$) then $P < 0$, that is active power flows from the grid into the STATCOM.

If we consider Equation 12-8 the reactive power equation for $\delta = 0$ then we have:

$$Q = \frac{|V_G|}{\omega L_S} [|V_S| - |V_G|]$$

Equation 12-9

which clearly shows that for $|V_S| > |V_G|$ we have $Q > 0$. From a network perspective this means that the STATCOM appears capacitive. Conversely, for $|V_S| < |V_G|$ then $Q < 0$ and the STATCOM appears inductive to the network. We must remember that $S = VI^*$ and thus;

- Capacitive current → current leads voltage → $Q<0$

- Inductive current → current lags voltage → $Q>0$

12.3 APPENDIX C – DC CAPACITOR PASSIVE CHARGING

As one of the questions within this dissertation is around the ability of the STATCOM to charge its DC bus (capacitors) at a voltage level that is greater than the RMS value of the network voltage.

There are two distinct modes which can be analysed when it comes to how the DC bus is built: active charge and passive charge.

- Active charge, thoroughly discussed throughout this dissertation, as the ability of the STATCOM to charge its DC bus based on the amount to Active Power absorbed by the unit during steady-state operation (heavily dependent on δ operational angle of the unit with respect to grid Voltage – V_G).

- Passive charge of the DC bus can occur when the STATCOM is initially synchronised to the network, but there is no demand

A helpful approach that can be taken to analyse this phenomenon is to use a RLC series circuit and observing the transient response of the system when a sinusoidal signal is applied onto the system. Also, by deriving the system equation from first principles allows us to assess the responses at different switching angles of the source sinewave.

When the STATCOM is initially synchronised on the grid (assuming that its DC bus is fully discharged), it starts to charge its DC bus (capacitors) before it can start its intended operation. This is generally done using passive charging through the freewheeling diodes. In some instances, the STATCOM control system may use series connected inrush resistors to limit the current flowing into the discharged capacitors. What is of interest is

the transient response of the DC capacitor charging and its effect on the capacitor initial voltage.

The transient response can be found using the classic second order system applied to the circuit depicted below:

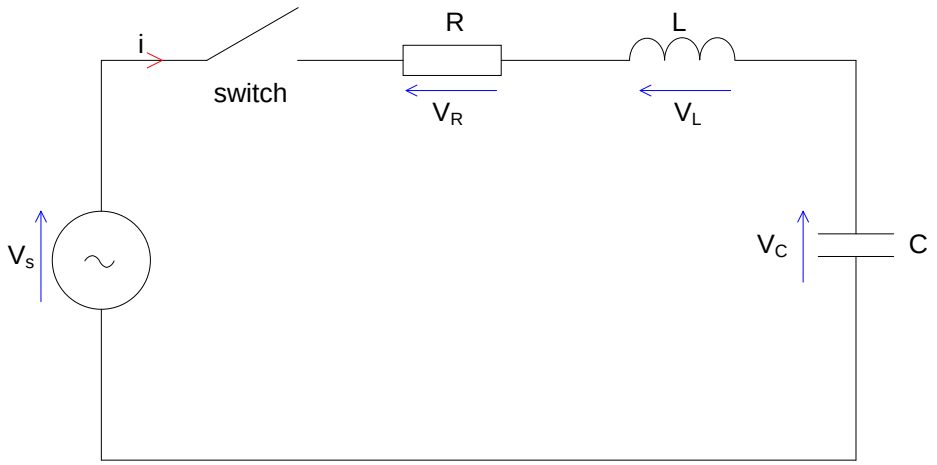

Figure 12-2 - STATCOM simplified to a RLC series circuit

By analysing the above circuit by using Kirchhoff's Voltage Law (KVL), we have:

$$\overrightarrow{V_R} + \overrightarrow{V_L} + \overrightarrow{V_C} = \overrightarrow{V_S} = \widehat{V}\, sin(\omega t + \Phi)$$

Equation 12-10

$$\Rightarrow i(t)R + L\frac{di(t)}{dt} + v_C(t) = \widehat{V}\, sin(\omega t + \Phi)$$

Equation 12-11

But we know that $i(t) = C\frac{dv_C(t)}{dt}$ and thus we can write:

$$\widehat{V}\ sin(\omega t + \Phi) = RC\frac{dv_C(t)}{dt} + LC\frac{d^2v_C(t)}{dt^2} + v_C(t)$$

Equation 12-12

$$\Rightarrow \frac{d^2 v_C(t)}{dt^2} + \frac{R}{L}\frac{dv_C(t)}{dt} + \frac{1}{LC}v_C(t) = \frac{\widehat{V}}{LC}\, sin(\omega t + \Phi)$$

Equation 12-13

To find the solution to this second order differential equation we need to find the following:

- The complementary solution -

The characteristic equation is:

$$S^2 + \frac{R}{L}S + \frac{1}{LC} = 0$$

Equation 12-14

which has roots:

$$S1 = \frac{1}{2L}\left(-R + \sqrt{R^2 - \frac{4L}{C}}\right)$$

Equation 12-15

and

$$S2 = \frac{1}{2L}\left(-R - \sqrt{R^2 - \frac{4L}{C}}\right)$$

Equation 12-16

Thus the complementary solution is:

$$v_{C_{comp}}(t) = K_1 e^{S1t} + K_2 e^{S2t}$$

Equation 12-17

where the constants K_1 and K_2 must be found using the initial condition for the complete system solution.

a) The particular solution – for a second order system with:

$$f(t) = forcing\ function = \ (V\ )\hat{}sin(\omega t + \Phi)$$

the particular solution will be the weighted sum of the $f(t), f'(t)$ and $f''(t)$. that is, the particular solution will contain the terms:

$$f(t) = \ (V\ )\hat{}sin(\omega t + \Phi)$$

Equation 12-18

$$f'(t) = \ \hat{V}\omega cos(\omega t + \Phi)$$

Equation 12-19

$$f''(t) = \ -\hat{V}\omega^2 sin(\omega t + \Phi)$$

Equation 12-20

and thus we can write the general form of the particular solution as

$$v_{C\_par}(t) = \ A\ sin(\omega t + \Phi) + B\ cos(\omega t + \Phi)$$

Equation 12-21

Substituting $v_{C\_par}(t)$ into the original differential equation

$$v_{C_{par}}(t) = A\ sin(\omega t + \Phi) + B\ cos(\omega t + \Phi)$$

Equation 12-22

$$\frac{d^2 v_C(t)}{dt^2} + \frac{R}{L}\frac{dv_C(t)}{dt} + \frac{1}{LC}v_C(t) = \frac{\hat{V}}{LC}\ sin(\omega t + \Phi)$$

Equation 12-23

we have:

$$\left(\frac{A}{CL} - \frac{BR\omega}{L} - A\omega^2\right) sin(\omega t + \Phi) + \left(\frac{B}{LC} + \frac{AR\omega}{L} - B\omega^2\right) cos(\omega t + \Phi) = \frac{\hat{V}}{LC} sin(\omega t + \Phi)$$

Equation 12-24

from which we can see that

$$\frac{A}{CL} - \frac{BR\omega}{L} - A\omega^2 = \frac{\hat{V}}{LC}$$

Equation 12-25

and

$$\frac{B}{LC} + \frac{AR\omega}{L} - B\omega^2 = 0$$

Equation 12-26

Solving for A and B gives

$$A = \hat{V}\left[\frac{\omega^2 LC - 1}{-\omega^4 L^2 C^2 + \omega^2(2LC - R^2C^2) - 1}\right]$$

Equation 12-27

and

$$B = \hat{V}\left[\frac{\omega RC}{-\omega^4 L^2 C^2 + \omega^2(2LC - R^2C^2) - 1}\right]$$

Equation 12-28

Given that the complete solution is given by

$$v_C(t) = v_{C_{comp}}(t) + v_{C\_par}(t)$$

Equation 12-29

we can now solve for constants K_1 and K_2 of the complementary solution using the following initial conditions;

$$v_c(t)\ at\ t = 0 = 0$$

Equation 12-30

that is the capacitor is assumed fully discharged at time = 0 when the switch is closed and

$$v_c{}'(t)\ at\ t = 0 = 0$$

Equation 12-31

The second initial condition comes from the fact that $i(t) = Cv_c{}'(t)$ which must be equal to zero at turn on as the inductor current is initially zero and cannot instantaneously change.

In matrix form these equations are given by:

$$\begin{bmatrix} v_c(t) \\ v_c{}'(t) \end{bmatrix} = \begin{bmatrix} e^{S1t} & e^{S2t} \\ S1e^{S1t} & S2e^{S2t} \end{bmatrix} \begin{bmatrix} K1 \\ K2 \end{bmatrix} + \begin{bmatrix} Asin(\omega t + \Phi) + Bcos(\omega t + \Phi) \\ -B\omega\, sin(\omega t + \Phi) + A\omega cos(\omega t + \Phi) \end{bmatrix}$$

Equation 12-32

Applying the two initial conditions the two constants (K_1 and K_2) can be readily found using;

$$\begin{bmatrix} K1 \\ K2 \end{bmatrix} = \begin{bmatrix} e^{S1t} & e^{S2t} \\ S1e^{S1t} & S2e^{S2t} \end{bmatrix}^{-1} \begin{bmatrix} -Asin(\omega t + \Phi) - Bcos(\omega t + \Phi) \\ B\omega\, sin(\omega t + \Phi) - A\omega cos(\omega t + \Phi) \end{bmatrix}$$

Equation 12-33

at $t = 0$ for a given Φ at which the switch is closed.

So considering 2 situations, such as switching angle of 0° and 90°, we find that at closing the switch we may have two considerably distinct maximum values of peak voltage, which will reflect on the maximum value at which the capacitor will be charged to during the positive semi cycle of the input waveform see in Figure 12-3 and Figure 12-4.

The below figures provide one reasonable explanation on how, during passive charging the DC bus voltage may reach a voltage amplitude greater than the source peak voltage without the need of complex power electronic devices or any consideration on the switching strategy of the STATCOM.

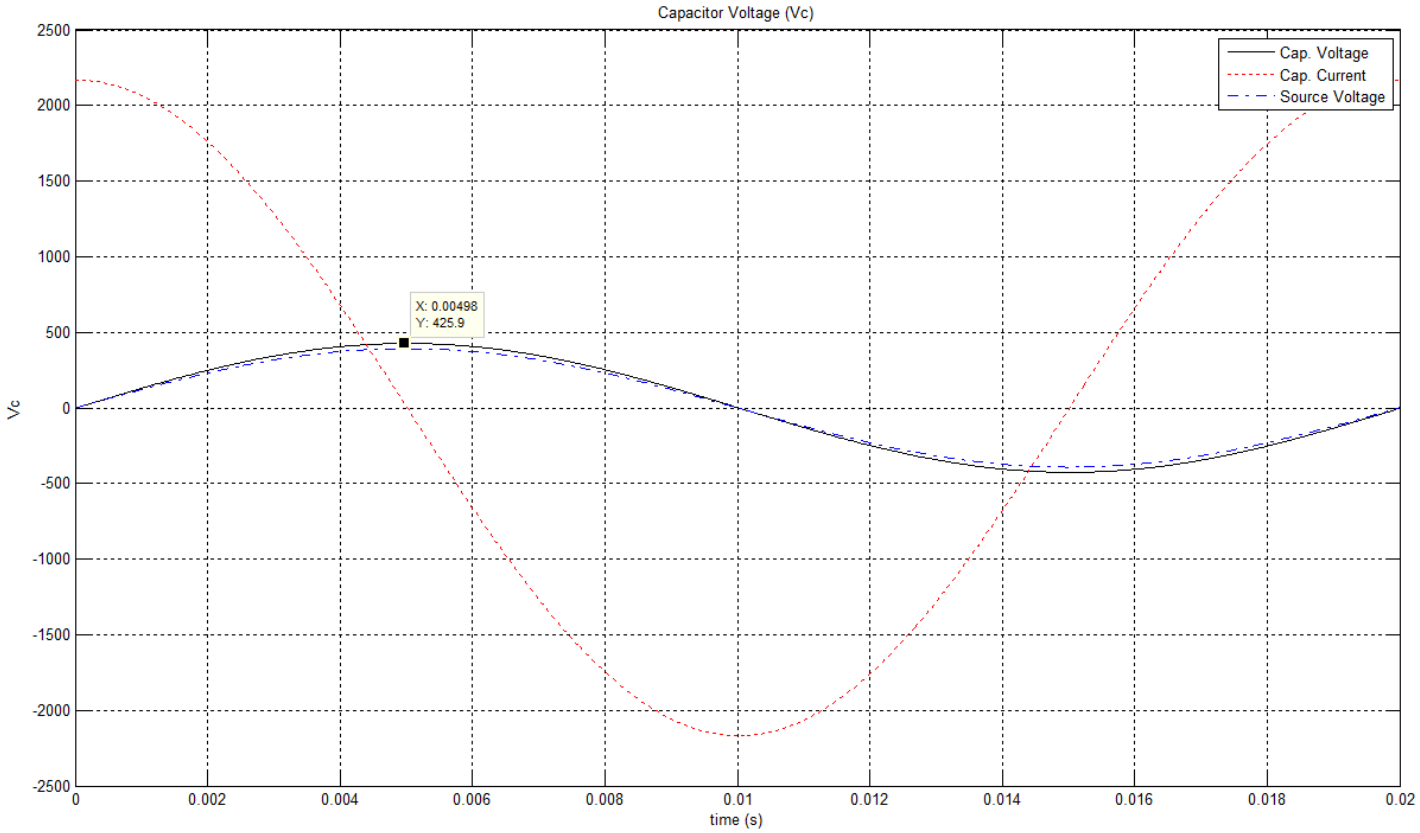

Figure 12-3 - RLC circuit switched at 0°*source angle*

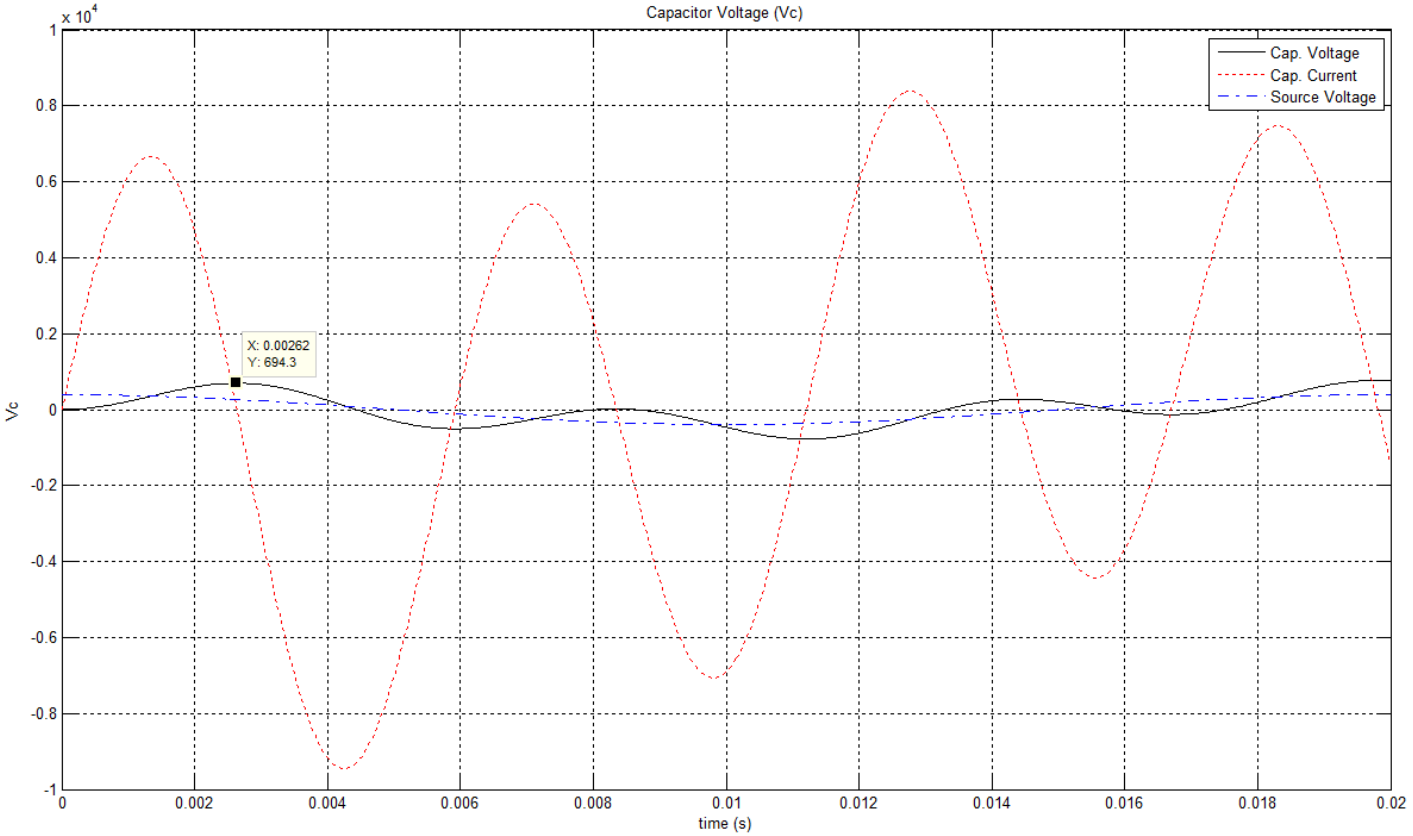

Figure 12-4 - RLC circuit switched at 90°source angle